Toward a greater understanding of the brain processes underlying handgrip and handgrip fatigue

By Michael T.C. King

Department of Exercise Science and Sports Medicine

Faculty of Health Sciences

University of Cape Town

February 2016

Submitted to the University of Cape Town

in fulfillment of the requirements for the degree

Doctor of Philosophy in Exercise Science

Supervisors:

Laurie Rauch

Department of Exercise Science and Sports Medicine
Faculty of Health Sciences
University of Cape Town, South Africa

Dan J Stein

Department of Psychiatry and Mental Health
Faculty of Health Sciences
University of Cape Town, South Africa

Samantha Brooks

Department of Psychiatry and Mental Health
Faculty of Health Sciences
University of Cape Town, South Africa

University of Cape Town

Faculty of Health Sciences

Department of Exercise Science and Sports Medicine

DECLARATION

I, Michael King, hereby declare that the work on which this dissertation/thesis is based is my original work (except where acknowledgements indicate otherwise) and that neither the whole work nor any part of it has been, is being, or is to be submitted for another degree in this or any other university.

I empower the university to reproduce for the purpose of research either the whole or any portion of the contents in any manner whatsoever.

Signature: Signed by candidate

Date: May 25th, 2016

Acknowledgements

This thesis is the culmination of an undertaking spanning four years across four continents packed with research and personal experiences that have made its completion possible. Particular individuals have graciously lent their expertise and mentorship and I would like to recognize them.

To my supervisors. Laurie - Thank you for your willingness to take on a neuroscience student without any previous experience in exercise science or fMRI imaging. Your reassurance that the project will work was a supportive pillar in these last four years. Leading by example, you demonstrated the importance of maintaining a calm attitude. Dan – You instilled a lasting confidence in my ability as a student, which is at the foundation of the work completed in this thesis. Thank you for setting high expectations and the guidance to achieve them. You have played a significant role in my development as a scientist. Samantha – Without your advice and assurance I'd still be scratching my head about how to create a comprehensive project. You were integral in my first PhD publication that connects the analyses performed in this thesis. The weekend reviews and coffee-shop meetings with Bob Lola enabled me to approach my project with confidence, thank you. Kai – You went above and beyond the role of a collaborator. You have made an invaluable contribution to my academic development. Your methodical and rigorous approach is inspiring and I have sincerely enjoyed working with you on this project, thank you.

There are others outside the typical supervisory role who I wish to thank. Karen Mearow – I suspect it is uncommon for a student to thank previous supervisors but it is necessary in this case. The skills you instilled during my MSc. continue to influence the way I approach questions and analyses. Jeanette Byrne – your interest in my work and review of my fellowship applications was essential for pursuing this degree. Your scientific demeanor has influenced how I approach working with others, thank you. Last but certainly not least Fabien Basset – In 2010, you walked into my office while I was

reading The Lore of Running and asked me how I'd like to do a PhD in Timothy Noakes' lab to search for the central governor. Honestly, I didn't believe it was possible but the following year we began the initial steps in Brasil, during which time you taught me valuable scientific and non-scientific skills for conducting a research project. Your persistent interest and involvement were instrumental in making this PhD a reality, thank you.

To the students that I met on my research stay in Brasil. Brunno and Guilherme, thank you for your welcoming attitude and for walking me through the basics of fMRI. Thiago and Marina, your day-to-day help in a foreign country, and friendship kept me focused throughout a challenging beginning, so thank-you. Rodrigo, thanks for the hospitality, lunch meetings, and above all, setting an example on how to be a great scientist against a suboptimal background.

To the remarkable staff and students of Exercise Science and Sports Medicine. Thank you for your generosity and logistical help. Your friendship and support made me feel at home. In this regard, special acknowledgements go to Marisce Blackaller-Smal, Philippa Skowno, Jordan Santos Concejero, Yoonus Abrahams, and especially, Nicholas Tam. Thank you for your constant encouragement, academic musings, and friendship throughout this degree.

To my family. Thank you to my wife Heather for understanding the pursuit of this degree in spite of the time apart, handling of at-home logistics, and always listening to my concerns. This degree would not have been possible without your support. Since this PhD is indeed the culmination of my formal education, thank you to my sisters Jennifer, Anna, and Stephanie for your help throughout grade school. Most importantly, to my Mom and Dad for always emphasizing the importance of education and hard work. It has taken over twelve years of post-secondary education to be satisfied with my student performance and I owe much of this to you. I am ever so grateful to you for allowing me the opportunity to pursue my interests freely, your belief in me, and everything you have and will continue to provide.

Acknowledgement of Funding

Project funding for this degree was supported in part by the:

a. Medical Research Council of South Africa
b. NLHARP – Newfoundland and Labrador Health and Applied Research Partnership Doctoral Research Grant
c. Tim Noakes Special Transformation - National Research Foundation
d. Novartis South Africa[1]

Personal funding for this degree was supported in part by:

e. NLHARP – Newfoundland and Labrador Health and Applied Research Partnership Doctoral Fellowship Award
f. R.A. Noakes Medical Research Fellowship

Funding for conferences, international travel was supported in part by:

g. NLHARP – Doctoral Research Grant
h. UCT - Doctoral Research Graduate Travel Award
i. CIHR/ICHR Doctoral Research Travel Award
ii. Psychiatry Department Research Fund

[1] Novartis did not participate or provide any communication that affected/influenced study design, data collection, analysis or interpretation of data. No one was paid by Novartis for their work.

Table of Contents

List of Figures

List of Tables

List of Abbreviations

ACC - anterior cingulate cortex

ANOVA -analysis of variance

ALE - activation likelihood estimation analysis

BA - brodmann area

BOLD - blood oxygen level dependent

CGM - central governor model

CNS - central nervous system

DA - dopamine

DCM - dynamic causal modeling

EC - effective connectivity

EEG - electroencephalogram

FC - functional connectivity

FDR - false discovery rate

fMRI - functional magnetic resonance imaging

FPCN - frontal parietal cerebellar network

FWE - family wise error rate

FWHM - full width half maximum

hem - hemisphere

hOC - human occipital

IC - insula cortex

IFG - inferior frontal gyrus

IPC - intraparietal cortex

M1 - primary motor cortex

METs - metabolic equivalent of task.

MPH - methylphenidate

MRCP - motor related cortical potential

MVC - maximal voluntary contraction

N - newton

OFC - orbital frontal cortex

PET - positron emission tomography

PPI - psychophysiological interaction

RF - radiofrequency

ROI - region of interest

S1 - primary sensory cortex

SD - standard deviation

SPM - statistical parametric map

TMS - transcranial magnetic stimulation

Thesis Preamble

In 2008, Timothy Noakes participated in an interview with the National Canadian Athletics Coaching Center at the University of Alberta, Canada. In this interview, he explained that exercise performance is regulated to protect homeostasis by a centrally located regulator known as the central governor. To provide support, he described the effect of stimulants in cycling performance. Noakes explained, "when they (cyclists) take stimulants its like the break is released and they can suddenly produce performances that were always there ... but could not access them". When then asked, "What's the interaction that the stimulants have for the break to be released?" Noakes' replied, "that's the fundamental question that if you can answer you'll know where the central governor works". In 2009, Noakes was involved in a study[1] that examined the effect of methylphenidate (MPH, Ritalin) on cycling performance during a fixed effort time trial. The main finding was that cyclists could exercise at higher cardiovascular and metabolic stress for ~32% longer than in the placebo condition. Authors interpreted that MPH altered the central interpretation of sensory feedback allowing for increased motor output. However, no data on the CNS was collected and the validation of this assertion could not be confirmed.

Soon after, a study at the University of Zurich by Lea Hilty, Kai Lutz *et al.* (2010)[2] used functional magnetic resonance imaging (fMRI) to determine that the insula cortex was an important region for the decision to quit a repetitive submaximal fatiguing handgrip task. Given that handgrip can generate intense sensations of muscle fatigue and can be completed in the fMRI, there was a clear incentive for examining the influence of MPH on the supraspinal mechanisms during muscle fatiguing exercise. As a result, a collaborative relationship was established between myself, Kai Lutz at the University of Zurich, and my supervisory committee at the University of Cape Town to unravel how MPH could influence neural mechanisms in the brain during handgrip muscle fatigue.

Reduced motor drive from the motor cortices is a core feature of supraspinal fatigue but the cerebral interactions leading to reduced drive are unknown. In order to address this

we first investigated the brain regions underlying the performance of handgrip using activation likelihood estimation analyses. Then, using fMRI and a fatiguing handgrip task we examined the effect of MPH on force output in three separate time resolutions: throughout the task, in the moments just prior to task failure, and during the recovery period after the task.

Abstract

Handgrip is a ubiquitous human movement that determines how we interact with our environment. It is involved in almost every aspect of daily life (e.g. opening a door, handling cutlery, using tools) and like all human movement, its application is limited by muscle fatigue. However, the supraspinal mechanisms of handgrip and handgrip fatigue are not fully understood despite the importance of this fundamental movement, numerous publications, and its presence as a longstanding research topic. This thesis investigates the brain mechanisms of handgrip and handgrip fatigue using fMRI. It begins with a review of the literature in Chapter one, which evaluates the theories and evidence for central control of handgrip and muscle fatigue as well as describing the rationale to perform the experiments in this thesis. The methodology and analyses are also reviewed to provide rationale for their use and to facilitate the interpretation of subsequent experimental results.

In order to understand the supraspinal mechanisms of handgrip and handgrip fatigue it is logical to first understand the most fundamental grip type (power vs. precision) and pattern (static vs. dynamic) by which handgrip can be performed. Using a neuroimaging meta-analysis method, activation likelihood estimation analysis (ALE), in Chapter two we analyzed data from 28 functional magnetic resonance data sets, which included a total of 398 male and female participants. Using ALE, we analyzed the blood oxygen level dependent (BOLD) activation coordinates during power, precision, static, and dynamic grip in a range of forces and age in right-handed healthy individuals. We found that power grip generates unique activation in area 1 and 3b and precision grip generates unique activation in area 6 and area 4a. Dynamic handgrip generates unique activation in area 4p and area 6 and of particular interest, both dynamic and static grip share activation in area 2, an area implicated in the human evolution of handgrip. According to effect size analyses, precision and dynamic grip generate stronger activity than power and static, respectively. This study highlights the differences in grip type and pattern. However, we found that there was a large degree of similarity, which indicates that mechanisms other than BOLD-related activation are potentially involved in regulating handgrip. In addition,

this study also served to generate regions of interest (ROIs) that were crucial in the analyses performed in this thesis.

Chapter three examines the supraspinal mechanisms during the performance of a fatiguing handgrip task. In addition to the commonly examined peripheral elements of muscle fatigue, there are also central nervous system (CNS) mechanisms that regulate muscle fatigue. The theories that address the role of the CNS in muscle fatigue are collectively known as central fatigue theory. CNS stimulants, such as methylphenidate (MPH), can increase force output during exercise. Central fatigue theory suggests that MPH may influence supraspinal mechanisms allowing for increased force but how this occurs is unknown. As a result, we sought to examine the effect of MPH on the force output and concomitant brain activity during a muscle fatiguing handgrip task. In a double blind, crossover design participants ingested MPH or a placebo before performing a muscle fatiguing handgrip task during fMRI scanning. We investigated force output, whole brain activation, and brain connectivity during the task and in the moments just prior to releasing the grip dynamometer (also known as task failure). Our findings confirmed previous stimulant-induced increase in force output and the role of the insula cortex (IC) in task failure. For the first time, we demonstrated findings indicating that MPH altered effective brain connectivity between the left IC and motor cortices throughout a muscle-fatiguing task, although not in the moments specifically prior to task failure. This finding is compelling given the proposed role of the IC in interoception of disturbed homeostasis and muscle fatigue. Indeed, the IC is thought to influence the motor cortex during fatiguing exercise. This study proposes a previously unknown neural mechanism between the IC and motor cortices during a muscle fatiguing handgrip exercise and may have broader implications for central fatigue theory and the study of sport performance.

Since muscles do not recover immediately after exercise has ceased, we sought to examine brain connectivity in the recovery period. In parallel with the study detailed in Chapter three, we conducted another study composing Chapter four, which examined ROI-to-ROI resting state functional connectivity (FC) before and after the performance

of the task. We were interested in the effect of fatigue and MPH on FC between several ROIs. We examined FC changes occurring: 1) between left and right primary motor cortices (M1) 2) right IC and hand motor area and 3) between the right orbital frontal cortex (OFC), and both the right IC and anterior cingulate cortex (ACC). We found: 1) a task-induced interhemispheric M1 FC disruption in the recovery period and that ingestion of MPH resulted in a trend toward a more pronounced M1 FC disruption. 2) Similar to connectivity results found in Chapter three, we observed MPH-induced increase in FC between the right IC and hand motor area during the recovery period. And 3) we observed reduced FC between the right OFC and both the right IC and ACC. These findings demonstrate that muscle fatigue influences FC in the recovery period after a fatiguing handgrip task.

Chapter five represents a synthesis of these results and summarizes the findings and implications for future research. This thesis examined the supraspinal mechanisms that control handgrip and handgrip fatigue on several different time resolutions. We demonstrate that grip type and pattern rely on unique activation patterns but also show substantial overlap, which suggests that handgrip is potentially regulated by other neural mechanisms. We demonstrate the that MPH allows for increased force output during a fatiguing handgrip task and offer potential supraspinal mechanisms coinciding with this ergogenic effect. We show that a muscle fatiguing handgrip exercise has dramatic effects on brain connectivity in the recovery period after exercise has ceased and suggests future research should examine how long brain connectivity is affected by fatiguing muscle exercise. Our results make a significant contribution to the study of handgrip and central fatigue theory and have implications for sport performance and further regulation of stimulant use during athletic endeavors.

Thesis structure

Using fMRI, this thesis aims to investigate the brain mechanisms underlying handgrip exercise and muscle fatigue in five chapters.

Chapter one is a review of the relevant literature and provides a rationale for performing the research questions covered in this thesis. It also provides a summary of the research questions and a rationale for the methods used to address them.

Chapter two is titled: "Understanding the regions that regulate handgrip: what are the similarities and differences between fundamental handgrip type and pattern?" and has been published in a modified form in *Neuroimage* (2014) 102 pp. 923–937. This chapter investigates the brain regions involved in controlling the two fundamental grip types: power and precision grip in the two basic patterns of force application: dynamic and static. This chapter reviews the scientific literature relevant to fMRI handgrip research, elucidates the different brain regions involved in the different forms of handgrip, and establishes regions of interest to be subsequently used for data analyses in chapters three and four, which investigate the brain's response to a fatiguing handgrip task.

Chapter three is titled "Supraspinal mechanisms of muscle fatigue during a fatiguing handgrip task" and has been submitted in a modified form to *Neuroscience*. This manuscript examined the effect of MPH on force output and the BOLD signal in response to a fatiguing handgrip task in fifteen participants during the task and in the moments just prior to task failure. This chapter demonstrates a MPH-induced increase in mean force output and altered effective brain connectivity. Activations generated during this experiment were used to create ROIs for analysis in the following chapter, which investigated FC changes in the recovery period after exercise.

Chapter four is titled "Supraspinal mechanisms of muscle fatigue after a fatiguing handgrip task" and a modified version of this manuscript is being prepared for submission to *Brain Connectivity* for publication. Using ROIs developed in chapters' one

and two; this chapter investigates fatigue-related FC changes *after* a muscle fatiguing handgrip exercise in sixteen participants. During the recovery period, we found that brain connectivity between some regions is disrupted. Yet, in other regions, task-related brain connectivity continues into the recovery period, a so-called bleeding effect of brain connectivity.

Chapter five of this thesis represents a synthesis of the studies performed, the novel findings, and potential implications. We also discuss potential direction of future research.

Chapter One

Review of relevant literature and rationale

1.1 Introduction

Human beings are unique in their ability to grip objects using four fingers and an opposable thumb[3]. The early hominid *Homo habilis* [3] distinguished itself by its ability to use its hands with two advantageous grips: the power and precision grip[4,5]. The power grip is thought to have been evolutionary selected for aggressive actions such as clubbing[5] while the precision grip was selected for accurate movements such as spear throwing[4,5], tool manufacturing[6] and use[5,7]. The ability to grip determines how we physically interact with our surroundings from early childhood to late adulthood. Infants develop the ability to power grip (e.g. holding a rattle) at 3-4 months of age while precision grip (e.g. picking up food) is developed later at 8-9 months. As we age, handgrip is a major predictor for late adulthood independence and mortality[8]. Although it appears simple in observation, the complex brain processes that regulate handgrip are still not fully understood. With this in mind, this vital ability is achieved partly through the supraspinal involvement of a network of regions that plan and execute handgrip.

Handgrip force is limited by muscle fatigue. Vocations that require repetitive or sustained hand use, such as assembly or mechanical repair, are particularly susceptible to experiencing intense handgrip fatigue, which presumably affects work-related performance and may lead to injury[9]. Muscle fatigue can be defined as a state characterized by a reduced ability to generate force or power[10]. Bodily tissues, including the CNS, do not recover immediately after exercise has ceased and require a period of rest. Central fatigue theory proposes that motor drive is limited by CNS processes that maintain bodily homeostasis and preservation of tissues[11]. However, scientists do not yet fully understand the mechanisms that regulate the limitation of motor drive during muscle fatiguing exercise.

CNS stimulants[12,13], such as MPH[1,14], enhance motor drive during muscle fatiguing exercise. For example, CNS stimulants have been shown to increase time to exhaustion during cycling[12], improve running and weightlifting performance[13], and reduce fatigue during repetitive cycling sprints[15]. This ergogenic effect has been attributed to modified

interpretation of feedback[1,16], feed forward[17] processes and/or a willingness to exert more effort[18]. However, the supraspinal mechanism(s) of stimulant use during muscle fatigue have not yet been fully elucidated.

The aim of this chapter is to review the central processes that regulate handgrip movement, handgrip muscle fatigue, and the potential central mechanism(s) by which MPH acts to improve force output. We review how fMRI can be used to elucidate the central mechanisms during and after muscle fatiguing exercise. Then, the chapter closes by reviewing the scientific questions related to this thesis. This chapter sets the framework for the subsequent experimental chapters that go on to empirically examine the central regulation of handgrip and handgrip fatigue.

1.2 Control of handgrip force

1.2.1 Neuromuscular control of handgrip force

We begin with the peripheral and central mechanisms that control handgrip force before moving into a discussion of the central processes related to muscle fatigue. Handgrip is a complex prehensile action that can be divided into two basic types: the power and precision grip[4,5]. Power grip involves grasping around an object using four digits and thumb where as precision grip involves pinching an object between the thumb, index, and second finger (Figure 1). The power grip relies on a larger proportion of extrinsic muscles in the forearm than the precision grip, which relies mostly on intrinsic muscles within the hand[4,19]. The primary extrinsic muscles used during power grip are the flexor digitorum profundus and the flexor digitorum superficialis (Figure 2A). The primary intrinsic muscles used during power grip are the radial interosseus, ulnar interosseus, and lumbrical muscles. Handgrip force during power grip is applied against the digits and palm where as precision grip is applied by the apical tuffs of the fingertips[5].

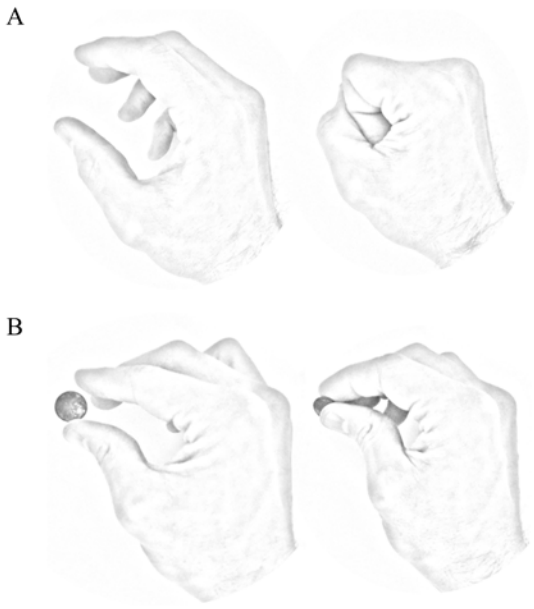

Figure 1. Schematic showing power (A) and precision (B) handgrips.

Like all voluntary muscle contraction, handgrip is coordinated by alpha and gamma motor neurons, which innervate motor units at the neuromuscular junction (Figure 2B). Alpha motor neurons innervate extrafusal muscle fibers to initiate contraction, where as gamma motor neurons innervate intrafusal muscle fibers to regulate muscle spindle mechanisms ensuring efficient contraction[20]. Muscle spindles are muscle-bound sensory receptors that generate spinal monosynaptic reflex mechanisms during voluntary contractions to facilitate tension during the stretch reflex and aid in efficient movement through reciprocal inhibition of opposing muscles. The actions of muscle spindles are controlled by gamma neurons and constitute part of the unconscious regulation of efficient voluntary muscle contraction (Chapter 36 in Kandel *et al*. (2000) [21]). Increased motor drive is achieved through recruitment of additional or increased firing of motor neurons. The supraspinal control of hand motor drive during muscle fatigue is a major topic of this thesis and throughout this chapter it will become clear that the command for motor drive during fatigue is modulated by voluntary and involuntary supraspinal mechanisms.

1.2.2 Supraspinal control of handgrip force

A network of brain regions interact to coordinate handgrip through feed forward and feedback processes[21]. Learned motor programs[22] are facilitated by the comparison of ongoing movement against a set of anticipated sensorimotor consequences, known as efference copies[23]. Efference copy is thought to be generated by the premotor cortex[24] and the supplementary motor area (SMA) [25]. Further, efference copy has been shown to influence perception of sensory stimuli[26] in the somatosensory cortex and may influence perception of physical effort[27]. The cerebellum has been implicated in efference copy[26] regarding rapid feed forward prediction and fine-tuning of movement[28]. With these ongoing processes, the pyramidal cells in the motor cortices (e.g. in M1, SMA[21,29,30]) generate descending command via corticospinal axons to motor neurons in the spinal cord[21] (Figure 2, D-B).

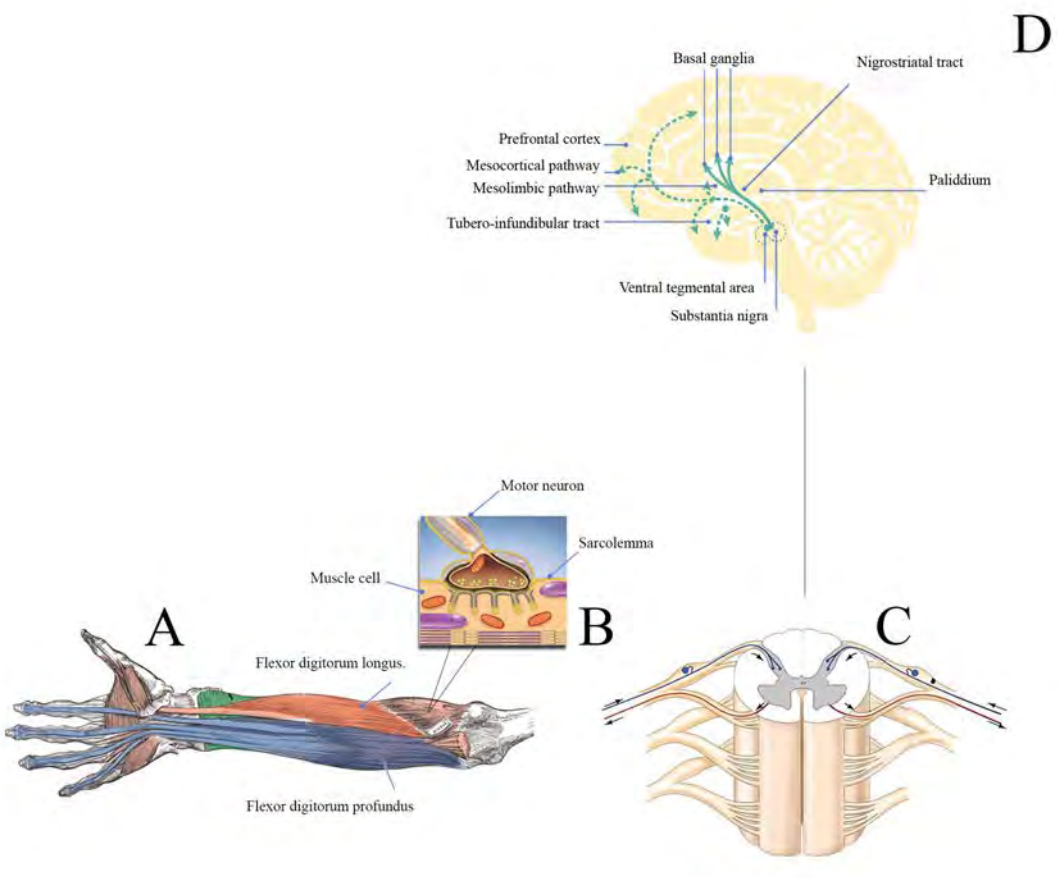

Figure 2. Schematic of the main peripheral and central components of the motor pathway.

The functional requirements of power and precision grip necessitate different brain activity. Power grip is commonly used for tasks requiring gross and more powerful forces, while the precision grip is used for delicate tasks requiring the precise application of force[19]. Brain activation during power and precision grip is comparable at lower forces[31] and power grip generates activation volume proportional to grip force [32-34]. In a direct comparison of power and precision grip, Takasawa *et al.* (2003)[35] used positron emission tomography (PET) to demonstrate that power grip generates greater volume of activation than precision grip, which is perhaps inherent to the volume of muscle recruitment orchestrated by the corticospinal tract. On the other hand, precision grip has been shown to generate greater ipsilateral brain activity in the premotor and parietal cortices [36] ; perhaps this is a result of the precise control required for its application of force. Indeed, for a variety of voluntary movements the more delicate force applied the greater the activity in the premotor cortices[37-39]. Dynamic handgrip is thought to generate greater activation than static handgrip due to the neurons associated with repetitive phasic activation[40 41] but this is region[40] and movement[42] specific. The differences between grip type and pattern have been investigated[35,36] but the regions that differentially regulate grip type and pattern remain equivocal.

1.3 Handgrip force is limited by peripheral and central muscle fatigue

The application of handgrip force is limited by muscle fatigue. Muscle fatigue develops during repetitive or maximal contractions and can be defined as a state characterized by a reduced ability to generate force or power[10].

It is common nomenclature to refer to fatigue as being centrally or peripherally regulated. Peripheral fatigue is the study of the efficacy of the motor system downwards of neuromuscular junction (Figure 2 A-B). These theories are the most prevalently discussed and understood in scientific and lay community, and are popular perhaps due to the ease of measurement. Peripheral fatigue theory focuses on the mechanisms of the muscle that are failing due to an inadequate blood supply from the heart[43], an increase in unfavorable

level of metabolites[44], and limitation of rephosphorylation of adenosine diphosphate[45]. In addition, muscle fatigue can be further characterized by neuromuscular changes such as disruption of excitation-contraction coupling[46], slowing of the conduction velocity along the sarcolemma[47], and decreasing sarcolemma excitability, all of which increase electromechanical delay[48]. On the other hand, central theories of muscle fatigue assert that the spinal cord and brain are critical components for regulating muscle fatigue and can be defined as a failure of muscle contraction by mechanisms occurring above the neuromuscular junction (Figure 2, B-D). For example, during maximal exercise a large proportion of muscles are not recruited despite the neuromuscular connections available to do so[11]. The body employs an exercise reserve[11,49] in order to maintain homeostasis and tissue integrity. For example, hypoxia induced poorer performance in a 5km cycling time trial in comparison to normoxia despite a lack of difference in peripheral failure[50], suggesting that central mechanism(s) reduces force output in the presence of critically low oxygen levels. For the remainder of this thesis, the term central fatigue will be used to refer to the central mechanisms of muscle fatigue.

The influence of central fatigue on muscle performance is well illustrated during maximal exercise tests. During such tests, a comparison of maximal voluntary contractions (MVC) before and immediately after exercise confirm a reduced ability to generate voluntary force (i.e. muscle fatigue). The presence of central fatigue can be illustrated if one induces an involuntary muscle contraction during a MVC[51]. The production of a stronger force by a superimposed electrically evoked contraction demonstrates that the muscle was capable of producing force greater than could be voluntarily generated.

1.4 Central fatigue: the neural processes of fatigue from the neuromuscular junction to the brain.

The study of central fatigue investigates neural mechanisms from the neuromuscular junction to the brain (Figure 2, B-D). Motor neuron activation frequency decreases during muscle fatigue[52], known as late adaptation[53], and may be caused by reduced motor neuron excitability[54,55] or reduced descending drive. Reduced motor neuron activation

during fatigue, as indicated by increased input required to maintain firing rate[56], may be caused by reduced activation of muscle spindles[57] leading to reduced reflex contributions to muscle contraction or by excessive activity-induced intrinsic changes in the motor neuron[53,58,59].

The contribution of reduced descending drive to muscle fatigue is supported by the observation that superimposed transcranial magnetic stimulation induced contractions at the cortical level increases force production during fatiguing MVCs. This illustrates an unused capacity in the pyramidal cells of the motor cortices to initiate a greater descending command [60,61]. This reduced drive is thought to be caused by 1) reduced efficacy of descending drive, which is perhaps caused by activity-induced changes in excitability of corticospinal axons (Figure 10-8 in Kandel *et al*. (2000)[21]) or by reduced efficacy of functional connections with motor neurons[54] and/or by 2) reduced output of descending drive caused by supraspinal mechanisms upstream of the motor cortices[51]. Supraspinal fatigue is a major component of this thesis and can be defined as an inability to generate optimal force as a result of suboptimal descending drive initiated at the level of the cortex (e.g. M1, Figure 2, D). However, the supraspinal mechanisms that lead to a decrease in motor drive during muscle fatigue are not fully known and should be further explored.

Functional imaging studies have begun to shed light on the supraspinal mechanisms of fatigue through activation and connectivity analyses. Activation in M1, primary sensory cortex (S1)[32-34,62], supplementary motor area (SMA), cingulate gyrus, prefrontal cortex, and cerebellum[34,62,63] is linearly proportional to force. However, brain activation increases at a non-linear rate in M1, S1, and SMA[64] as forces reach ~70% of MVC, possibly from increasing cortical neuron firing rate[62]. Similarly, Liu *et al.* (2003)[63] demonstrated that activation volume in M1 and S1 increased non-linearly throughout a 30% MVC static power grip (i.e. isometric). Activation volume in M1, S1, SMA, prefrontal, and cingulate cortex was shown to linearly increase up until a point when activation began to decrease, while force linearly decreased from start to finish, despite maximum effort from participants to maintain force[65]. These results as well as

converging evidence from cell recordings[10], electroencephalogram (EEG) [66] and PET studies[42], support the notion that increased cortical activation volume and/or frequency occurs in response to increased demand, which eventually decreases with declining muscle activity[63]. The functional connectivity (FC) between two or more brain regions may provide valuable insight into supraspinal mechanisms of fatigue since FC infers how regions relate to, or interact, with one another (see section 1.10.4). Jiang *et al*. (2012)[67] demonstrated a fatigue related increase in connectivity between the premotor cortex, SMA, and M1 in the latter stages of a fatiguing handgrip task and interpreted that strengthened connectivity may be facilitating motor output. However, Deshpande *et al.* (2009) [68] demonstrated conflicting evidence by dividing task analyses into early, middle, and end phases. Authors demonstrated that the premotor cortex, SMA, S1, and M1 were strongly interconnected early in the task but decreased in connectivity in the middle and end phases, suggesting a weakening of connectivity during muscle fatigue.

To summarize, cortical activation increases proportionally to force output until muscle capacity is challenged. At which point the motor cortices show a failed attempt to increase[65] volume, firing rate, and/or modify connectivity with other regions[67] in order to maintain efficacy[51] of descending command via the corticospinal tract to motor units, which respond to these signals by increasing frequency and/or number of recruited units in an attempt to compensate for reduced force[69]. Given that EEG, fMRI, and PET data well-correlate with excitatory changes in local field potentials[70,71], these results suggest that at the cortical level, force is partly maintained through motor cortex drive via excitatory mechanisms that occur up until a point, at which time cortical drive is possibly inhibited by mechanisms upstream of the motor cortex[72]. It is thought that these upstream mechanisms are potentially mediated by cortical processing of signals from afferent myelinated Aδ (group III) and unmyelinated C (group IV) fibers[51] fibers.

1.5 Central homeostatic structures process afferent feedback during muscle fatigue

Homeostasis can be defined as a process that ensures the functioning of biological systems through the stabilization of bodily states that are modified and informed by

behavioral, feed forward[26,72,73], and feedback[68,74,75] processes. The concept of homeostasis was initially proposed in 1878 by Claude Bernard in *Leçons sur les phénomènes de la vie communs aux animaux et aux végétaux* (see Cooper *et al.* (2008)[76] for translation) and the term was later coined in 1932 by Walter Cannon in *The Wisdom of the Body*[76]. The failure to regulate homeostasis during exercise can result in severe tissue damage or even death (e.g. exercise induced hyperthermia[77]).

Specific structures for relaying homeostatic signals and subsequent autonomic responses during muscle contraction have been identified (Figure 3)[78]. Afferent stimuli, such as pain, temperature, and pressure, from the musculoskeletal system generate action potentials that travel through myelinated Aδ (group III) and unmyelinated C (group IV) fibers to the dorsal horn of the spinal cord where they synapse with spinal lamina 1 cells.

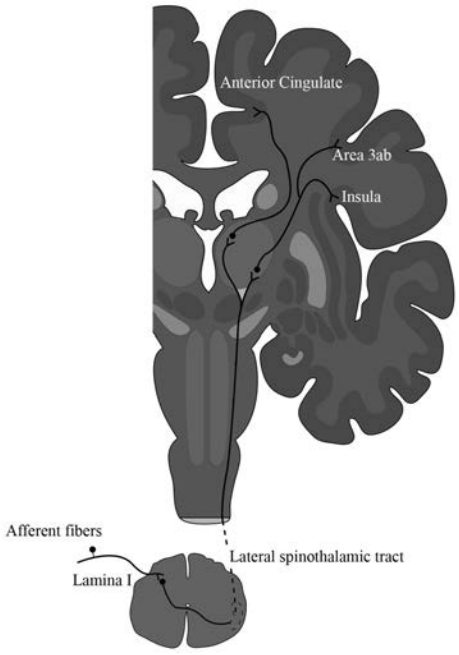

Figure 3. Cortical substrates of homeostatic signal processing. Painful stimuli from the periphery travel through small afferent fibers to the spinal cord where they synapse and ascend to higher cortical areas such as the insula cortex, anterior cingulate and sensory cortex (Redrawn from Craig *et al*. (2003)[79])

These fibers are sensitive to muscle contraction[80,81], tendon stretch[81], pain, hydrogen ions, and notably, phosphate[82], all of which are associated with muscle fatiguing exercise. Indeed, increased firing rate of these fibers occur during muscle fatigue[83,84] and induce a

cardiovascular response[85]. Afferent homeostatic information from the cardiovascular system during exercise is transmitted via the vagus nerve to the nucleus of the solitary tract in the brainstem, which also contributes to the efferent (feed forward) control of lung inflation. Efferent homeostatic reflexes controlling the cardiovascular response to exercise, such as increases in heart rate, stroke volume, and vasodilation/constriction, is modulated by the periaqueductal grey[86]. Interestingly, group III and IV fibers, which innervate practically every tissue in the body[87], have been implicated in central processes involved in muscle fatigue[74,75]. For example, group III and IV fibers have been shown to inhibit motor neuron firing rate[88] (excluding elbow flexors[89]) and voluntary drive after a muscle fatiguing task in both exercised and unexercised muscles[90]. Sensory information from lamina 1 decussates to the right anterior horn and ascends contralaterally through the anterolateral spinothalamic tract until synapsing in the basal and posterior ventromedial thalamic nuclei[91]. The thalamus then relays afferent sensory information to higher processing cortical areas such as the IC[92], right OFC[91], sensory cortex[87], and ACC[79].

The conscious awareness and emotional response engendered by disturbed homeostasis are collectively known as interoception [91]. The IC, ACC, and OFC are key structures forming the interoceptive system thought to be responsible for interpreting the sensations associated with disturbed homeostasis (e.g. pain, air hunger) [79,91] and muscle fatigue[93,94]. This system (Figure 3)[78] is larger in primates and rudimentary or non-existent in other mammals[21] supporting the suggestion that primates have a unique protective ability to perceive and be consciously aware of fatigue during exercise[94]. This ability to exercise safely within the confines of homeostasis is presumably an important factor for the proposed theory that humans evolved as efficient endurance runners[95,96].

1.6 Brain structures implicated in the interoception of disturbed homeostasis

The IC has been identified as an important structure for processing disturbed homeostasic[79,97] signals. The IC has been shown to be important for the processing of alarming stimuli[98] and afferent signals leading to pain[99], breathlessness[100], and thirst [101].

Interestingly, the IC has been associated with the cardiovascular response to exercise[102] and its activation is proportional to exercise intensity[103]. The IC's involvement in the interoception of pain and exercise suggests that it might be an important brain structure for regulating muscle fatigue.

The notion that the IC integrates signals of disturbed homeostasis during muscle fatigue is supported by functional and structural connections between the periphery, IC[91,104,105] and motor cortices[106 107,108]. Stimulation of group III and IV fibers lead to increased anterior IC activation[109] and direct stimulation of the IC evokes sensations of pain[110]. The IC projects to the OFC[104,108], ACC[111] and the motor cortices, such as SMA [107,108], which is functionally connected to M1[106]. Further, muscle pain activates right anterior IC[112,113] and the IC has been proposed as an important region for interpreting perceived exertion during exercise[114]. Indeed the IC has consistently been implicated in neuroimaging studies of exercise[2,31,36,115-117]. Thus, the IC and motor cortices provide a potential functional connection that may be employed for the interoception of muscle fatigue.

The IC's involvement in the decision to terminate exercise[2] during a submaximal fatiguing handgrip task and its proposed role in the limitation of motor drive via inhibition of the primary motor cortices[116] suggests that the IC could be a supraspinal substrate for the limitation of force output upstream of the motor cortex. Indeed, it has frequently been suggested that cortical regions and networks upstream of motor cortex are playing a role in fatigue and should be investigated[72 93,118,119].

In an attempt to examine muscle fatigue over the course of a task, Jouanin *et al*. (2009)[120] found a shift towards medial IC activation, indicating that the IC may change activity patterns throughout increasing muscle fatigue. The authors suggested that this change in activation may have been mediated by increasing pain and exhaustion. A drawback to this study is that they did not specifically address the time period just prior to terminating the task (i.e. a period known as task failure), which could inform on an important decision to terminate exercise related to muscle fatigue. Further, they did not examine the periods immediately after performing the fatiguing task. Previous research indicates that

the brain continues to be influenced during the recovery period after exercise has ceased. Muscle exercise reduces corticospinal motor evoked potentials[121] and increases alpha (7.0 - 12.5 Hz) frequency activity[122-124]. Exercise fatigue induces a temporary disruption in interhemispheric FC in both frontal[124,125] and M1[126]. OFC activation increases in the recovery period after fatigue [127] and is activated during sensations of mental fatigue [128] These findings support the line of research proposing that muscle and mental fatigue are interconnected[129,130]. The right OFC[91] (Figure 3 in Craig (2002)[91]), ACC, IC together are thought to play a role in the interoception of disturbed homeostasis and potentially, muscle fatigue[93,131]. Despite that muscles require a period of recovery after exercise has ceased[10] there is comparatively less literature on the supraspinal response during this period.

1.7 Models of central fatigue

1.7.1 The psychobiological and central governor model

Thus far, we have seen that muscle fatigue is regulated by peripheral mechanisms in the muscle and by central mechanisms from the neuromuscular junction to the brain. With this in mind, researchers have attempted to create a cohesive model of how the brain controls the limitation of motor drive.

The psychobiological model proposed by Marcora[27] and the central governor model (CGM)[132] by Noakes explains how the brain regulates exercise but they differ in how motor drive is influenced. The psychobiological model asserts that exercise termination (i.e. task failure) is regulated by the perception of feed forward drive, (i.e. efferent copy, corollary discharge) in response to increasing demand from skeletal and respiratory muscles[72], and psychological factors (e.g. motivation, effort). The CGM recognizes these factors[132] but includes the presence of an unconscious teleoanticipatory regulator that controls exercise fatigue based on rate of perceived exertion (RPE), physiological and psychological factors, which are regulated by both feed forward and feedback homeostatic mechanisms[11]. RPE is defined as the task-related effort, strain, discomfort,

and/or fatigue and is classically measured on a 6-20 RPE scale[133]. RPE has been linked to both psychological (e.g. mental fatigue[130] and sleep deprivation[129,134]) and physiological factors[135,133]. The two models also differ on the involvement of a teleoanticipatory regulator. Teleoanticipation is defined as the processes that manages RPE in anticipatory manner so that a maximum RPE is reached near the end of exercise[49,136]. Further, the CGM asserts that RPE is regulated in a teleoanticipatory manner to prevent physiologically threatening temperatures[137].

1.7.2 The neurotransmitter model

Acute exercise-induced changes in neurotransmitter levels, particularly the monoamines, have been long thought to play an important role in muscle fatigue[138]. Chronic changes in neurotransmitters also play a role in long term fatigue[139]. Monoamines have an intuitive connection with exercise and fatigue: increases in serotonin is associated with sensations of lethargy, decreased motivation, and sleep while dopamine (DA) has been associated with movement[140] willingness to exert physical effort[18], motivation[141] and reward[142], and norepinephrine with attention and arousal[143]. Indeed, if the brain has been proposed to regulate mechanisms of exercise fatigue then an examination of the neurotransmitters involved in synaptic communication should be conducted. As a result, human pharmacological interventions that modulate synaptic levels of monoamines have received a great deal of scientific investigation[144,145], perhaps due to the feasibility by which neurotransmitter systems can be non-invasively investigated by administration of a capsule in a double blind exercise trial.

The proposed effect of monoamines to improve exercise performance is inconsistent[145]. Norepinephrine was thought to enhance exercise via increased arousal and reward, but it does not improve performance. For example, norepinephrine reuptake inhibitors have resulted in no difference[146,147] or even a decrease in performance[148]. Serotonin agonists and antagonists have been shown to decrease and increase exercise performance in rodents, respectively[149,150]. But findings from human studies modulating serotonin levels have been less convincing. Branch chain amino acids, which indirectly reduce

serotonin[151], have been shown to improve performance on executive function tests after exercise[152], which suggests that low levels of serotonin could reduce mental fatigue associated with exercise and result in improvement based on the theory that mental fatigue contributes to exercise fatigue[130]. Early serotonin pharmacological interventions[153,154] demonstrate reduced performance with selective serotonin reuptake inhibitors (i.e. increased serotonin transmission). However, later nutritional[154,155] and other pharmacological interventions[156,157] have not replicated serotonin's involvement in exercise fatigue. This can potentially be explained by the strong influence of other neurotransmitters, such as DA, which during exercise has been shown to decrease while serotonin increases, leading Davis and Bailey (1997)[144] to propose that ratio of DA and serotonin influence exercise fatigue rather than serotonin alone.

The role that DA plays in submaximal exercise[158] is partly responsible for its proposed role in exercise fatigue. Marshall *et al.* (1979)[159] demonstrated apomorphine and L-dopa improved swimming impairment thought to be caused by an age-related deficit in the DA system. This was supported by Heyes *et al.* (1985)[138] who demonstrated that administration of apomorphine, an amphetamine DA agonist, could rescue exercise in rats after injection of a selective DA neurotoxin, 6-hydroxydopamine (6-OHDA). By showing that clonidine, a norepinephrine agonist, did not rescue exercise, authors concluded that both the reduction and recovery in exercise was DA mediated. Destruction of DA by the neurotoxin 1-methyl-4-phenyl-1,2,3,6-tetrahydropyridine in rodents[160], monkey's[161], and humans[162] lead to Parkinson's syndrome, which can be treated by administration of L-dopa or neural stem cells implanted into the basal ganglia to improve DA transmission[163]. It is clear that voluntary movement heavily depends on dopaminergic transmission, however the use of varied protocols to investigate DA's role in exercise make it difficult to pin down its specific role(s) in exercise regulation[164]. Further, DA's role in exercise has not always been replicated[165,166 167]. Thus, although it is certain that DA is important for exercise, its exact role remains unclear. In order to better understand DA's role in exercise we will next discuss the movement related neural pathways in which DA is heavily involved.

1.7.2.1 Dopaminergic pathways and the facilitation model

With advances in MRI scanning protocols and analyses, such as diffusion tensor imaging and functional network analyses, exercise scientists became increasingly interested in how brain networks influence exercise fatigue. Dopamine (DA) is largely synthesized in the cell bodies of the ventral tegmental area and substantia nigra but can influence neurotransmission in other parts of the brain through several dopaminergic tracts (Figure 2D): (1) the basal ganglia[168] via the nigrostriatal tract, which is important for movement[169], (2) the pituitary and hypothalamus via the tubero-infundibular tract (3) the nucleus accumbens via the mesolimbic pathway and (4) the frontal cortex via the mesocortical tract. The mesocortical and mesolimbic pathway overlap in the ventral tegmental area and together form a mesocorticolimbic pathway, which are together important for emotion and motivation[170,171].

In conjunction with these pathways, DA-regulated[21] re-entrant basal ganglia-cortical loops allow for moment-to-moment modifications to regulate motor control[172,173]. The mesocorticolimbic pathway is thought to be a critical part of the motor facilitation system proposed by Tanaka and Watanabe[174] where by motivational input into the basal ganglia can influence motor output[175,176]. The basal ganglia and areas of the prefrontal cortex, such as the OFC, and ACC, are thought to perform a facilitating role in order to compensate for reduced motor drive during fatigue[174] and have been recognized elsewhere as important regions during muscle fatigue[93]. Although, authors do not specify how sub regions of the ACC or basal ganglia are specifically involved. Evidence from Liu *et al*. (2007)[177] suggests that regions such as the ACC and prefrontal cortex compensate for handgrip muscle fatigue by increasing activation throughout the task, while Jiang *et al*. (2007) proposed strengthening of FC between motor cortices as a possible compensatory mechanism. Both of these results are in line with the proposed facilitation model.

The facilitation network is a set of structures that could be important substrates for regulating motivation during muscle fatigue. However, it is important to note that it is

challenging to empirically integrate motivation and mechanisms of supraspinal muscle fatigue into a single cohesive model. Indeed, the proposed facilitation network model non-specifically describes ROI to ROI involvement. Further, despite that motivational aspects described by the facilitation network and reduction of motor drive are intuitively related, the facilitation network and processes reducing motor output are separate constructs. Hence, Tanaka and Watanabe[174] separately proposed an inhibitory model in the same review. A key region of the proposed inhibitory system is the IC, which is a region thought to be important for the perception of effort, decision for the disengagement of exercise[2,72,116], and interoception of disturbed homeostatic stimuli[91]. Further, the IC is thought to influence M1 during fatiguing cycling[116]. Thus, the IC's role as a region influencing descending drive during muscle fatigue is warranted.

Other dopaminergic pathways important for the regulation of movement are the indirect and direct pathways. The subthalamic nucleus and caudal substantia nigra influence the motor cortex via dopaminergic indirect and direct pathways to putamen and the internal and external segment of the globus pallidus (Figure 43-6 in Kandel *et al*. (2000)[21]), which then influence the motor cortex via the thalamus[178] and caudate[179]. However, the indirect/direct pathways are more commonly associated with movement inhibition/excitation and the generation of involuntary motor actions in disease. For example, disruption of these pathways lead to hypo- or hyperkinetic disorders such as parkinson's disease and chorea, respectively. There is a potential role of the subthalamic nucleus and caudal substantia nigra for dopaminergic influence and would be excellent substrates of a region specific hypothesis but these areas particularly difficult to directly investigate in human populations given the small volume of brain matter and the deep brain location of these regions[180]. Further, the indirect/direct pathways contain many gamma-aminobutyric acid-mediated segments. Thus, although the regions of the indirect/direct pathways play a potential role, they are not ROIs in this thesis for elucidating a dopaminergic mechanism involved in the regulation of muscle fatigue during voluntary movement.

In the subsequent section, we discuss the literature and rationale for investigating the effect of an ergogenic stimulant and DA reuptake inhibitor, MPH, on supraspinal mechanisms during a muscle-fatiguing task.

1.8 Investigating supraspinal mechanisms of muscle fatigue using an ergogenic stimulant and functional imaging

The CGM predicts[181] that stimulants that dampen regulatory controls[14] and increase motivation should enhance motor drive during exercise. The psychobiological model proposes, although somewhat vaguely, that stimulants influence efference copy[17,182], which in turn influence motor drive perhaps via a reduction of RPE or increased motivation. While on the other hand, the neurotransmitter hypothesis suggests that reduced DA transmission can potentially be rescued by increasing failing neurotransmission.

MPH is a norepinephrine and DA reuptake inhibitor that increases synaptic norepinephrine and DA transmission by blocking reuptake transporters[183,184] on the presynaptic terminal. Although, its affinity for DA transporters is five-fold greater than for norepinephrine[185]. CNS stimulants have been shown to increase time to exhaustion during cycling[12], to improve running and weightlifting performance[13], and reduce fatigue during repetitive cycling sprints[15]. MPH's ergogenic effects may be explained by the increase in DA transmission [145,186]. MPH increases motivation and willingness to exert more effort[18,187]. Indeed, MPH binds [188] and acts on the mesocorticolimbic pathway, which according to Chaudhuri and Behan (2000, 2004)[175,176] increases force output via increases in motivational input. This concept was later reformulated by Tanaka and Watanabe (Figure 2, in Tanaka and Watanabe (2012) [174]) as previously discussed. However, investigation into this model as a source for increased motor output via M1 must be done with caution since there is not a specific ROI to ROI data to formulate a specific functional hypothesis between the facilitation network and the motor cortices. Although part of their rationale is supported by dysfunction of these tracts in disease

states, the presence of disease offers confounding factors in interpreting fatigue mechanisms for healthy individuals.

In a randomized double blind crossover design, Swart *et al.* (2009)[1] demonstrated that participants were able to cycle for 32% longer in a fixed RPE trial after having taken MPH. Further, participants reached a higher percentage of maximal oxygen consumption (13%) heart rate (12%), and arterial lactate (43%). Authors concluded that MPH may have altered "the central interpretation of afferent sensory feedback from some, but not all, homeostatic regulators" (i.e. interoception). This study attempted to integrate the CGM with the neurotransmitter model by showing that feedback could be influenced by neurotransmitter manipulation. By showing that initial force outputs in placebo and MPH conditions were equal they further interpreted that MPH induced changes in somatosensory feedback, rather than feed forward mechanisms, were the source of improved performance.

Roelands *et al.* (2008)[14] demonstrated that cyclists completed a time trial 16% faster in 30°C but not in 18°C after ingestion of MPH compared to control trials. Additional research by this group replicated this effect in humans [16] and rats[189] using bupropion, also a norepinephrine and DA reuptake inhibitor. In human studies, participants reached higher heart rate and body temperature in MPH conditions, but interestingly maintained the same rate of perceived exertion (RPE), which normally increases with these variables. Authors concluded that MPH may have increased motivation and maintained RPE while overriding thermoregulatory mechanisms during exercise. Further, Roelands *et al.* (2008)[14] suggested that these effects were of dopaminergic origin[145], instead of norepinephrine, based on bupropion's temporal dopaminergic influences[190]. Furthering the notion that dopamine plays a role in MPH-induced increases in motor drive, it has been shown that rats bred for increased wheel running have higher dopaminergic tone than controls[191] but do not ergogenically respond to MPH[192]. Conversely, control rats have lower dopaminergic tone[191] and respond ergogenically[192].

A recent meta-analysis[193] demonstrated that caffeine induces a ~7% increase in force output. This study further demonstrated that although caffeine could have an impact anywhere along the motor pathway[194] (e.g. on the muscle[195]), the collective data points to a supraspinal effect since caffeine has a greater effect on voluntary contraction than during superimposed involuntary stimulation[193]. Other independent reviews[196] have made similar conclusions for caffeine's ergogenic effect. Indeed, caffeine antagonistically acts on adenosine receptors leading to increased dopaminergic transmission[197], motor activity[198], and increased motivation[197]. However, the supraspinal neural mechanism(s) behind stimulant-related force increases are unknown.

The influence of stimulants on the supraspinal regulatory mechanisms during exercise has infrequently been directly investigated using neuroimaging methods. Using EEG, Moree *et al.* (2014)[17] examined motor cortical related potentials (MRCPs) during knee extensions with or without administration of caffeine. Caffeine caused a ~5% increase post-task MVC, a reduction in task-related RPE, and reduction in MRCP in the SMA and premotor cortices during the task, which are regions thought to be important for efference copy and perception of effort[199]. Authors proposed that the caffeine-induced reduction in MRCP in the SMA and premotor cortices was indicative of reduced corollary discharge associated with the concomitant decrease in perception of effort. Their study[17] supports the notion that stimulants may affect efferent copy, leading to reduced RPE and potentially improved force output. Surface-level imaging methodologies have been used to examine the relationship between the CNS and muscle fatiguing exercise. For example, Subudhi *et al.* (2009)[200] used near-infrared spectroscopy to show that prefrontal, premotor, and motor cortex deoxygenation during maximal exercise may contribute to a decision to stop exercise. In addition, Hilty *et al.* (2011)[116] demonstrated increased EEG intracortical communication between the IC and M1 after fatiguing cycling exercise. The authors postulated that the IC was providing an inhibitory influence on M1. Although these studies greatly contribute to our understanding of the role of the brain in muscle fatigue (particularly for whole body exercise), they do not well-examine brain structures with a resolution offered by fMRI. Given that the proposed effect of ergogenic stimulants is thought to be centrally mediated, a double blind handgrip trial performed during fMRI

scanning provides an excellent model by which to study the supraspinal regulation of force output during muscle fatigue.

1.9 Functional Magnetic Resonance Imaging (fMRI)

fMRI enables us to indirectly map neural activity of the entire brain into three-dimensional brain images with higher temporal and spatial resolution than other imaging methods (e.g. PET, EEG, near-infrared spectroscopy). fMRI is a safe non-invasive widely-used tool to examine task related neurophysiological events in a variety of experimental designs and populations. As a result, fMRI has become the preferred technique to examine whole brain activation from the BOLD signal. However, a significant drawback to fMRI is that the head must be in a fixed position, which is difficult to achieve during large extremity movement, such as cycling. As a result, muscle fatigue is often examined in the fMRI using either a maximal or submaximal fatiguing handgrip paradigm. Further, the fMRI environment is experimentally limited, as it must not include any paramagnetic material. In order to understand the methodology implemented in this thesis, we will next review fMRI and its analyses in advance of discussion of the aims, hypotheses, and experimental design.

1.9.1 Nuclear spin and dipole moment generate nuclear precessing

The protons and neutrons that make up atomic nuclei have an intrinsic characteristic known as spin (Figure 4A). Nuclear spin generates a magnetic dipole, which when in the presence of an external magnetic field (B_0) interact to produce a precessing movement around the magnetic field axis (B_0). The spinning nuclei itself also rotate around an axis. Like all spinning objects, precession is a result of angular momentum. The frequency of nuclear precession is known as the Larmor frequency (ν_0). In the absence of a magnetic field the orientation of nuclei precession is random (Figure 4B) and net magnetization (M_0) is equal to 0.

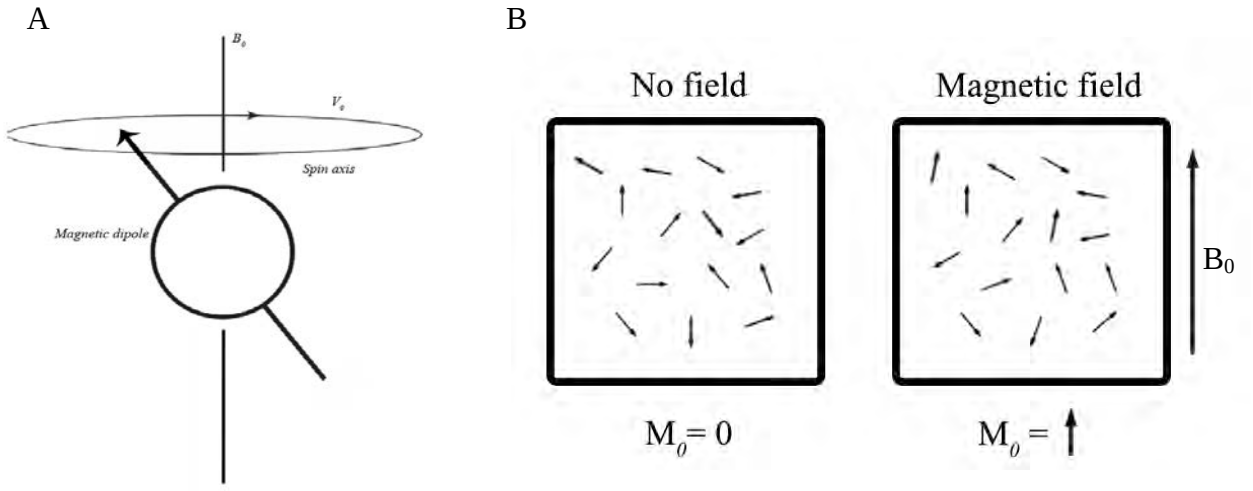

Figure 4 Schematic of nuclear spin (A) in the presence and absence of a magnetic field (B). (Redrawn from Buxton *et al*., (2009) [201])

However, in a magnetic field (B_0) M_0 aligns to form a weak equilibrium, where the difference in the number of spins now in line with B_0 is approximately 1 in 1 000 000. Nuclear spin and precession are the basis for generating the nuclear magnetic resonance signal[201].

1.9.2 Generating the nuclear magnetic resonance (NMR) signal

Hydrogen, which has a single proton in its nucleus, produces a particularly strong angular momentum and precesses around B_0 axis of a magnetic field at a Larmor frequency of 64Mhz. By using a radiofrequency (RF) pulse equal to hydrogen's Larmor frequency the orientation of precession can be gradually tipped out of alignment following a declining spiral path. With this pulse, the precessing hydrogen protons become out of alignment to the magnetic field (B_0) to form a high-energy state. Net magnetization is now slightly out of orientation. Once the RF pulse is switched off the H protons are free to change orientation, or relax, to re-align with the magnetic field, which reverses the process and produces a detectable electromagnetic current. The duration of time required for the magnetic dipole to realign is known as T_1 relaxation. Energy is released during relaxation

because a magnetic dipole out of alignment has a higher energy state than one that is aligned.[202]

1.9.3 Free induction decay and the nuclear magnetic resonance (NMR) signal

The NMR signal is derived from free induction decay. Free refers to the freely processing nuclei, induction refers to the electromagnetic current generated by a changing magnetic field (using a RF pulse), and decay describes that this signal decreases over time (during T_1 relaxation). The longer the RF pulse the larger the displacement angle known as flip angle, the larger the change in net magnetization, and the larger the NMR signal. There is a delay between a series of RF pulses known as scan repeat time (TR) that allows for relaxation. It's during relaxation that a change in net magnetization creates a detectable current received by the receiver coil. Repeating this process generates MRI images. This signal is proportional to the length of the RF pulse and proton density, which in turn impacts the strength of M_0 and strength of B_0[201].

1.9.4 Spatial encoding and voxel organization

The nuclear phenomenon explained thus far describes the processes that create the NMR signal. However, one of the invaluable characteristics of MRI is the generation of high-resolution three-dimensional images. Three processes that spatially localize the NMR signal generate MRI images: 1) Slice selection is achieved during a pulse sequence through the application of a varying gradient magnetic field along the z-axis. Since protons precessing at the Larmor frequency selectively respond to the RF pulse, the NMR is narrowed down to a thin slice of brain tissue on the z-axis. 2) Next, opposing gradient fields are applied transversely in the x-axis generating a net signal that is composed of varied range of precessing frequencies, which can be subsequently separated and spatially localized using the fast Fourier transform. 3) Lastly, the y-axis is spatially encoded by repeatedly performing this process around the x-axis until a complete data set is formed. With this information in the z, x, and y planes an MRI image can be created[201].

The MRI signal is spatially organized into three-dimensional units known as voxels. In fMRI each voxel contains a time series of MRI data (i.e. one time series of data per voxel per image), thus generating a four-dimensional data set. The physiological signal associated with fMRI is the BOLD signal.

1.10 fMRI Analyses of the blood oxygen level dependent (BOLD) signal

MRI's most common research application measures the BOLD signal. The BOLD signal is dependent on the hemodynamic response, which can be defined as a localized increased in blood flow and oxygenation. The hemodynamic response occurs in order to supply oxygen to metabolically active cells and can be modeled with the hemodynamic response function[203]. Since deoxygenated blood is paramagnetic and oxygenated blood is isomagnetic, a sudden increase in the ratio of oxygenated to deoxygenated blood creates a localized change in surrounding magnetic field, which is detected and localized in space with a pulse sequence. Despite that neural activation well correlates to single cell recordings and local field potentials[204] it should be noted that oxygen consumption by supporting glial, and not neuronal, cells could influence the intensity of the BOLD signal[205]. Indeed, the signaling process that regulate the hemodynamic response is not well understood and recently, it has been proposed that it may not be driven by an energy deficit but by neurotransmitter-mediated signaling involving glutamate[206] and dopamine[207]. For example, dopaminergic modulation has been associated with both increases[207] and decreases[208] in cerebral blood flow, which is thought to be mediated by post-synaptic action of astrocytes or dopaminergic receptors on microvessels. Nonetheless, the BOLD signal is a proxy for brain activity with high temporal and spatial resolution[203], which satisfies the methodological requirements of the questions addressed in this thesis.

1.10.1 Activation Likelihood Analyses (ALE) of the blood oxygen level dependent (BOLD) signal

ALE is a meta-analytic method used to compile activation coordinates from multiple studies that have examined a similar imaging question using varying experimental design. ALE analysis attempts to form a cluster of activation illustrating a three-dimensional probability distribution of activation and provides a probabilistic summary of the BOLD response in hundreds of participants, which is otherwise difficult to achieve in a single fMRI experiment. ALE is a particularly useful method for three reasons: (1) The number of participants that contribute to ALE data can be considerably larger than a single fMRI study (2) it reveals brain areas that are consistently active between studies, which through common activation demonstrates reliability and (3) it does so with statistical measure, which is particularly useful given the inter-participant, -scanner, and -experiment variability typical of a single fMRI study[209]. ALE studies assume a null hypothesis that brain activation occurs randomly and computes the probabilistic distribution of activation in a region.

1.10.2 Task related and resting state analyses

In task-based studies, fMRI research is interested in uncovering hidden neurophysiological processes related to a cognitive or motor task. Each voxel contains a time series of fMRI data (i.e. one data point per voxel per *x* number of images) and the fMRI signal time series is tested against a task model using a general linear model. In a block design, the task follows an on/off design (Figure 5A) and a task model is a function created from the convolution of the task time course (Figure 5D) and the canonical hemodynamic response function (Figure 5C). A convolved model allows for a more accurate estimation of the hemodynamic response than an on/off stimulus function.

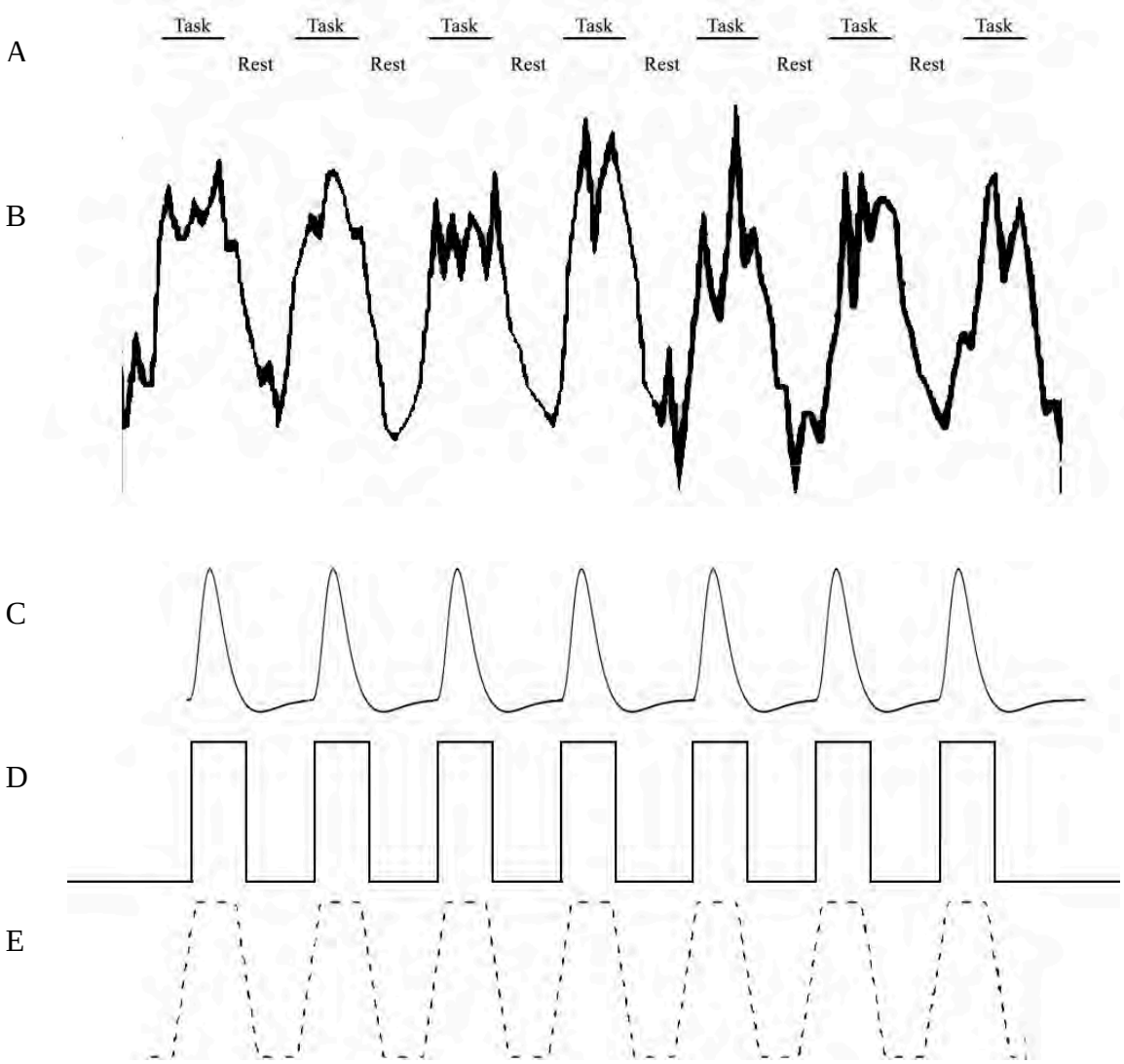

Figure 5. fMRI analysis modelling. A timecourse of a task (i.e on/off performance of a task) (A) and sample fMRI signal (B). The canonical hemodynamic function (C) is convolved with the boxcar function (D) to create the task model (E). Using the general linear model, the task model (E) is correlated with the fMRI signal (B). Figure adapted from Poldrack *et al.* (2011)[203].

Statistical parametric maps (SPMs) are created by testing the correlation between the task model (Figure 5E) and the time series data (Figure 5B) using the general linear model at every voxel. Resting-state studies, on the other hand, examine task-free temporal correlations (i.e. FC) between slow oscillating BOLD signals from two or more brain regions.

1.10.3 Correction for multiple comparisons and inference

One of the unique statistical implications of fMRI analyses is that the GLM is performed at every voxel in the brain. This creates a situation where multiple testing corrections are required. By using family wise error rate (FWE) correction for multiple comparisons, voxel-level inference involves assessing whether the test statistic (T or F statistic) has reached significance in a single voxel with consideration for multiple testing across the whole brain.

Voxel level inference may not be the optimal type of inference because spatial normalization and data signal smoothing spread the signal over neighboring voxels. Cluster-level significance is also used to assess activation that occurs in neighboring voxels. Taking into account the spatial connectedness or clustering of activated voxels reaching a defined threshold, a cluster-level significance describes a region of neural activity. However, an inherent problem with cluster-level significance is that the threshold is arbitrarily set. In practice, it is common to select a threshold of 0.01 or 0.001[203]. Cluster level significance is a more sensitive approach of inference[210].

An alternative FWE correction to multiple testing is false discovery rate (FDR). FDR[211] helps avoid arbitrarily set thresholds and controls for the presence of false positives amongst the subset of significant tests that have rejected the null hypothesis[212]. Further, FDR corrected testing is well suited to exploratory analyses[213], which is appropriate for brain connectivity analysis when a specific hypothesis cannot be established.

1.10.4 Functional and Effective Connectivity Analyses

Task-related BOLD analyses do not make conclusions on how regions function together[206]. An increasingly common method of analyses of the BOLD signal is functional and effective connectivity (EC). FC and EC analyses attempt to relate the time course of the MRI signal between regions. Then with BOLD activations and structural pathways we can gain a greater understanding of how regions are working in unison

during a task. Although similar, there is a clear difference between the two analyses: FC is a correlative measure typically used in resting state fMRI that may or may not reflect meaningful interactions[214] (which is inherent to a task-free rest period), where as EC determines if brain regions are correlated in a meaningful way. Since we are interested in the relationship between specific brain regions during and after a fatiguing handgrip task we employed both EC and FC analyses using ROI-to-ROI psychophysiological interaction (PPI) and ROI-to-ROI FC to better understand these relationships.

PPI is a measurement of effective connectivity[214] and is the *task dependent* percent signal change between a seed and target ROI. A key feature of PPI is that a task-dependent regressor, known as the PPI regressor, is created from a moment-by-moment product between the task regressor (e.g. periods of grip) and seed region signal. The PPI regressor attempts to predict changes in correlated neuronal activity occurring only during the task (see Figure 2 in O'Reilly *et al.* (2012) [215]). The PPI regressor is tested in a regression model with the task time course and a target signal in a ROI. PPI coefficients are measures of task dependent signal change where as, FC is quantified by Pearson correlation coefficients. Although PPI coefficients are an indicator of effective connectivity[214], it is important to note that PPI does not predict directional influences between ROIs. Other effective connectivity methods, such as dynamic causal modeling (DCM), are used to measure directional links between multiple regions in the brain. However, we did not implement DCM in this thesis since DCM requires task activation in both investigated areas as a prerequisite [214]. We plan to investigate IC and motor cortex PPIs during the task and in the moments prior to task failure. Previous research implementing the identical grip paradigm used in this thesis did not show activation in the hand motor cortex area[2] just prior to task failure and grip-related contrasts were not performed in the previous study. Further, and of more practical and dissemination reasons, PPI is well translatable [214] to those who do not have a background in mathematics required to fully understand DCM. Thus, in this thesis we implemented PPI effective connectivity.

There are many methods of analyses to address resting state FC. Popular types of analyses include independent or principle component network analyses. Although an attractive method for isolating changes in networks we did not have specific hypothesis regarding this network connectivity (e.g. the default mode network). Instead, we sought to examine brain connectivity changes between well-defined, functionally specific, and hypothesis driven ROIs, such as bilateral M1, IC, and others regions associated with the interoception of disturbed homeostasis[79] and fatigue[93], such as the OFC and ACC.

1.11 Research purpose, questions and overview:

1.11.1 Research purpose

It is clear that the regulation of handgrip muscle fatigue is a complex phenomenon influenced by a multitude of peripheral, central, and task specific factors. The CGM, psychobiological, and neurotransmitter models recognize that motor drive is centrally regulated[1,72] and proponents of these models refer to "brain regulatory centers"[11] or neural pathways "upstream of the motor cortex" [72,93]. Although, these pathways have been investigated[68,177,216], the interactions that lead to reduced motor drive and the subsequent effects of muscle on the CNS have not been well established. The aim of this thesis is to understand the brain processes that regulate handgrip and handgrip muscle fatigue by using fMRI and several analysis methods described above.

To investigate the brain regions associated with central fatigue of handgrip it is best to first establish task-specific ROIs and then form directed hypotheses prior to data collection and analyses. The ROI to be examined should be chosen independently of the data being analyzed. This is done to circumvent circularity errors described by Vul *et al*. (2009)[217] and others[218]. This can be achieved using localizer tasks however given the aforementioned benefits to ALE (i.e. number of participants etc. see section 1.10.1) as well as the variability associated with the hand motor cortex[219], this analysis method is chosen to develop ROIs. Understanding the supraspinal mechanisms influencing decreased motor drive and during the recovery period after a fatiguing handgrip trial will

enable us to gain a greater understanding of how muscle fatigue affects the brain. Thus, to address the purpose of this thesis the following research questions have been highlighted:

1.11.2 Research questions:

Chapter Two - How does the brain control handgrip?

If we are to fully understand the supraspinal mechanisms behind handgrip then it is logical to examine the differences between the fundamental type and pattern of grip. Although the differences between grip type and pattern have been investigated[35,36], the regions that differentially regulate grip type and pattern remain equivocal. Thus, the primary focus of Chapter two is to examine the similarities and differences between grip type and pattern using ALE analyses. Further, a major component of this thesis is directed at examining the supraspinal mechanisms of handgrip fatigue and thus an ALE analysis of the brain activations associated with handgrip will provide important regions of interest to examine fatigue.

Chapter three - How does MPH affect force output, brain activation, and effective connectivity during a submaximal fatiguing handgrip task?

MPH has been shown to increase force production during exercise[1]. A central fatigue theory proposes that motor drive is limited to maintain homeostasis. Recently the IC, which is a brain region critical for interoception of disturbed homeostasis[220], was shown to be a important structure for the decision to terminate exercise (i.e. task failure)[2] during a submaximal fatiguing handgrip task. The IC's proposed role in the limitation of motor drive via inhibition to the motor cortices[116] suggests that the IC could be a supraspinal substrate for the limitation of force output upstream of the motor cortex. Given that force output is increased with MPH administration then it is possible that this relationship could be modified by MPH. On the other hand, MPH increases dopaminergic transmission and may influence the mesocorticolimbic pathway to increase force

production via increased willingness to exert more force. Thus, we aim to determine 1) whether MPH will improve mean trial force and 2) alter brain activation and effective connectivity during a muscle fatiguing handgrip and/or in the moments prior to task failure. We specifically investigate effective connectivity between the IC and motor cortices, as well as the facilitation network proposed by Tanaka and Watanabe (2012)[174].

Chapter Four - How does a fatiguing handgrip task and MPH interact to influence functional connectivity in the recovery period *after* exercise?

Previous research indicates that the brain continues to be influenced during the recovery period after exercise has ceased[124] (e.g. interhemispheric M1 disruption[221]) and that tasks may influence subsequent resting state brain activity[222]. Task-related networks have also been shown to persist into subsequent resting state periods[222]. Indeed, muscle fatigue is a lasting disturbed homeostatic state characterized by a temporary inability to produce or maintain force output[10]. Thus, we sought to investigate brain functional connectivity changes in the recovery period after a fatiguing handgrip exercise. We aim to determine if brain connectivity observed during the task persist into the recovery period after exercise. Further, we investigate whether performing a fatiguing handgrip task will disturb functional connectivity in the period after exercise and whether this will occur to a greater extent after performing handgrip with MPH.

1.11.3 Overview of experimental chapters:

To address the question related to Chapter two, I performed an ALE meta-anlysis of handgrip. Then to address the question related to Chapter three and four, I performed two studies in parallel on the same participants to address the effect of MPH and handgrip muscle fatigue on brain activation and connectivity. In a double blind counter balanced design participants ingested placebo or MPH and subsequently performed three scans 1) pre-task resting state scan (green rectangle) 2) task scan during a fatiguing handgrip exercise (red rectangle) and 3) post-task resting state scan (red gradient rectangle).

Chapter three examined the task-related data *during* muscle fatiguing handgrip task and Chapter four examined the resting state data before and *after* the task.

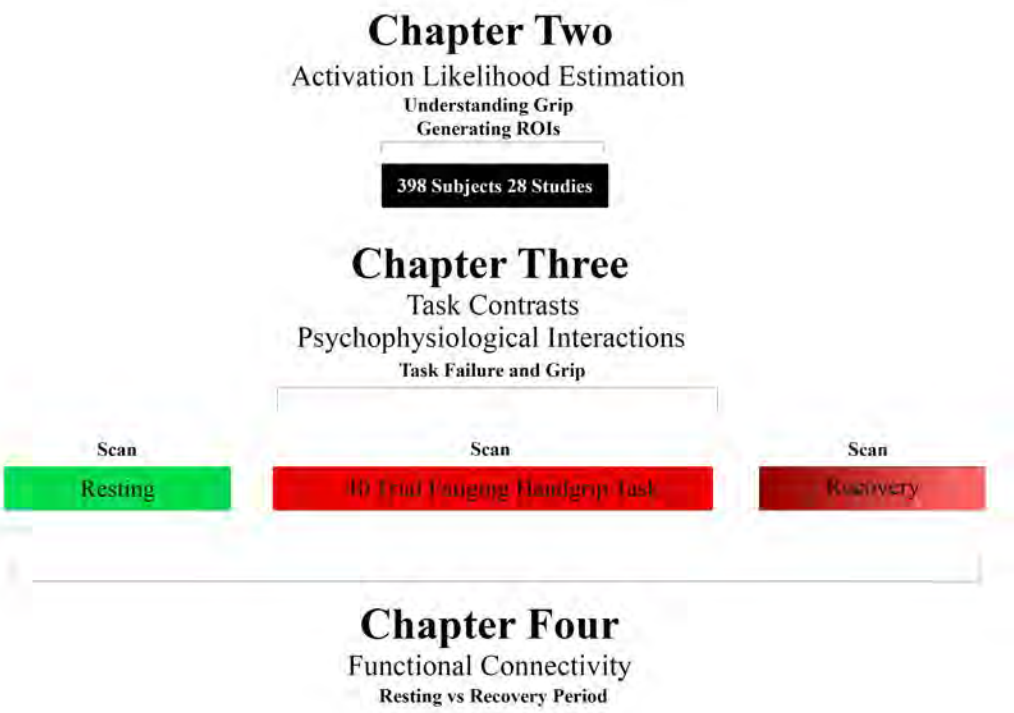

Figure 6. Overview of experimental chapters and data collection.

Chapter Two

Understanding the regions that regulate handgrip; what are the similarities and differences between fundamental handgrip type and pattern

2.1 Abstract

Handgrip is a ubiquitous human movement that was critical in our evolution. However, the differences in brain activity between grip type (i.e. power or precision) and pattern (i.e. dynamic or static) are not fully understood. In order to address this, we performed ALE analysis between grip type and grip pattern using fMRI data. ALE provides a probabilistic summary of the BOLD response in hundreds of participants, which is often beyond the scope of a single fMRI experiment. We collected data from 28 functional magnetic resonance data sets, which included a total of 398 male and female participants. Using ALE, we analyzed the BOLD response during power, precision, static and dynamic grip in a range of force and age in right handed healthy individuals without physical impairment, cardiovascular, or neurological dysfunction using a variety of grip tools, feedback, and experimental training. Power grip generates unique activation in the postcentral gyrus (area 1 and 3b) and precision grip generates unique activation in the supplementary motor area (SMA, area 6) and precentral gyrus (area 4a). Dynamic handgrip generates unique activation in the precentral gyrus (area 4p) and SMA (area 6) and of particular interest, both dynamic and static grip share activation in the area 2 of the postcentral gyrus, an area implicated in the evolution of human handgrip. According to effect size analysis, precision and dynamic grip generates stronger activity than power and static, respectively. This chapter demonstrates specific differences between grip type and pattern. However, there was a large degree of overlap in the pre and postcentral gyrus, SMA and areas of the frontal-parietal-cerebellar network, which indicates that other mechanisms are potentially involved in regulating handgrip. Further, this chapter provides empirically based regions of interest that will be used to study muscle fatigue during a fatiguing handgrip task performed in the power grip position.

2.2 Introduction

In Chapter one, I explained that human beings are unique in their ability to grip objects using four fingers and an opposable thumb. Early in human evolution, *Homo habilis* (taken from Latin to mean 'able handyman')[3] distinguished itself from other early hominids by its ability to use its hands with two advantageous grips: the power and precision grip[4,5]. The power grip (Figure 1A) has been extensively studied[4,31,36,40,64,223-226] and is thought to have been selected for aggressive actions such as clubbing[5]. The precision grip[4,36-38,227,228](Figure 1B) is used for actions requiring accuracy and was selected for actions such as spear throwing[4,5], tool manufacturing[6] and tool use[5,7]. These grips can be applied in either a dynamic or static pattern[7]. Dynamic handgrip is a series of intermittent or rhythmic forces, where as static is a fixed force. Despite the fundamental role of handgrip in human evolution[4,5], a consensus of the similarities and differences between them remains elusive. The brain mechanisms involved in hand movement have been recently reviewed[229],[229,230] but a meta-analysis of the brain's BOLD sinal associated with the grip type or pattern, using ALE, a method of meta-analysis for fMRI, has not been performed. fMRI measures the alteration of the magnetic field caused by an imbalance between oxy- and deoxyhaemoglobin[231] and the BOLD signal is thought to be a proxy for brain activity[231].

Previous research suggests that grip type[31] and pattern[228,232] have differing brain activity. Indeed, power and precision grip are physiologically and anatomically different[7]; there are grip specific bone and muscular adaptations for each[6], both thought to be developed near the origin of hominid lineage[5]. The power grip requires a much larger proportion of extrinsic muscles, where as the precision grip relies more on intrinsic muscles[4,19]. Further, the application of these grips are primarily for force and precision, respectively, and thus the muscle volume, force and sensory feedback generated during power grip is greater than precision grip[19]; after all how often does one precision grip a sledge hammer or power grip a dart. On the other hand, dynamic grip involves the repetitive recruitment and deactivation of opposing muscle groups, where as static grip is the holding of a

sustained force (i.e. isometric contraction). Thus, brain activation should greatly differ between grip pattern.

Currently, the relationship between grip type or pattern and brain activation is equivocal. Brain activation during power and precision grip is comparable but only at lower forces[31]; at greater force power grip produces greater brain activation[32-34]. Further, precision is thought to generate more ipsilateral brain activity in the premotor and parietal cortices[36]. On the other hand, dynamic forces produce greater activation than during static force but this trend is region[40]and movement[42] specific.

The ALE meta-analysis presented here analyzes the BOLD signal for handgrip type and pattern. Such an analysis has not been performed and an ALE meta-analysis will provide a description of the brain regions involved in grip, which can be subsequently used as empirically derived *apriori* ROIs for further analysis in this thesis. The purposes of this chapter are: 1) to elucidate the similarities and differences that exist between grip type (power vs precision) and grip pattern (static vs dynamic). 2) to determine which grip type and pattern generates stronger activations and 3) to provide empirically based ROIs to be implemented in Chapter three and four of this thesis. In doing so we hope to to give a comprehensive illustration of the brain areas associated with a fundamental and evolutionary important human movement.

2.3 Methods

2.3.1 Activation likelihood analysis (ALE)

A voxel can be defined as a unit of volume specified within a coordinate system to indicate spatial location in the brain. In fMRI imaging, voxels are assigned a coordinate to indicate location of activation. An ALE voxel represents a brain coordinate that is consistently active over *n* number of studies. ALE is used to compile peak activation coordinates from multiple studies that have examined a similar question using varying experimental design. ALE analysis attempts to form a cluster of activation illustrating a

three-dimensional probability distribution of activation and provides a probabilistic summary of the BOLD response in hundreds of participants, which is otherwise difficult to achieve in a single fMRI experiment. ALE is a particularly useful method for three reasons: (1) The number of participants that contribute ALE data can be considerably larger than a single fMRI study (2) it reveals brain areas that are consistently active between studies, which through common activation demonstrates reliability and (3) it does so with statistical measure, which is particularly useful given the inter-participant, -scanner, and -experiment variability typical of a single fMRI study[209]. ALE studies assume a null hypothesis that brain activation occurs randomly and computes the probabilistic distribution of activation in a region. A more detailed description of ALE[209] and other neuroimaging meta-analysis techniques, such as kernel density analysis and signed differential mapping, can be found in Radua *et al*. (2012)[233].

2.3.2 PRISMA

We used Preferred Reporting Items for Systematic Reviews and Meta-Analyses (PRISMA) framework[234] to collect and report our meta-analysis.

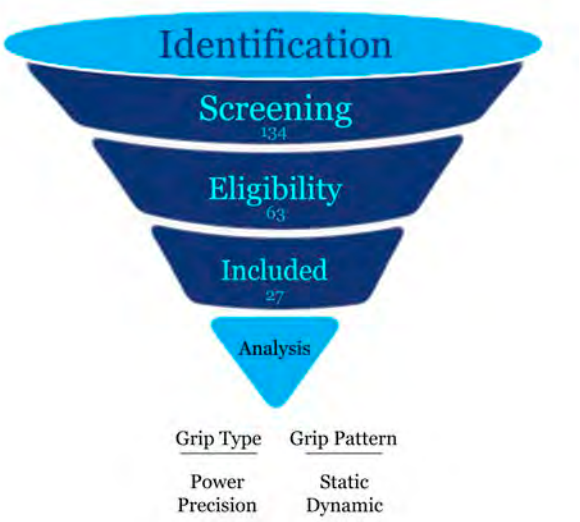

Figure 7. The Preferred Reporting Items for Systematic Reviews and Meta-Analyses (PRISMA) framework. We performed our meta-analysis according to PRISMA. Various combinations of Handgrip, MVC, MRI, fMRI, hand grip search criteria were searched in PubMed and 134 results were subsequently identified, screened, determined to be eligible and included for analysis. Data from 398 participants within 28 data sets were analyzed.

2.3.2.1 Identification

134 distinct search results were identified using the following terms: Handgrip fMRI, Handgrip MRI, Handgrip BOLD, "hand grip" fMRI, "hand grip" MRI, "hand grip" BOLD, MVC fMRI, MVC MRI, MVC BOLD, grip force fMRI, grip force MRI and grip force BOLD. Both “maximal voluntary contraction” and “MVC” were used and precision and power grip were used in place of handgrip. This search criteria was last performed on November 12th, 2013.

2.3.2.2 Screening

Papers were excluded that investigated other modalities (left hand, finger and wrist flexion, etc., n = 46 for precision), non-brain fMRI studies (skeletal, cardiac, eye etc., n = 40,) case studies (n=6) or clinical studies (multiple sclerosis, stroke, lesions etc., n=65) not containing healthy controls, non-BOLD fMRI or other imaging modalities (diffusion tensor imaging or positron emission tomography, n=22). Papers were also excluded if they were not written in English (n=4) or unrelated to handgrip in the fMRI (n=68). It often occurred that papers were excluded on more than one criterion.

2.3.2.3 Eligibility

Thirty-two power and 31 precision papers remained after screening and were not eligible when: (1) authors did not perform their analysis on a voxel by voxel basis (e.g. using percent signal change, n=21) (2) regression analysis was performed with another variable other than age and force (e.g. effect of muscle ischemia, n=2) (3) when left and right handed grip were performed simultaneously (n=1) and (4) in any of the above cases when we were not able to make contact with authors to request data.

2.3.2.4 Included

Thirteen papers (Table 1) examining right hand power grip and 15 papers (Table 2) examining right hand precision grip in healthy participants, ages 10-80 years were included in the meta-analysis. These studies employed dynamic (n=10), static (n=15), or both patterns (n=3) of grip. Keisker *et al*. (2009)[236] and Keisker *et al*. (2010)[40] used the same fourteen participants in two distinct studies. We used whole brain data in male and female participants, except for one ROI data set[237]. Coordinates that were reported as a regression to force[238], or age[239], were included in the analysis.

2.3.3 Co-ordinate conversion and GingerALE

Activated coordinates were recorded in a spreadsheet and subsequently converted into a text file. Any coordinate provided in Montreal Neurological Institute (MNI) standard space were converted to Talairach space using GingerALE's (Version 2.3 www.brainmap.org) convert foci tool; MNI standard space differs from Talairach space[235] and this step was performed to ensure consistency between foci. The text file was then formatted according to the user manual and analyzed using the import tool on GingerALE's graphic user interface. ALE images were generated and visualized on the Talairach brain "colin.nii" (downloaded here: http://www.brainmap.org/ale/colin1.1.nii), using Mango (Jack Lancaster, Michael Martinez: http://ric.uthscsa.edu/mango). A cluster-level inference threshold method was used with $p<0.05$ at 1000 permutations. Each image is thresholded with a minimum cluster threshold that includes clusters composed only of coordinates with a significant ALE statistic[209]. Mask size was set as "more conservative (smaller)" with dimensions 80 x 96 x 70mm. The cluster forming details were as follows: full width half maximum minimum value = 8.696mm, median value = 9.501mm, and maximum value = 11.373, cluster-forming method = uncorrected p value, cluster-forming value = 0.0010.

2.3.4 Analysis

This chapter compiles the BOLD response during voluntary grip in a range of force, age, grip type (power and precision) and pattern of grip (dynamic and static) in right handed healthy individuals (males and females without physical impairment, cardiovascular or neurological dysfunction) using a variety of grip tools, force feedback (visual or tactile) and experimental training (Table 1, Table 2). A description of these variables can be seen in section 2.3.7. Coordinates within a single study that utilized power and precision[31,36] or dynamic and static[228,236] were not used if reported activations combined modality, as activation related to this is potentially different. This chapter attempts to compare grip type and pattern and this is best selected separately and then computed in GingerALE. Coordinates generated from brain activity associated with other upper extremity movements such as finger[242] and wrist[226] flexion were excluded to maintain the purposes of this meta-analysis (see section 2.2.).

2.3.5 Types of activation likelihood estimation images

In order to determine the brain regions associated with grip type and pattern we first generated ALE images for grip type and grip pattern. Secondly, we performed conjunction and subtraction analysis between these images.

A conjunction analysis is performed from two ALE images and isolates commonly active regions, where as a subtraction analysis is performed from two ALE images and isolates unique activations. Thirdly, we generated a supplementary ALE image of all studies involved in a supplementary analysis. Given that we had four conditions from which to analyze we performed an ALE image for each type and pattern, a conjunction between each type and pattern, two subtractions per type and pattern and one ALE combining all studies for a total of 11 potential images.

2.3.6 Analysis of effect size

After performing ALE analysis we wanted to determine the strength of activation between grip type and grip pattern; ALE is suitable for determining the location of converging foci between experiments but not the strength of activation. To address this, we calculated the effect size per voxel from the original data sets and then the mean effect size for each condition (i.e grip type and pattern). We calculated Cohen's d from *z* and *t* statistics that were reported with activated coordinates using $2t/\sqrt{df}$ and $2z\sqrt{n}$, respectively. Knowing that previous work has shown that the force-activation relationship is linear in the SMC[32-34] we sought to normalize the strength of activation in this region by mean % MVC. In order to do this we divided the mean effect size per condition (i.e. grip type or pattern) by the mean % MVC employed in the studies, which were 35.33±28.27, 12.68±11.44, 23.08±19.80 and 30.22±26.89 (SD) % MVC for power, precision, dynamic and static, respectively. We also performed effect size analysis between grip type and pattern in the ipsilateral cerebellum as Keisker *et al.* (2010) demonstrated that ipisilateral cerebellum generated stronger activations during dynamic than static[40] (see 2.4.2). While this these steps are not typically included in an ALE analysis, it may help elucidate which type and pattern generates stronger brain activation.

2.3.7 Variables considered

fMRI has been used in a plethora of research designs to reveal the effect of type [36,229] and pattern of grip[40], age[39,64,225], force[33,64,237] handedness[238] and disease[39,239,240]. In our analysis we considered how these variables should be included in our ALE and are described next.

2.3.7.1 Voluntary force and age

Voluntary force is measured as either absolute force in Newton (N), (where $N = Kg \cdot m/s^2$) or a percentage of a participant's maximal ability (% MVC). This study excludes brain

activation data from involuntary handgrip, such as those produced by electromuscular or transcranial magnetic stimulation. Two of the power grip studies[39] included some participants who were greater than 60 years of age. Nearing this age the strength of activation during handgrip is different than that of younger participants[64]. Given that the study wasn't a homogeneously aged population, that the mean ages of these studies were below 50 years and that aged participant's data represents a small fraction of the total sample size it will provide little influence on the results. Excluding the entire data set would reduce statistical power and consequently we maintained the use of this data.

2.3.7.2 Right handed healthy individuals

This study included right handed healthy males and females, except for 1 of the 26 participants in Ward's 2003 study [39] who performed the task with their dominant left hand. We included this data assuming that 1 of 238 participants would not significantly impact the outcome of our analysis. Excluding the entire data set would reduce statistical power and consequently, we maintained the use of Ward's data. Sclocco *et al*. (2012)[224] used alternating right and left handed grips in right handed participants. To resolve this we contacted the authors directly to obtain only those coordinates during right handgrips.

2.3.7.3 Pattern of grip

Researchers typically examine handgrip movement in a dynamic or static grip pattern. Dynamic handgrip is a series of intermittent or rhythmic grips typically lasting 0 - 3.5 seconds where as static handgrip is a fixed grip lasting greater than 3.5 seconds. For example Keisker *et al*. (2010)[40] used 2 and 21 seconds for their dynamic and static

Table 1. Gender, reported participant statistics, force, grip pattern, tool, study design and type of feedback for studies included for power grip.

a. Participants were asked to grip lightly at a force of 2Hz and through personal correspondence authors indicated that although unspecified in the publication that participants were gripping at roughly 10% of their maximum.

Study	Participants	Reported Statistics	Force (%MVC)	Grip	Tool	Analysis	Force Feedback
Goswami *et al.* 2011[226]	12 (8F)	25±3 (range)	35%	Static	Dynamometer	Block	External: visual
Keisker *et al.* 2009[249]	14 (7F)	21-33 (range)	10, 20 and 30%	Static	Dynamometer	Block	External: visual
Keisker *et al.* 2010[40]	14 (7F)	21-33 (range)	20%	Static	Dynamometer	Block	External: visual
Schmidt *et al.* 2009[223]	20 (10F)	21±1 (range)	100%	Static	Plastic cylinders surrounding compressed air tube	Block	External: visual
Ehrsson *et al.* 2000[36]	5M	21-27 (range)	4.8%	Dynamic	Plastic cylindrical tube	Block	External: vibrotactile cue
Ward *et al.* 2003[39]	26 (9F)	M= 50.2, 27±80, F= 44.7, 26±66 (mean, range)	10, 20, 40 and 60%	Static	Molded plastic with force transducer	Block	External: visual
Hilty *et al.* 2010[2]	15M	26.4±4.5 (mean±SD)	70%	Static	Dynamometer	Block	External: visual
Kurniawan *et al.* 2010[241]	18 (5F)	27±3 (mean±SD)	40 and 85%	Static	Cylinders compressed air	Event	External: visual
Talelli *et al.* 2008[251]	27 (9F)	19-78 years, 42.2 ±19.8 years (range, mean±SD)	15.8-54.9%	Dynamic	Manipulandum	Block	External: visual
Halder *et al.* 2006[252]	Adult:17 (10F), Adolescent: 17 (10F), Children: 17 (7F)	Adult= 25±3 years Adolescent=16±0.5 Children=10±0.5 (mean±SD)	20, 40 and 75%	Dynamic	Sphygmomanometer rubber bulb	Block	External: visual
Wong *et al.* 2007[238]	17 (9F)	25±4 (mean±SD)	35%	Static	Inflated rubber bladder	Block	External: visual
Kuhtz-Buschbeck *et al.* 2008[31]	14 (7F)	26±5, 21-38 (mean ±SD, range)	1.15-7.36%	Dynamic	Non-metallic force transducers	Block	External: visual/Internal: proprioception
Sclocco *et al.* 2012[224]	5 (2F)	39.2 ± 16.3 (mean±SD)	~10%[a]	Static	Rubber ball	Block	Internal: proprioception

Table 2. Gender, reported participant statistics, force, grip pattern, tool, study design and type of feedback for studies included for precision grip.

a We calculated a percentage value from typical MVCs associated with precision grip (Ehrsson *et al.* (2000)[36]). Percentage values were not reported in these studies.**b** Authors could not be reached for the grip force generated. Our meta-analysis included activations from both high and low grip force.

Study	Participants	Reported Statistics	Force (%MVC)	Grip	Tool	Analysis	Force Feedback
Sulzer *et al*. 2011[227]	5 (1F)	27-32 (range)	10,20,30%	Dynamic	MR-compatible force sensor	Event	External: visual
Ehrsson *et al*. 2001[38]	6M	21-28 (range)	40%	Dynamic	Nonmagnetic flat parallel transducers	Event	External: vibrotactile cue
Kuhtz-Buschbeck *et al.* 2001[37]	8M	22-23 (range) 28.5 (mean)	1.7-5.5%	Static	Dual flat grip force transducers	Block	Internal: proprioception
Vaillancourt *et al.* 2003[242]	10 (7F)	21-35 (range)	15%	Static	Custom designed pinch tool	Block	External: visual or Internal: proprioception
Galléa *et al.* 2005[243]	11(3F)	Not reported	6.3 ±2.5% (5 ± 2N[a])	Dynamic	Circular grip tool	Block	External: visual
Ehrsson et al. 2007[244]	6M	20-32 (range)	2.5±1.1% (2.0 ± 0.95N[a])	Static	Dual flat grip force transducers	Block	Internal: proprioception
Kuhtz-Buschbeck *et al.* 2008[31]	14 (7F)	26±5, 21-38 (mean,range)	1.28-9.77%	Dynamic	Non-metallic force transducers	Block	External: visual or Internal: proprioception
Spraker *et al.* 2009[245]	12 (7F)	19-34	15%	Static	Polycarbonate apparatus	Block	External: visual
Mosier *et al.* 2011[236]	16 (6F)	22-54, 32 (mean)	36.2-42.5% (29-34N) [a]	Dynamic and Static	MR-compatible springs	Event	Internal: proprioception
Neely *et al.* 2013[228]	17 (8F)	21-33 (range)	15%	Dynamic and Static	Precision grip apparatus	Block	External: visual
Holmström *et al.* 2011[246]	16M	32 ± 4 years (mean ± SD)	High/Low (Unspecified)[b]	Dynamic	MR-compatible springs	Block	Internal: proprioception
Wasson *et al.* 2010[247]	11 (6F)	21-33 (range)	15%	Dynamic	Polycarbonate device	Block	External: visual
Spraker *et al.* 2012[259]	11 (6F)	20-37 (range)	5-80%	Static	Custom grip device	Block	External: visual
Galléa *et al.* 2008[248]	12 (7F)	26.7 ± 4.8 (mean ± SD)	6.25% (5N[a])	Static	Force transducer	Block	External: visual
Ehrsson *et al*. 2000[36]	5M	21-27 (range)	4.5%	Dynamic and Static	Nonmagnetic flat parallel transducers	Block	External: vibrotactile cue

paradigm, respectively. More simply, dynamic grips are short and frequent where as static is lasting and infrequent. Historically, the study of regularly timed dynamic limb movements (i.e the study of central pattern generators), such as walking, have been of great interest to scientists[249-252]. Although the studies used in this ALE included rhythmic contractions, which perhaps necessitate the use of central pattern generators our study was not *per se* designed to investigate them. Further, central pattern generators are thought to exert their control of movement largely from the spine [249]. Our study investigated results of both arhythmic and rhythmic grip patterns in dynamic and static handgrip and consequently our results do not distinguish between activations involving the potential existence of supra-spinal central pattern generators. Since the frequency of grips is not associated with different brain activity[232] we did not distinguish between the duration of rests in between the dynamic grips. The reasoning for these restrictions was to allow for sufficient statistical power and to maintain the purposes of the study.

2.3.7.4 Grip tool, feedback, and experimental training

The current analysis includes data regardless of the tool, feedback provided and experimental training. Handgrip studies employ various tools, either commercial or lab-made, and our study included a variety of designs (Table 1, Table 2. In fMRI studies, participants are typically instructed to squeeze at a predetermined force; often the grip paradigm is practiced during an experimental training session and participants are instructed prior to performing the grip task. It is often the case that participant instructions are not reported despite the value[235] for the interpretation and replication of brain imaging data. Handgrip force levels are often maintained in real time with the aid of visual or tactile feedback. Most of the studies used here employed external force feedback (e.g. visual or tactile), except for those that used a combination of both, or internal feedback generated from proprioceptive sensations learned during experimental training (Table 1, Table 2).

2.3.8 Atlas' used

We interpreted our results using the SPM Anatomy Toolbox 1.7, a probabilistic cytoarchitectonic atlas. The SPM Anatomy Toolbox is a probabilistic atlas used within MATLAB to locate brain regions for neuroimaging research as defined by cytoarchitecture structure[253]. This atlas was created to resolve the problematic use of macro-anatomical landmarks, which do not take into account the microscopical architectonic organization[254]. Further, this atlas accounts for the inherent variation that exists in human neuroanatomy and provides a probability of a co-ordinate being located in a particular area. The probability assigned to a co-ordinate describes the frequency that a co-ordinate occurred in a cytoarchitectonic area out of ten post-mortem brains. Previous work[255,256] has recommended that a probabilistic template be used when interpreting the location of activation and consequently we have used it here. It should be noted that the cytoarchitectonic atlas may have less optimal performance in areas such as the frontal and parietal lobes[253]. In Table 3 to Table 8, we indicate the probability of activation occurring in an area within the cytoarchitectonic atlas. We reported the cytoarchitectonic area with the highest frequency and included multiple areas when two or more areas were equally likely. Each cytoarchitectonic area occurs within a larger macroscopic feature and we have discussed our findings with references to these features. For example, area 4a is a cytoarchitectonic region within the anatomical feature precentral gryus. See respective references for a more detailed description of the following cytoarchitectonic areas: area 1[257], area 2[258], area 3[257], area 4[259] and area 6[260].

2.4 Results

2.4.1 ALE images

A total of 398 participants from 28 data sets were included in our ALE analysis. We generated single (Figure 8, Figure 9, Figure 12, Figure 13) conjunction (Figure 10, Figure 14) and subtraction (Figure 11, Figure 15) ALE contrasts for grip type and grip pattern. In addition we collapsed all groups for an ALE image including all studies (see section,

Figure 17). Cluster coordinate size, extrema, and locations comparing grip type and pattern can be seen in Tables 3-8. Images were interpreted according to extrema and location. Extrema represent the peak probability of converging activation between studies[209] and we reported the area with the highest frequency in a given cytoarchitectonic area. In the case where two areas were equally likely we reported both areas. ALE results per condition are listed below:

2.4.1.1 Power grip results

For the power grip ALE (Table 3, Figure 8) we found cluster extrema in the L. precentral gyrus (area 4a), R. cerebellum (lobule V), L. SMA (area 6), L. middle cingulate cortex (area 6), R. supramarginal gyrus (hIP2 and IPC), L. rolandic operculum and L. inferior frontal gyrus (p. opercularis, area 44), L. cerebellum (lobule IV), L. precentral gyrus (area 44) and R. cerebellar vermis (lobule VI).

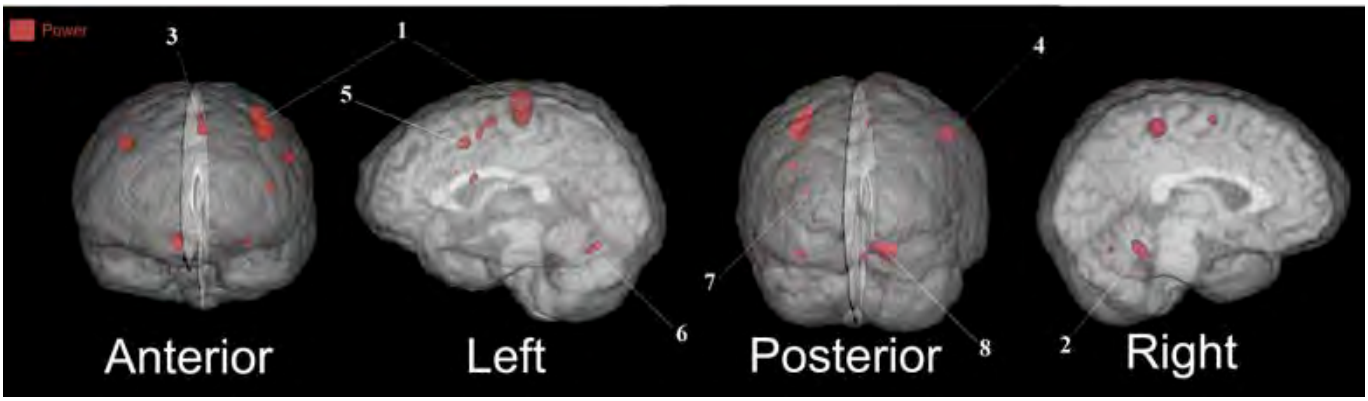

Figure 8. ALE showing the BOLD response to power grip in the (1) L. precentral gyrus (area 4a), (2) R. cerebellum (lobule V), (3) L. SMA (area 6) and L. middle cingulate cortex (area 6) and (4) R. supramarginal gyrus (hIP2 and IPC), (5) L. rolandic operculum and L. inferior frontal gyrus (p. opercularis, area 44), (6) L. cerebellum (lobule IV), (7) L. precentral gyrus (area 44) and (8) R. cerebellar vermis (lobule VI). Cluster details can be seen in Table 3. Cluster forming threshold and cluster-level inference used were uncorrected $p<0.001$ and $p<0.05$, respectively. Anterior and posterior images are rotated 5 degrees clockwise. Abbreviations: ALE – activation likelihood estimation, BOLD – blood oxygen level dependent signal, hIP1, 2 - intraparietal sulcus 1, 2, IPC - intraparietal cortex.

Table 3. Activation co-ordinates generated from power grip. ALE cluster coordinates were assigned an area using the SPM Anatomy Toolbox 1.7 and probability indicated in brackets (column 3). We reported the highest probable area and multiple areas were listed when the assigned probability was equal for two or more areas. Areas were assigned based on extrema coordinates ± 5mm and multiple extrema were reported within a cluster when the cluster spanned over more than one brain area (cluster #3,5). Clusters are displayed in Figure 8. Abbreviations: ALE – activation likelihood estimation analysis, SMA - supplementary motor area, hIP1, 2 - intraparietal sulcus 1, 2, IFG - inferior frontal gyrus IPC - intraparietal cortex.

Cluster # / Figure	**Cluster Size(s) (mm^3)**	**Cytoarchitectonic Area and Probability**	**Cytoarchitectonic Label**	**Coordinate Extrema (x,y,z)**	**Cluster Location (x,y,z to x,y,z)**
#1 Figure 8	3792	L. Area 4a (40%)	L. Precentral Gyrus	-37,-25,56	-50,-32,42 to -28,-18,66
#2 Figure 8	1712	R. Lobule V (56%)	R. Cerebellum	15,-49,-20	4,-58,-28 to 24,-42,-14
#3 Figure 8	1560	L. Area 6 (70%)	L. SMA	-3,-2 ,51	-10,-10,42 to 4,4,60
-	-	L. Area 6 (40%)	L. Middle Cingulate Cortex	-6,0,44	-
#4 Figure 8	1184	R. hIP2 (30%) R. IPC (30%)	R. SupraMarginal Gyrus	48,-38,44	42,-42,38 to 54,-32,50
#5 Figure 8	976	L. Rolandic Operculum (N/A)	L.Rolandic Operculum	-40,-2,14	-60,-6,8 to -38,10,20
-	-	L. Area 44 (50%)	L.IFG(p. Opercularis)	-56,6,14	-
#6 Figure 8	792	L. Lobule VI (44%)	L. Cerebellum	-30,-68,-20	-34,-72,-26 to -24,-58,-16
#7 Figure 8	744	L. Area 44 (20%)	L. Precentral Gyrus	-50,2,30	-56,-2,24 to -46,8,34
#8 Figure 8	368	R. Lobule VI (70%)	R. Cerebellar Vermis	6,-68,-22	42,-42,38 to 54,-32,50

2.4.1.2 Precision grip results

For the precision grip ALE (Table 4, Figure 9) we found cluster extrema in the L. SMA (area 6), L. precentral gyrus (area 6), L. postcentral gyrus (area 3b), R. cerebellum (lobule V), R. inferior frontal gyrus (p. opercularis, area 44), R. rolandic operculum (area 44), and R. precentral gyrus (area 44). L. precentral gyrus (area 6) and R. postcentral gyrus.

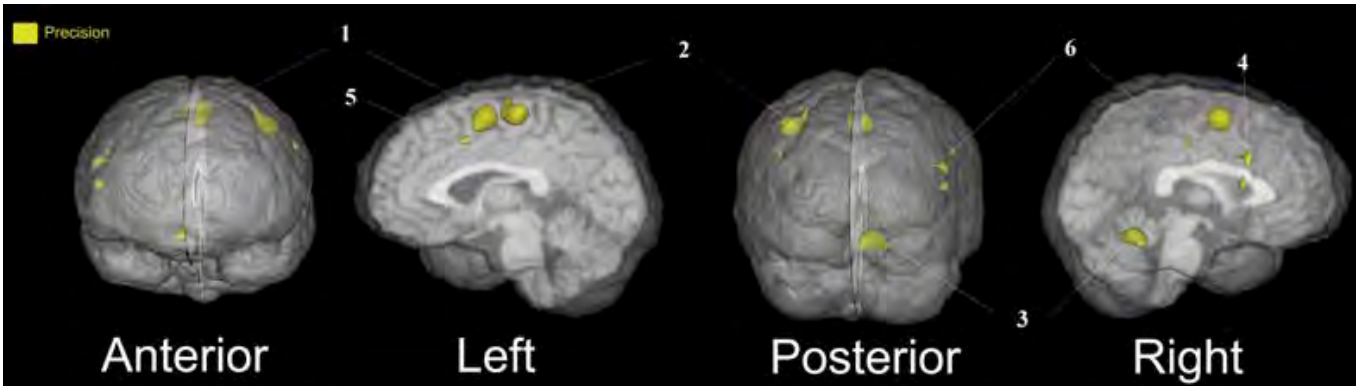

Figure 9. ALE showing the BOLD response to precision grip in the (1) L. SMA (area 6), (2) L. pre and postcentral gyrus (area 6 and 3b), (3) R. cerebellum (lobule V), (4) R. inferior frontal gyrus (p. opercularis, area 44), R. rolandic operculum (area 44) and R. precentral gyrus (area 44), (5) L. precentral gyrus (area 6) and (6) R. postcentral gyrus (IPC). Cluster details can be seen in Table 4. Cluster forming threshold and cluster-level inference used were $p<0.001$ and $p<0.05$, respectively. Anterior and posterior images are rotated 5 degrees clockwise. Abbreviations: ALE – activation likelihood estimation, BOLD – blood oxygen level dependent signal

2.4.1.3 Power and precision conjunction and contrasts

For the power + precision conjunction (Table 5, Figure 10) we found cluster extrema in the L. postcentral gyrus (area 3b) and L. precentral gyrus (area 4a), L. SMA (area 6), and L. middle cingulate cortex (area 6), R. cerebellum (lobule V), L. precentral gyrus (area 44), and R. cerebellar vermis (lobule VI). For the precision - power contrast (Table 5, Figure 11, brown clusters) we found cluster extrema in the R. and L. SMA (area 6), L. precentral gyrus (area 4a), and L. precentral gyrus (area 6). For the power - precision contrast (Table 5, Figure 11, yellow clusters) we found cluster extrema in the L. postcentral gyrus (Area 1, 3b) and R. supramarginal gyrus (hIP2).

Table 4. Activation co-ordinates generated from precision grip. ALE cluster coordinates were assigned an area using the SPM Anatomy Toolbox 1.7 and probability indicated in brackets (column 3). Areas were assigned based on extrema coordinates ± 5mm and multiple extrema were reported within a cluster when the cluster spanned over more than one brain area (cluster #2, 4). Clusters are displayed in Figure 9. Abbreviations: ALE – activation likelihood estimation, SMA - supplementary motor area, IFG - inferior frontal gyrus, IPC - intraparietal cortex.

Cluster # / Figure	**Cluster Size(s) (mm^3)**	**Cytoarchitectonic Area and Probability**	**Cytoarchitectonic Label**	**Coordinate Extrema (x,y,z)**	**Cluster Location (x,y,z to x,y,z)**
#1 Figure 9	3832	L. Area 6 (70%)	L. SMA	0,-4,54	-10,-14,44 to 8,4,60
#2 Figure 9	2976	L. Area 6 (60%)	L. Precentral Gyrus	-32,-20,60	-50,-30,42 to -30,-14,62
	-	L. Area 3b (70%)	L. Postcentral Gyrus	-42,-24,48	-
#3 Figure 9	2440	R. Lobule V (71%)	R. Cerebellum	8,-54,-18	0,-64,-24 to 22,-46,-12
#4 Figure 9	1496	R. Area 44 (40%)	R. IFG (p. Opercularis)	54,8,26	42,0,8 to 58,10,30
	-	R. Area 44 (30%)	R. Rolandic Operculum	54,4,12	-
-	-	R. Area 44 (20%)	R. Precentral Gyrus	46,2,26	-
#5 Figure 9	432	L. Area 6 (60%)	L. Precentral Gyrus	-56,2,34	-58,-2,30 to -52,6,38
#6 Figure 9	368	R. IPC (70%)	R. Postcentral Gyrus	56,-22,32	52,-26,28 to 60,-20,36

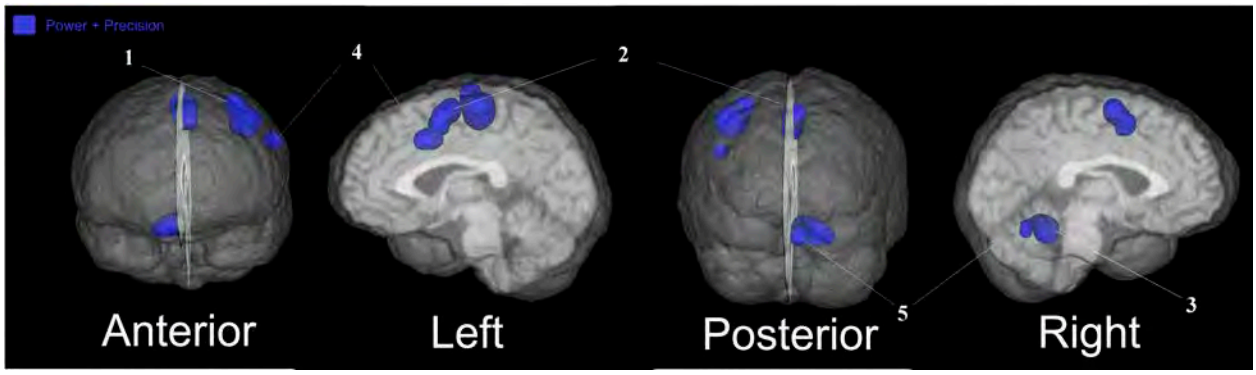

Figure 10. ALE showing the common activations between power and precision grip in the (1) L. post and precentral gyrus (area 3b and 4a), (2) L. SMA and L. middle cingulate cortex (area 6), (3) R. cerebellum (lobule V, VI), and (4) L. precentral gyrus (area 44). Cluster details can be seen in Table 5. Uncorrected $p<0.05$. Anterior and posterior images are rotated 5 degrees clockwise. Abbreviations: ALE – activation likelihood estimation, SMA – supplementary motor area

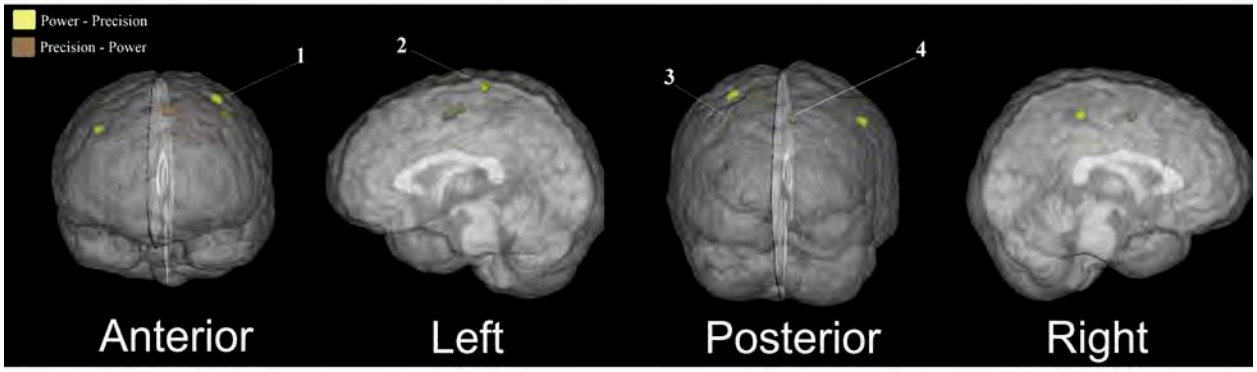

Figure 11. ALE showing the differences between grip type. For the power - precision subtraction (yellow) our analysis revealed activation in the (1) L. postcentral gyrus (Area 1 and 3b) and (2) R. supramarginal gyrus (hIP2). Cluster details can be seen in Table 5. For the precision - power subtraction (brown) our analysis revealed (3) L. precentral gyrus (area 4a and area 6) and (4) R. and L. SMA (area 6). Cluster details can be seen in Table 5. Uncorrected $p<0.05$. Anterior and posterior images are rotated 5 degrees clockwise. Abbreviations: ALE – activation likelihood estimation, SMA – supplementary motor area

Table 5. Activation co-ordinates generated from the conjunction of power + precision grip, power - precision grip and precision - power. ALE cluster coordinates were assigned an area using the SPM Anatomy Toolbox 1.7 and probability indicated in brackets (column 4). Areas were assigned based on extrema coordinates ± 5mm and multiple extrema were reported within a cluster when the cluster spanned over more than one brain area (e.g. power + precision cluster #1). Clusters are displayed in Figure 10 (blue) and Figure 11 (yellow and brown). Abbreviations: ALE – activation likelihood estimation, SMA - supplementary motor area, hIP2 - intraparietal sulcus 2.

Contrast	Cluster # / Figure	Cluster Size(s) (mm^3)	Cytoarchitectonic Area and Probability	Cytoarchitectonic Label	Coordinate Extrema (x,y,z)	Cluster Location (x,y,z to x,y,z)
Power + Precision	#1 Figure 10	1984	L. Area 3b (60%)	L. Postcentral Gyrus	-38,-24,50	-48,-30,42 to -30,-18,62
	-		L. Area 4a (50%)	L. Precentral Gyrus	-34,-20,58	-
	#2 Figure 10	1168	L. Area 6 (80%)	L. SMA	0,-8,56	-6,-10,44 to 4,4,60
	-		L. Area 6 (40%)	L. Middle Cingulate Cortex	-6,0,44	-
	#3 Figure 10	1096	R. Lobule V (56%)	R. Cerebellum	16,-50,-20	4,-58,-24 to 22,-46,-14
	#4 Figure 10	176	L. Area 44 (20%)	L. Precentral Gyrus	-52,2,32	-56,-2,30 to -52,6,34
	#5 Figure 10	40	R. Lobule VI (56%)	R. Cerebellar Vermis	6,-64,-22	4,-64,-22 to 6,-64,-18
Power - Precision	#1 Figure 11	430	L. Area 1 (30%) L. Area 3b (30%)	L. Postcentral Gyrus	-30,-32,64	-38,-32,58 to -28,-26,66
			L. Area 3b (50%)	L. Postcentral Gyrus	-34,-32,62	
	#2 Figure 11	432	R. hIP2 (30%)	R. SupraMarginal Gyrus	50,-34,40	44,-38,40 to 52,-32,46
Precision - Power	#3 Figure 11	1088	R. Area 6 (40%)	R. SMA	8,-4,48	-10,-14,4 to 8,0,56
	-	-	L. Area 6 (70%)	L. SMA	-6,-10,52	-
	#4 Figure 11	384	L. Area 4a (50%)	L. Precentral Gyrus	-42,-16,48	-
	-		L. Area 6 (30%)	L. Precentral Gyrus	-34,-14,50	-44,-18,44 to -32,-14,54

2.4.1.4 Static grip

For the static grip ALE (Table 6, Figure 12) we found cluster extrema in the L. postcentral gyrus (area 2), R. cerebellum (lobule V, VI), L. SMA (area 6), L. middle cingulate cortex (area 6), R. supramarginal gyrus (hIP2, IPC), R. inferior parietal lobule (hIP1, 2, 3), L. IC and L. rolandic operculum, R. rolandic operculum (area 44), and R. and L. thalamus (Th-prefrontal).

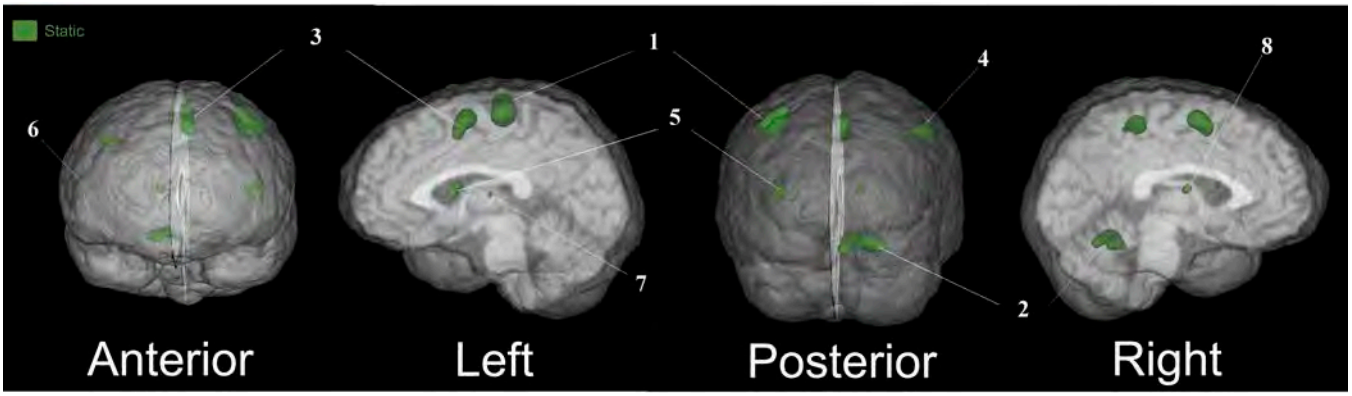

Figure 12. ALE showing the BOLD response to static grip in the (1) L. postcentral gyrus (area 2), (2) R. cerebellum (lobule V, VI). (3) L. SMA and L. middle cingulate cortex (area 6), (4) R. supramarginal gyrus (hIP2 and IPC) and R. inferior parietal lobule (hIP1, 2, 3), (5) L. IC and L. rolandic operculum, (6) R. rolandic operculum (area 44), and (7) L. and (8) R. thalamus (Th-prefrontal). Cluster details can be seen in Table 6. Cluster forming threshold and cluster-level inference used were $p<0.001$ and $p<0.05$, respectively. Anterior and posterior images are rotated 5 degrees clockwise. Abbreviations: ALE – activation likelihood estimation, BOLD – blood oxygen level dependent signal, SMA – supplementary motor area, IC – insula cortex.

2.4.1.5 Dynamic grip

For the dynamic grip ALE (Table 7, Figure 13) we found cluster extrema in the L. postcentral gyrus (area 3b), L. precentral gyrus (area 6), R. cerebellum (lobule V), L. SMA (area 6) and L. precentral gyrus (area 44).

Table 6. Activation co-ordinates generated from static grip. ALE cluster coordinates were assigned an area using the SPM Anatomy Toolbox 1.7 and probability indicated in brackets (column 3). Areas were assigned based on extrema coordinates ± 5mm and multiple extrema were reported within a cluster when the cluster spanned over more than one brain area (cluster #2, 3, 4, 5). Clusters are displayed in Figure 12 Abbreviations: ALE – activation likelihood estimation, SMA - supplementary motor area, hIP1, 2, 3 - intraparietal sulcus 1, 2, 3 IPC – intraparietal cortex – IC – Insula cortex

Cluster # / Figure	**Cluster Size(s) (mm^3)**	**Cytoarchitectonic Area and Probability**	**Cytoarchitectonic Label**	**Coordinate Extrema (x,y,z)**	**Cluster Location (x,y,z to x,y,z)**
#1 Figure 12	3816	L. Area 2 (40%)	L. Postcentral Gyrus	-40,-26,52	-52,-34,44 to -30,-18,64
#2 Figure 12	3560	R. Lobule V (82%)	R. Cerebellum	8,-56,-16	0,-70,-26 to 28,-42,-12
-		R. Lobule VI (84%)	R. Cerebellum	20,-52,-20	-
-		R. Lobule V (42%)	R. Cerebellar Vermis	4,-64,-20	-
#3 Figure 12	3464	L. Area 6 (70%)	L. SMA	-2,-4,56	-12,-12,40 to 6,6,62
		L. Area 6 (50%)	L. Middle Cingulate Cortex	-8,0,44	-
#4 Figure 12	1760	R. hIP2 (30%) R. IPC (30%)	R. SupraMarginal Gyrus	48,-38,44	32,-50,38 to 54,-32,50
		R. hIP1 (20%) R. hIP2 (20%) R. hIP3 (20%)	R. Inferior Parietal Lobule	36,-46,42	-
#5 Figure 12	1320	L. IC (N/A)	L. IC	-40,-2,12	-56,-6,4 to -36,4,16
		L. Area 44 (30%)	L. Rolandic Operculum	-52,2,14	-
#6 Figure 12	768	R. Rolandic Operculum (N/A)	R. Rolandic Operculum	50,2,12	36,0,10 to 58,6,18
#7 Figure 12	568	R. Th-Prefrontal (60%)	R. Thalamus	12,-10,12	8,-16,8 to 16,-8,16
#8 Figure 12	416	L. Th-Prefrontal (75%)	L. Thalamus	-12,-18,8	-16,-22,2 to -8,-14,12

2.4.1.6 Static and dynamic conjunction and contrasts

For the static + dynamic conjunction ALE (Table 8, Figure 14) we found cluster extrema in the L. postcentral gyrus (area 2, 3b) and L. precentral gyrus (area 4a), R. cerebellum (lobule V, VI), and L. SMA (area 6). For the dynamic - static contrast (Table 8, Figure 15) we found cluster extrema in the L. precentral gyrus (area 4p), L. SMA and L. middle cingulate cortex (area 6), L. precentral gyrus (area 6). For the static - dynamic contrast we did not find any ALE clusters.

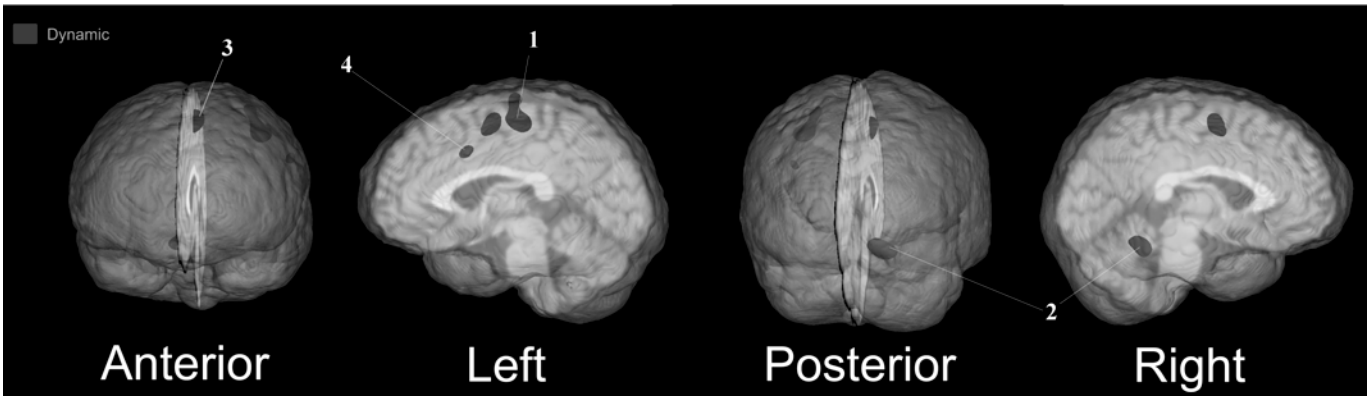

Figure 13. ALE showing the BOLD response to dynamic grip in the (1) L. post and precentral gyrus (area 3b and 6), (2) R. cerebellum (lobule V), (3) L. SMA (area 6) and (4) L. precentral gyrus (area 44). Cluster details can be seen in Table 7. Cluster forming threshold and cluster-level inference used were $p<0.001$ and $p<0.05$, respectively. Anterior and posterior images are rotated 5 degrees clockwise. Abbreviations: ALE – activation likelihood estimation, SMA – supplementary motor area

2.4.2 Effect size results

ALE measures the occurrence but not strength of activation between studies. In order to resolve this, we assessed the strength of activation using effect size. Our analysis indicated that precision and dynamic grip generated stronger whole brain activation than power and static, respectively (ANOVA, Bonferroni, $p<0.0001$ see Figure 16 A). To further investigate this we separated effect sizes by region and tested for effect size differences between grip type and pattern in the SMC and ipsilateral cerebellum[40]. Knowing that activity in the SMC is dependent on MVC[32-34] we sought to

perform effect size analysis in this region normalized by MVC (see section 2.3.6). Precision and dynamic grip demonstrated higher normalized effect sizes in the SMC than in the power and static grip (ANOVA, Bonferroni, $p<0.0001$, Figure 16B). Dynamic grip demonstrated higher effect sizes than static grip in the ipsilateral cerebellum (ANOVA, Bonferroni, $p<0.05$, Figure 16C) but not in grip type.

Table 7. Activation co-ordinates generated from dynamic grip. ALE cluster coordinates were assigned an area using the SPM Anatomy Toolbox 1.7 and probability indicated in brackets (column 3). Areas were assigned based on extrema coordinates ± 5mm and multiple extrema were reported within a cluster when the cluster spanned over more than one brain area (cluster #1). Clusters are displayed in Figure 13. Abbreviations: ALE – activation likelihood estimation, SMA – supplementary motor area

Cluster # / Figure	**Cluster Size(s) (mm^3)**	**Cytoarchitectonic Area and Probability**	**Cytoarchitectonic Label**	**Coordinate Extrema (x,y,z)**	**Cluster Location (x,y,z to x,y,z)**
#1 Figure 13	2832	L. Area 3b (80%)	L. Postcentral Gyrus	-40,-24,46	-48,-30,42 to -28,-14,66
	-	L. Area 6 (60%)	L. Precentral Gyrus	-32,-20,62	-
#2 Figure 13	2016	R. Lobule V (80%)	R. Cerebellum	12,-50,-20	4,-62,-26 to 22,-44,-14
#3 Figure 13	2000	L. Area 6 (80%)	L. SMA	0,-6,54	-8,-14,42 to 4,2,60
#4 Figure 13	648	L. Area 44 (20%)	L. Precentral Gyrus	-54,4,30	-58,-2,26 to -50,8,34

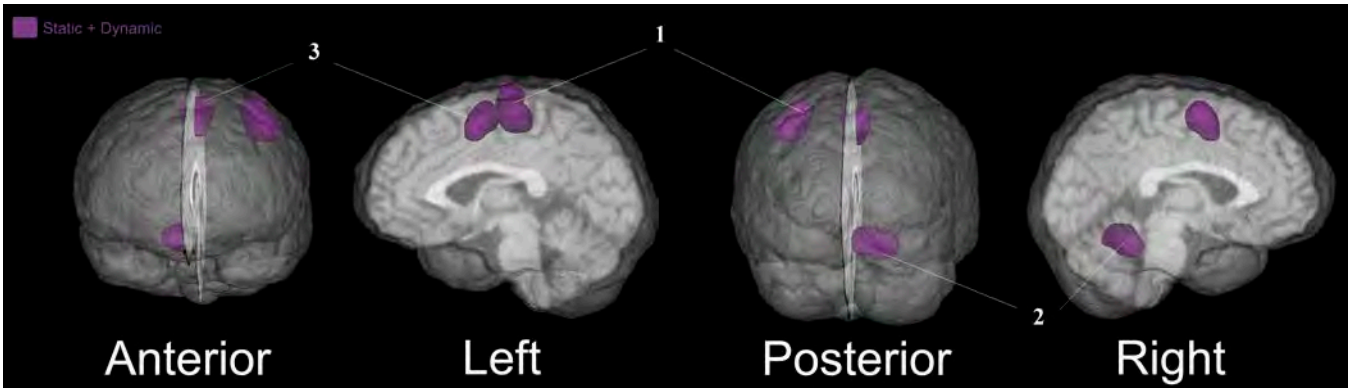

Figure 14. ALE showing the BOLD response to common activations between grip pattern in the (1) L. postcentral gyrus (area 2, 3b) and L. precentral gyrus (area 4a), (2) R. cerebellum (lobule V, VI), and (3) L. SMA (area 6). Cluster details can be seen in Table 8. Uncorrected $p<0.05$. Anterior and posterior images are rotated 5 degrees clockwise. Abbreviations: ALE – activation likelihood estimation, SMA – supplementary motor area

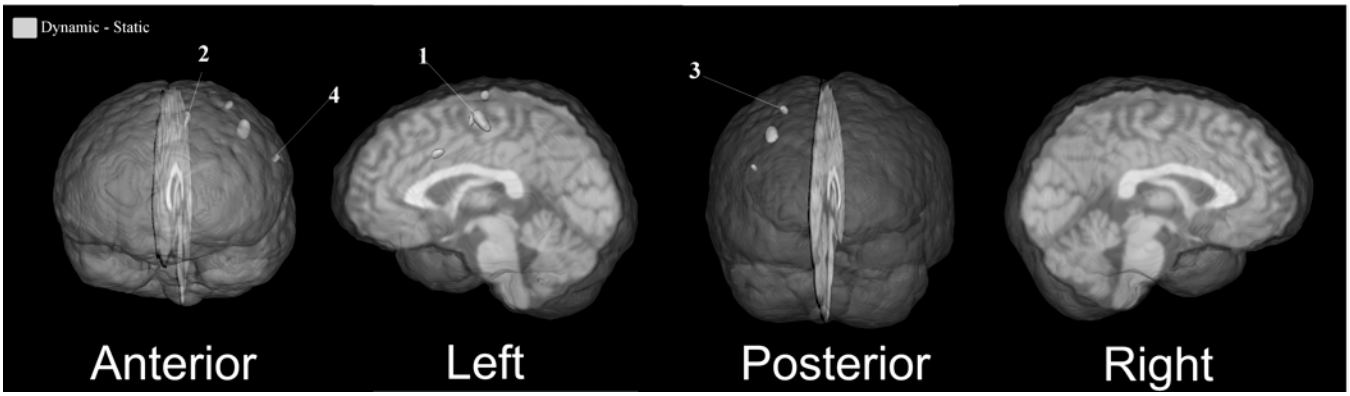

Figure 15. ALE showing differences between grip pattern. For the dynamic - static grip subtraction our analysis revealed activation in the (1) L. precentral gyrus (area 4p), (2) L. SMA and L. middle cingulate cortex (area 6), (3) L. precentral gyrus (area 6) and (4) L. precentral gyrus (area 6). Cluster details can be seen in Table 8. Cluster forming threshold and cluster-level inference used were $p<0.001$ and $p<0.05$, respectively. Anterior and posterior images are rotated 5 degrees clockwise. Abbreviations: ALE – activation likelihood estimation, SMA – supplementary motor area.

Table 8. Activation co-ordinates generated from the conjunction of static + dynamic grip and dynamic – static grip. No clusters were generated from the static - dynamic contrast. ALE cluster coordinates were assigned an area using the SPM Anatomy Toolbox 1.7 and probability indicated in brackets (column 4). Areas were assigned based on extrema coordinates ± 5mm and multiple extrema were reported within a cluster when the cluster spanned over more than one brain area (e.g. static + dynamic cluster #1). Clusters are displayed in Figure 9. and Figure 10. Abbreviations: SMA - supplementary motor area., ALE – activation likelihood estimation

Contrast	**Cluster # / Figure**	**Cluster Size(s) (mm^3)**	**Cytoarchitectonic Area and Probability**	**Cytoarchitectonic Label**	**Coordinate Extrema (x,y,z)**	**Cluster Location (x,y,z to x,y,z)**
Static + Dynamic	#1 Figure 14	1552	L. Area 2 (50%) L. Area 3b (50%)	L. Postcentral Gyrus	-40,-26,48	-48,-30,44 to -30,-18,62
			L. Area 4a (40%)	L. Precentral Gyrus	-34,-24,60	-
	#2 Figure 14	1384	R. Lobule V (82%)	R. Cerebellum	8,-54,-16	4,-62,-26 to 22,-44,-14
	-		R. Lobule VI (70%)	R. Cerebellum	18,-50,-20	-
	#3 Figure 14	1384	L. Area 6 (80%)	L. SMA	0,-6,54	-8,-12,44 to 4,2,60
Dynamic - Static	#1 Figure 15	680	L. Area 4p (60%)	L. Precentral Gyrus	-39,-18 ,47	-44,-26,42 to -32,-14,54
	#2 Figure 15	432	L. Area 6 (60%)	L. SMA	-8,-12,58	-8,-14,42 to 2,-4,60
	-	-	L. Area 6 (70%)	L. Middle Cingulate Cortex	-4,-10,46	-
	#3 Figure 15	288	L. Area 6 (90%)	L. Precentral Gyrus	-30,-20,66	-34,-24,58 to -28,-16,66
	#4 Figure 15	248	L. Area 6 (40%)	L. Precentral Gyrus	-58,2,28	-58,-2,26 to -54,8,32

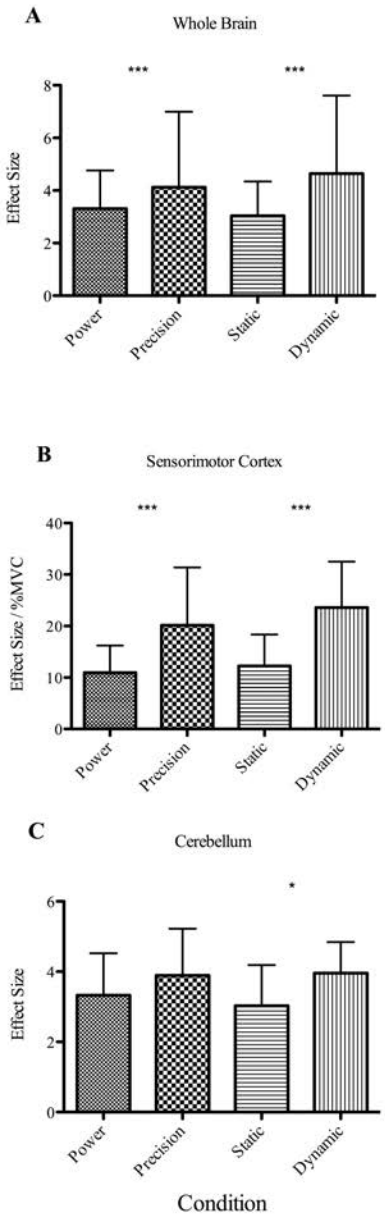

Figure 16. Effect sizes of grip type and pattern in whole brain (A), sensorimotor cortex (B) normalized by percent MVC, and cerebellum (C). Precision and dynamic grip generated stronger activation in the whole brain than power and static, respectively (A, ANOVA, Bonferroni, $p<0.0001$) When normalized by percent MVC, precision grip and dynamic grip generated stronger activation than power and static grip, respectively (B, ANOVA, Bonferroni, $p<0.0001$). Dynamic grip generated stronger activation than the static grip in the ipsilateral cerebellum but not in grip type (C, ANOVA, Bonferroni post-test, $p>0.05$). *$p<0.05$, ***$p<0.001$. Abbreviations: MVC – maximal voluntary contraction

2.5 Discussion

2.5.1 Main findings

This chapter comprises an ALE meta-analysis of the BOLD signal associated with handgrip type and pattern. Our analysis revealed 3 main findings: (1) There are similar and distinct activation clusters for grip type (Figure 10 and Figure 11, respectively) and grip pattern (Figure 14 and Figure 15, respectively) (2) Effect size analysis indicates that brain activation was stronger for precision and dynamic grip than power and static, respectively (Figure 16) (3) There was a large degree of overlap between grip type (Figure 10) and pattern (Figure 14) and this suggests that mechanisms, such as oscillatory patterns of brain activation, may be partly responsible for neural coding of different grip functions[261]. To our knowledge, this is the first meta-study to compare grip type and pattern.

2.5.2 The similarity between power and precision grip

Activity in power and precision overlapped in the L. postcentral gyrus (area 3b), L. precentral gyrus (area 4a, 44), the L. SMA (area 6), L. middle cingulate cortex (area 6), and R. cerebellum (lobule V, VI) (Table 5, Figure 10). It is clear from our results and others[31] that both power and precision grip rely on these brain regions, which are classically known to be involved in voluntary movement (Chapter 42, Kandel *et al.* (2000)[21] and have previously been implicated in numerous handgrip studies[36,40,64,223,225,226]. Indeed, the middle cingulate cortex, SMA, and area 4a all project via the corticospinal tract to motor neurons controlling the muscles of the hand[29,30]. Voluntary movement at any force in the presence or absence of externally generated cues is executed by a complex coordination between cortical and subcortical structures[21,262]. The force applied during grip is modulated by feed forward[26,263,264] and feedback[21,229,265] mechanisms delivered to and arriving from the periphery, respectively, and are modified by the cerebellum and area 6[266]. Thus, it is not surprising that these regions are active in both power and precision grip since both grips necessitate these processes. The difference

between the two types of grip is equivocal and our ALE sought to examine the differences.

2.5.2.1 The differences between power and precision grip

The power - precision contrast generated clusters in the L. postcentral gyrus (area 1, 3b) (yellow clusters in Figure 11). Power grip inherently generates more force, volume of muscle activation, and sensory feedback than precision grip[19] and has been shown to increase activation in the contralateral SMC[267]. Further, force related changes typically occur in the SMC, cerebellum and parietal cortex[31]. Thus, it is possible that unique regions were generated in our ALE by the presence of a broader activation response in the SMC, which is perhaps due to a larger neural response[33] caused by the larger force, feedback and muscle recruitment associated with power grip[19]. Previous work [32-34] in power grip has shown that the force-activation relationship in the SMC is linear.

To address the potential effect of force we calculated the effect size at all reported voxels in the SMC and normalize these values by mean % MVC. While controlling for % MVC, precision grip generates significantly higher effect sizes than power grip (Figure 16). From this, our interpretations are somewhat limited given that the current version ALE can't perform an ANCOVA for variables such as % MVC. Nonetheless, our interpretation is that power grip generates broader activations in the SMC but that precision grip generates stronger activations than power grip in the SMC.

We also saw ALE clusters in the parietal lobe (R. supramarginal gyrus), which as stated above typically increases with an increase in force. The involvement of this brain region will be discussed subsequently in section 2.5.4.

The precision - power contrast generated clusters in the R. and L. SMA (area 6) and the L. precentral gyrus (area 4a) (brown clusters, Figure 8) The SMA is particularly known to be involved in the planning and execution of movement[21,262]. This may be the result of the fine dexterity and lighter forces required to perform precision grip; for a variety of

voluntary movements the lighter the force applied the greater the activity in the premotor cortices[36-39]. Area 6 and area 4a were uniquely activated in the precision grip subtraction, which highlights a specific difference between grip types. This finding is supported by research demonstrating specific cortical neurons in M1 are activated during precision but not power grip[285], perhaps due to their direct monosynaptic connections into intrinsic muscles in the hand, which are often more associated with precision grip[19]. Further, SMA (area 6) activation spanned left and right hemispheres, indicating that precision grip requires bilateral involvement of the premotor cortices. It is thought that the involvement of ipsilateral activity is due to an increase in neural demand associated with more precise tasks[36] or in the SMC, a lack of inter-hemispheric inhibition[267]. It is possible that one of these mechanisms is functioning during precision grip to generate activation in the R. and L. SMA (area 6) and L. precentral gyrus (area 4a, Figure 11)

2.5.3 The similarities between static and dynamic grips

We found that dynamic and static grip shared activity in the L. postcentral gyrus (area 2, 3b), L. precentral gyrus (area 4a), the R. cerebellum (lobule V, VI) and L. SMA (area 6, Figure 14). The data presented here confirms that area 2 is important for both patterns of unilateral force application[268]. Locating extrema in area 2 in both patterns of force application is particularly interesting given its potential involvement in human evolution[268]. Area 2 is an important region for dominant hand[268] tactile processing and kinaesthesia[288,289] and thought to be a critical area in the development of hand use made possible by an opposable thumb[268]. Indeed, old world monkeys and the cebus monkey, the only new world monkey with an opposable thumb[290], uniquely possess a well developed area 2 and are exclusive in their use of feeding tools in the wild[268]. In conjunction with other research examining the role of area 2, our results provide support for the general involvement of area 2 in handgrip force application[268].

2.5.3.1 The differences between static and dynamic grip

The static - dynamic subtraction did not reveal any clusters. However, the subtraction between dynamic - static revealed activations in the L. precentral gyrus (area 4p), L. SMA (area 6), L. middle cingulate cortex (area 6), and precentral gyrus (area 6) (Figure 15). Previous work indicates that dynamic movements produce greater SMC and cerebellum activation during power handgrip[40] and finger flexion[32], perhaps suggesting a general mechanism for dynamic movements in the hand. Indeed, other motor cortex regions, such as the SMA, activate to a larger extent during dynamic gripping versus static gripping[269]. While we found the cerebellum to be active in both dynamic and static ALE images alone, the comparison dynamic - static did not reveal activation in the cerebellum. Our analysis of effect sizes between dynamic and static grip in the cerebellum (Figure 16C) revealed that dynamic grip generated stronger activation in the cerebellum. As seen Table 8, rows 7-9, area 6 was the most prominent cytoarchitectonic area isolated from this contrast. This is perhaps due to the planning or movement initiation/cessation[40] that is involved in repetitive dynamic movements.

2.5.4 Voluntary handgrip, motor cortices and the fronto-parietal-cerebellar network

In addition to investigating the similarity and differences between grip type and grip pattern, one might also be interested in studying handgrip mechanisms in general; typically one does not perform handgrip exclusively in a grip type or grip pattern and often performs a mixture of the two. Thus, we performed a supplementary ALE analysis of all studies to illustrate a generic description of brain activity during handgrip, regardless of grip type and pattern (Figure 17).

This ALE meta-analysis highlights a number of structures important for voluntary grip, such as the thalamus, rolandic operculum (area 44), and putamen that have not yet been discussed. The putamen, a component of the basal ganglia, has recently been implicated in precision grip[229], while the thalamus[32,36,37,62,238] have been heavily implicated in handgrip. Wong *et al*. (2007)[238] demonstrated a correlation between heart rate and

activation in these regions and the thalamus has been shown to be activated just prior to handgrip fatigue[2] and perhaps during nociception[97]. It is possible that the thalamus is active due to autonomic function[270], visceral awareness[271], proprioceptive feedback[26], perception of effort and/or fatigue to some degree[2,116] . A combination of these is also possible since these variables are difficult to separate[26]. In several of our ALE conditions, we found clusters in the rolandic operculum, confirming previous findings of its involvement in voluntary movement [272,273].

The remaining regions generated by the generic ALE are part of the fronto-parietal cerebellar network (FPCN) and have previously been shown to be invovled[242] during voluntary hand movement. The involvement of the parietal cortex during hand movements such as grasping has been well established in both primate[274-277] and human studies[278-283], suggesting conservation between species. This work led to the development of the FPCN that involves the premotor cortical areas, SMA (area 6), postcentral gyrus (areas 3a, 3b, 2) and cerebellum, which interact with the parietal lobe during feedback, feed forward and cognitive processes associated with movement[236]. Visual or auditory feedback is often part of handgrip experimental design and the FPCN is thought to adjust motor output carried out by the motor cortices according to the integration of visual[284,285], efference copy or sensory feedback, presumably from the cerebellum and premotor cortex[26]. However, the role of the FPCN is not clear. Vaillancourt *et al.* (2005)[285] demonstrated that the premotor cortices and parietal cortex were activated independent of feedback frequency during grip. Christensen *et al*. (2007)[26] removed sensory feedback using an ischemic nerve block and showed an increased correlation between activated FPCN regions. Author ascribed efference copy to the premotor cortices and suggested that without sensory feedback the FPCN may be computing expected and actual sensory input. This is supported by a Ghez and Thach's (Chapter 42, Kandel *et al.* (2000)[21]) proposed role of the cerebellum in motor control as a comparator for actual versus intended movement. Further, Haller *et al*. (2009)[284] demonstrated that the anterior parietal cortex and SMA are important for force and timing during precision grip task in the presence of visual feedback; while others[31,36] have found this without visual feedback. Other research has suggested that regions of the FPCN are associated with cognitive and

attention processes that are ongoing during handgrip. The posterior parietal cortex, which is sub-divided into the superior parietal lobule and inferior parietal lobule, has been implicated in cognitive processes[230,280,286], for example object assessment and execution of hand movement[281-283] and object manipulation[278,287]. Further, previous literature[286] suggests that brain activation is specific to functional tools rather than neutral objects; thus the activation we demonstrated during power and static forces could indicate that activity in the inferior parietal lobule is potentially specific to the grip tool itself.

2.5.5 Other Mechanisms regulating grip

We found that there was a large degree of cluster overlap between handgrip type and pattern. Indeed, we were able to see elements of the FCPN in all conditions. This brings about the question that if the areas between grip and type are similar then how is the brain coding for different grip actions? A theory of oscillating brain activity has emerged to explain how the motor system functions to modulate sensorimotor mechanisms during and prior to movement by oscillating between neural activation frequencies[261]. It has been well established that the frequency of activation is associated with specific brain states, such as a relaxed or aroused state[288]. The oscillation between these electrophysiological frequencies is thought to play a functional role in the brain [261] and may be modulated according to local network and cellular diferences[289]. Activation frequencies have been shown to be differentially modulated in movement related regions, such as the motor[290], parietal and cerebellum (i.e. the FPCN), during steady holding, preparation and execution of movement[314,315]. For example beta-band (13-30Hz) activity is prominent during steady holding but decreases during preparation and execution[290]. It is thought that beta-band dominant activity represents a more efficient way of processing sensorimotor feedback and becomes interrupted when a new movement is planned and executed during which time gamma-band (>30Hz) frequencies become dominant (see Figure 3, in Engel and Fries, (2010)[261]). The BOLD signal has been shown to be positively correlated to EEG gamma frequency in the cerebellum [316]. This is particularly interesting in the context of the current study, where we observed higher effect sizes (

Figure 16) during dynamic grips in the cerebellum, which necessitate repetitive transitions between gripping and rest. Thus, if dynamic grips necessitate the switching between beta- and gamma-band frequencies then it is possible that this results in a greater BOLD signal than steady grip alone, which is more commonly associated with only the beta-band. Other forms of functional integration could be coding for grip type and pattern such as temporal, rate, synchrony, and/or transient coding as discussed by Friston (1997)[291].

2.5.6 Limitations and future directions

Presumably regions within the FCPN network are not acting independently to generate grip. The study of brain connectivity examines how two or more regions relate or influence one another (see section 1.10.4). ALE activations do not draw inferences about how activated regions function together, nor do BOLD activations alone[206]. Methods such as functional connectivity (FC) or effective connectivity (EC) have been developed and can be used in concert with meta-analysis methods[233] to indicate the brain regions activated in unison. One can then, with structural pathways, infer a network of regions involved in a task. Indeed, we apply this approach in chapters 3 and 4 to investigate the brain's response to handgrip muscle fatigue.

We discussed our ALE results using BOLD, frequency, and connectivity literature in order to draw inferences about the regions revealed by our meta-analysis that might be working to produce voluntary handgrip. Notwithstanding, there are inherent statistical limitations of ALE[209,233]. For example, ALE does not compute positive and negative BOLD together, but separately, thus generating a bias towards neural activation as opposed to deactivation. Methods such as signed differential mapping[233,292] have been developed to resolve this issue. However, the inclusion of negative BOLD presumes that this signal represents a decrease in brain activity but that may not be the case[293]. Thus, we maintained use of ALE to summarize brain activation according to positive BOLD in the variables specified (see section 2.3.7). Lastly, because ALE does not take into account the strength of activation we calculated effect sizes for the entire brain and specific

regions between grip type and pattern. Given that the power grip studies employed a larger MVC we normalized the effect sizes in the SMC by mean MVC. This was performed given that previous work[32-34] demonstrated activation in the sensorimotor cortex was linear to force output. However, three of our studies included voxel activations that were in part generated by forces greater than 70%, at which point activation becomes non-linear[64]. Thus, normalizing by % MVC linearly in a non-linear trend may affect our results. Notwithstanding, we performed an additional power grip ALE without forces greater than 70% and no differences were observed.

The purpose of this chapter was to elucidate brain activity associated with handgrip and the potential differences between grip type and grip pattern. However, our design and analysis was partially limited by broader experimental factors. At a single study level experimental designs of even a simple task are often not decomposed sufficiently to perform statistical interactions between all variables that are not always known. Further, task analysis presumes the knowledge of all variables involved in a task, which is being investigated in the first place. Our study includes a variety of experimental designs and modeling, which may introduce variation unrelated to our investigation in a number of ways. It is known that the degree of parietal cortex activation in imaging experiments is variable and heavily dependent on experimental task parameters, such the distance[281] participants are required to reach during gripping and whether participants are specifically asked to assess[280] or report[286] what it is they are grasping. For example, power grip studies typically employ greater force than in precision grip studies. In addition, most of our studies employed block design, which captures neurophysiological processes over a short window, which may include a set of heterogeneous psychological events during handgrip task. A homogenous data set is difficult to obtain given the wide variety of variables (e.g. age and MVC) and psychological processes that occur. More broadly, there is anatomical[294,295] and cytoarchitectural variation[254,294] between participants and the assigned location of activation may vary. Notwithstanding, the ALE method of selecting commonly activated voxels should ameliorate this and we used a probabilistic atlas to interpret ALE clusters, which further reduces the effect of participant-to-participant variation.

2.5.7 Conclusions

Using ALE contrast analysis we highlighted key similarities and differences between grip type and grip pattern. We found that power grip generates unique activation in the SMC (area 1 and 3b), while precision grip generates stronger activation here. Further, precision grip generates more activation in the premotor cortices (area 6) and precentral gyrus (area 4a), which is potentially due to the fine motor forces and control associated with this grip type. Dynamic handgrip relies more on areas 4a and 6 than static grip and generates stronger activation in the cerebellum, which is perhaps necessitated by the coordination of repetitive opening and closing of hand digits or due to an increased BOLD requirement potentially associated with the oscillation between beta and gamma frequencies. Dynamic and static grip share activity in the postcentral gyrus (area 2), an area which has been strongly implicated in the evolutionary development of handgrip[268].

We found a striking similarity between grip type and pattern. There was a large degree of overlap within grip type and grip pattern in the precentral, postcentral, and SMA, which suggests that these regions are conserved for handgrip. This suggests that handgrip is regulated by other factors such as brain connectivity or oscillatory mechansims.

In our combined ALE (Figure 17) we outlined that brain regions could be: (1) functioning within the FPCN to adjust force production according to sensory perception with[285] or according to efference copy (2) related to the associated cognitive processes inherent within a motor task (i.e. assessment, execution and manipulation of a tool) or (3) an unknown process, which is potentially the case. FPCN activity could be modulated according to grip force[38] or age[39,64,225] and this could be an opportunity for future ALE research; recently, correlational methods have been used[296,297] to address these questions, although they are not yet widely available.

More practically, our results provide empirically based ROIs that can be used in order to more effectively study handgrip. In the following chapters, we are particularly interested in investigating central fatigue processes occurring during and after a fatiguing handgrip

task. As such, the motor cortex regions revealed in this chapter (e.g. area 4ap and 6) will provide ROIs from which to study the role of the motor cortices during handgrip fatigue.

2.6 Supplementary analyses

We performed an ALE analysis including all studies without differentiating between grip type of pattern. We found activation in the L. postcentral gyrus (area 3b), R. SMA (area 6), R. cerebellum (lobule VI), R. supramarginal gyrus (intraparietal cortex, IPC), R. postcentral gyrus (IPC), R. inferior parietal lobe (hIP3), R. inferior frontal gyrus (area 44, p. opercularis), R. rolandic operculum (area 44), L. thalamus (prefrontal), L. putamen, L. precentral gyrus (area 6), L. rolandic operculum, L. cerebellum (lobule VI), and L. cerebellum (lobule V, VI, VII).

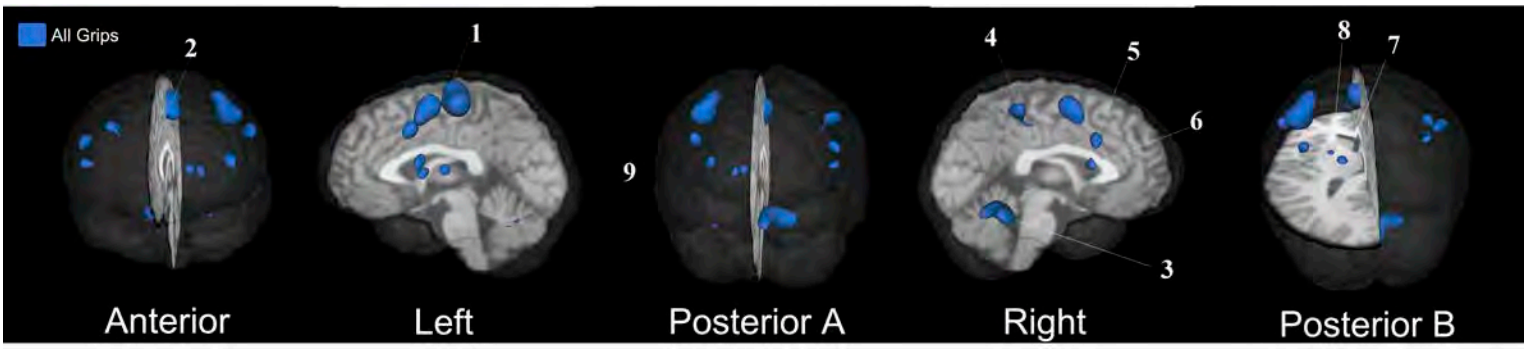

Figure 17. ALE showing the BOLD response to grip type and pattern in the (1) L. postcentral gyrus (area 3b), (2) R. SMA (area 6), (3) R. and L. cerebellum (lobule V, VI, VII), (4) R. supramarginal gyrus (IPC), R. postcentral gyrus (IPC), and R. inferior parietal lobe (hIP3), (5) R. inferior frontal gyrus (area 44, p. opercularis), (6) R. rolandic operculum (area 44), (7) L. thalamus (Th-prefrontal), (8) L. putamen, (9) L. precentral gyrus (area 6), and L. rolandic operculum. Cluster forming threshold and cluster-level inference used were uncorrected $p<0.001$ and $p<0.05$, respectively. Posterior A and B showing the same image from two views, A the standard view and B with left axial slice to demonstrate activation in subcortical structures. Anterior and posterior A images are rotated 5 degrees clockwise and posterior B image are rotated 30 degrees superior to anterior.

Chapter Three

Supraspinal mechanisms of muscle fatigue during a fatiguing handgrip task

3.1 Abstract

Central fatigue theory proposes that motor drive is limited to maintain homeostasis. Stimulants, such as MPH, can improve exercise performance and it is thought that MPH alters central processes during muscle fatigue. However, the ergogenic mechanism of MPH is unknown. This study examines the effect of MPH on force output and the brain's response to a muscle fatiguing handgrip task. In a double blind, crossover design participants ingested MPH or a placebo before performing a muscle fatiguing handgrip task during fMRI scanning. We analyzed mean force output, whole brain activation, and effective connectivity during the task and in pre-task failure windows. Pre-task failure was defined as the moments just prior to releasing the grip dynamometer. **Force output results:** our results show that participants increased their grip force during the task but that this increase was not significantly present during pre-task failure windows. **Whole brain activation results:** in the placebo condition, we observed task related increase in neuronal activation in bilateral cerebellum and motor cortices whereas in MPH conditions we observed increase in neuronal activation in motor cortices but not the cerebellum. Furthermore, during pre-task failure in the placebo condition we observed increased BOLD signal in the right IC and inferior frontal gyrus while in MPH condition, pre-task failure was associated with increased BOLD in the left IC, right ACC, sensory cortex, supplementary motor area and visual cortex. **Connectivity results:** MPH increased effective connectivity between the IC and hand motor cortex during grip, but again, this was not present in the time windows shortly before task failure. Similarly, MPH also increased effective connectivity between the IC and supplementary motor area. There were no observed differences in effective connectivity within a previously proposed facilitation network (e.g. OFC, ACC, basal ganglia, see 1.7.2.1). This chapter demonstrates: 1) MPH increases grip force and 2) alters IC effective connectivity during grip but not during task failure. 3) Effective connectivity within the facilitation network is not altered by MPH. 3) The inferior frontal gyrus may be involved in the decision to terminate exercise. This study proposes a previously unknown neural mechanism of MPH during a muscle fatiguing exercise.

3.2 Introduction

As discussed in Chapter one, primates possess a network of structures that transmit and interpret signals of disturbed homeostasis[97] (Figure 3). Muscle fatigue can be defined as a reversible state characterized by a reduced ability to generate force or power[298] and is partly modulated by the CNS[11,299,300]. Central fatigue theory proposes that motor drive is limited to maintain homeostasis[2,11,298] according to feed forward[26,72,73] or feedback processes[68,75,298].

Investigations of exercise related to pacing strategy[301] show that muscle fatigue is regulated throughout exercise[132] and that the culmination of fatigue occurs with a decision to stop (i.e. task failure)[2,302]. It is thought that the CNS terminates exercise according to homeostatic regulation[11] in advance of catastrophic tissue failure. Interestingly, the IC, which is located in the temporal area, has been identified as an important brain structure for processing disturbed homeostasis[79,97] , task failure[2] and muscle fatigue[120]. The IC has been shown to integrate afferent feedback from the periphery[102,303] and is thought to be the site of viscerosensory integration [220] of alarming stimuli[98]. Interestingly, the limitation of motor drive during muscle fatigue has been proposed to involve interactions between the IC and M1[116]. Other examples for IC involvement in homeostatic processes are the processing of afferent signals leading to pain[99] air hunger[100], and thirst[101].

MPH[1,14] and other CNS stimulants[12,13,15] improve exercise performance and MPH is used to treat fatigue-related illness[304] and to enhance interest[305] and attention[306]. The ergogenic effect of MPH is suggested to occur via a modification of central processes during exercise fatigue [1,12] but the neural mechanisms of MPH during muscle fatigue are unknown. MPH and other CNS stimulants[12,13], increase motivation and willingness to exert more effort[18,187] that allows for exercise closer to maximal ability[1,16], which is potentially achieved by increasing synaptic DA and norepinephrine transmission[183,184] in the mesocorticolimbic pathway[174]. Some[174,175] have proposed that a dopaminergic

facilitation network involving the OFC, ACC, basal ganglia and motor cortex may be acting to overcome fatigue and deficits in force output.

Against this background, this study investigates MPH's influence on the central processes of muscle fatigue during a fatiguing handgrip task using fMRI. This study address' whether MPH influences brain activation and effective brain connectivity between the IC and motor cortices and/or within a proposed dopaminergic motor facilitation network[174,175]. Using the results of our ALE in Chapter two, we investigate effective connectivity in the motor cortices, using the hand motor area of M1 and SMA. In a double blind, crossover design participants ingested MPH or placebo prior to performing a 40-trial fatiguing handgrip task[2]. The hypotheses of this study are 1) MPH will improve mean trial force[1] and 2) will alter brain activation and connectivity during handgrip and/or in the moments prior to task failure.

3.3 Methods

3.3.1 Ethical approval

Participants provided written informed consent before participation. This study was approved by the human research ethics committee of the University of Cape Town, South Africa (REF:214/2013) and was carried out in accordance with the *Declaration of Helsinki* on the use of human participants in experiments.

3.3.2 Participants

Participants were assessed for handedness using the Edinburgh handedness inventory[307] and completed a neuropsychological evaluation performed by a trained psychologist using the Mini International Neuropsychiatric Interview [308]. Fifteen right-handed participants (9 male, 6 female) without a history of neuropsychological disease, drug use (e.g. stimulants, amphetamines, tranquilizers), or recent use (1 month) of prescription medication participated in the study. Participant data such as age, height, weight, and

physical activity levels using the generalized physical activity questionnaire [309] were collected during a familiarization session. This was collected in order to indicate participant's level of physical activity. Demographic data is summarized in Table 9. Participants participated in the study in three separate handgrip sessions that occurred over 3-4 weeks.

Table 9. Subject data illustrating mean and standard deviations of age, height, weight, BMI, and levels of physical activity in METs/week measured by the Generalized Physical Activity Questionnaire. Abbreviations: METs – Metabolic equivalent of task.

Sex	Age	Height (m)	Weight (Kg)	BMI	Physical Activity (METs/week)
9 Male 6 Female	28.4±5.2	1.75± 0.10	71.88± 11.58	23.4±2.32	492.4±311.1

3.3.3 Experimental design

3.3.3.1 Familiarization session

Participants were familiarized with the task in a custom-built mock fMRI scanner (Figure 18). Prior to the mock-fMRI session, participants were given an overview of the study using a power point presentation and completed the identical task while listening to scanner sounds through on-ear headphones (Bose Corporation, Framingham, MA, USA).

Figure 18. Custom built mock-fMRI used during familiarization session.

3.3.3.2 Experimental sessions

Participants began experimental testing one week after familiarization. Experimental sessions occurred 1-2 weeks apart and the task was reviewed in detail before each session. In a double-blind cross-over design, participants ingested a non-identifiable pill that contained either 20 mg of immediate-release MPH or glucose 90 min[1,310] before the start of the task. Participants were asked not to engage in stressful exercise and heavy lifting two days prior to an experimental session. Participants were asked to refrain from caffeine on the day of the test and abstain from food or drink three hours prior to ingesting the pill, which was consumed with a low fat[311] standard snack consisting of an 80g piece of fruit (an apple or pear), a 30g slice of whole grain bread, and 300-400ml of water. Prior to the start of the scan participants were asked to verbally rate how they felt on a scale from 1-10, where 1 represented completely calm and 10 represented very nervous[312]. Participants did not differ between placebo and MPH conditions (Figure 19). Each participant took part in both, placebo and MPH conditions.

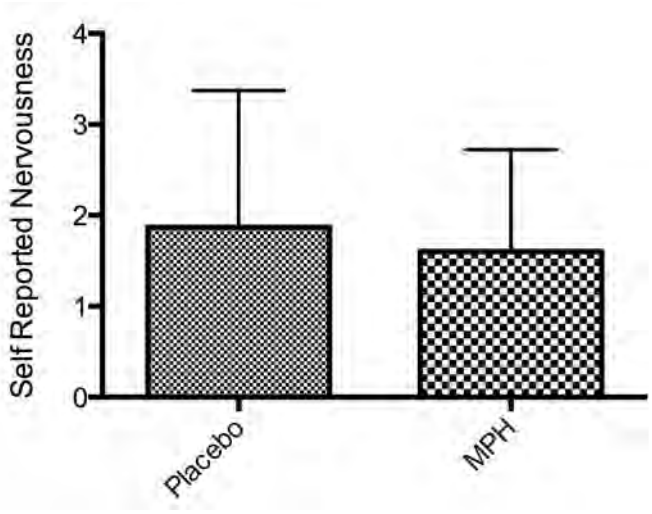

Figure 19. Self reported level of scanner related nervousness. Prior to the start of the scan participants were asked to verbally rate how they felt on a scale from 1-10, where 1 represented completely calm and 10 represented very nervous[312]. Participants did not differ between placebo and MPH conditions. Abbreviations: MPH - methylphenidate

3.3.3.3 Handgrip task

The fatigue generated during submaximal exercises is composed of a higher proportion of supraspinal fatigue than the fatigue generated from maximal exercises, which are more peripherally based[313]. In addition, dynamically applied force[40] is typically associated with more intense activations in the sensorimotor cortex (Figure 17, Chapter two) than during static grip, which suggests that a grip paradigm using repeated, rather than a static hold, may be the most appropriate paradigm to study muscle fatigue. Together, this would imply that a submaximal repetitive handgrip exercise is an optimal paradigm to study central fatigue. Further, the task used in this study has previously been shown to generate activation related to disturbed homeostasis during muscle fatigue[2].

Participants were asked to perform their MVC prior to the start of the task. Participants were asked to perform 40 submaximal grip trials (Figure 20) by flexing all digits around a custom-made MRI-compatible isometric handgrip dynamometer (Sensory-Motor Systems Laboratory, ETH Zurich and University of Zurich, Switzerland) in the power grip position[314]. The start of the first trial was set to trigger image acquisition and each trial was composed of alternating grip and rest durations lasting 12-13 and 5-7 seconds, respectively. During rest, a white cross was presented in the middle screen. Grip and rest durations were jittered to minimize anticipatory responses at the end and start of each trial and the entire task lasted 13 minutes and 20 seconds.

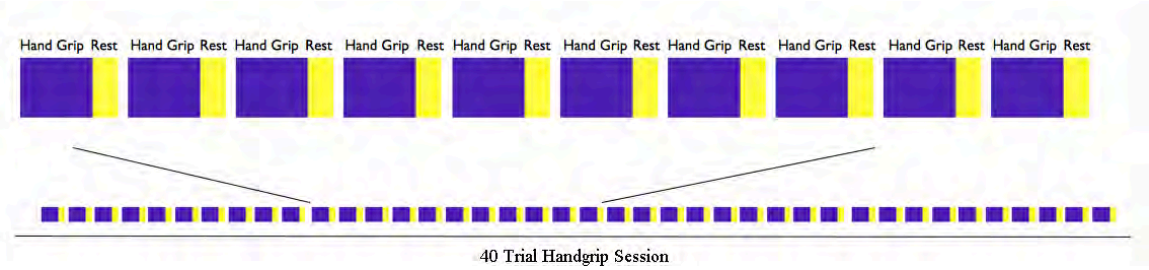

Figure 20. Schematic of 40-trial fatiguing handgrip task.

During the grip task, applied force resulted in the vertical movement of a red bar that rested on the bottom of a screen, which was visible to participants throughout the experiment. Participants were asked to raise the bar to the top of the screen into a green shaded area during each trial for as many trials as possible. The desired force was indicated at the top of the screen by a green shaded area and when the target force was reached the red bar changed to light green.

Participants began the task at a target force of 70% of their MVC. A grip trial was defined as failed if a participant's force dropped below the target force by more than 10% after having reached the target force. A trial was defined as successful if the participant maintained the target force until the end of the trial. After two consecutive failed trials, there was an 80% chance of the target force being reduced by 20% and the opposite was true after two consecutive successful trials. This was coordinated using a custom written Presentation 16.5 (Neurobehavioral Systems, Inc. CA, USA) program. The purpose of this design was to maximally fatigue participants and ensure that participants would generate a comparable number of both successful and failed trials.

3.3.4 Force recording

The timing and amplitude of the applied force were recorded at a sampling frequency of 60 Hz into a text file and later analyzed using a custom designed Matlab 2014b (The MathWorks Inc. Natick, MA, USA) program previously used by our group[2]. In order to address the effect of MPH on grip force (hypothesis one), we compared mean trial force between experimental conditions. Since we are attempting to assess neural mechanisms related to MPH's improved motor drive, mean force is the most appropriate measure of force output. Although muscle fatigue has been shown to increase the amplitude of fluctuations of forces during isometric contractions[315] we did not investigate this behavioral attribute since previous experiments[2] using the identical grip paradigm did not display fatigue-related force variations. In order to address the effect of MPH on BOLD and effective connectivity (hypothesis two), we used the timing of the applied force to define the onset times and duration in our design matrices.

3.3.5 fMRI data acquisition

We used a Siemens 3T Magnetom Allegra Syngo MR 2004A cerebral scanner to acquire 311 images per experimental session using an interleaved ascending acquisition with a repetition time of 2.58 s. The field of view was 300 mm, 34 slices were taken per repetition time and voxel size was 2.3×2.3×3.5 mm. A 90-degree flip angle and echo time of 35 ms was used. Head padding was used to minimize head movement. At the end of each experimental session we collected whole-brain T1-weighted multi-echo fast spoiled radient (FSPGR) anatomical images (TR=2 s, TE=1.53, 3.21, 4.89, 6.57 ms, voxel = 1×1×1.5 mm, field of view: 256x256 mm, 128 slices), for the purpose of anatomical localization.

3.3.6 Image preprocessing, contrasts and analyses

Image data were processed and analyzed using SPM12(http://www.fil.ion.ucl.ac.uk/spm/) within Matlab. Two dummy images were collected ahead of the task to allow the MRI signal to calibrate and were subsequently discarded from the time series before any further processing. Images were realigned to the first image in the time series, normalized to the ICBM152 MNI template, and spatially smoothed using a 8mm full-width-at-half-maximum Gaussian filter. Next, functional images were aligned to structural images using movement parameters.

In order to address hypothesis two, we investigated whole brain activation and effective connectivity using PPI analyses during grip and pre-task failure windows in placebo and MPH conditions. Motion parameters were obtained during realignment and included as covariates of no interest at the first level. In second level analyses, we used age and sex as covariates. Grip and pre-task failure contrasts are described below.

3.3.6.1 Grip contrast

To obtain first level grip images, we constructed a design matrix containing: all times during grip trials when participants were applying grip force (i.e., force, pre-task failure, and yoked windows into one regressor; see section 3.3.6.2 and Figure 21 for exact definitions) and all times during grip trials when participants were not applying grip force (i.e. no force windows, Figure 21). Rest periods were not modeled. Then, we contrasted grip windows versus those windows when participants were not applying grip. The contrast performed was grip force > no grip force. This contrast was designed to isolate the neurophysiological event associated with grip during the fatiguing task.

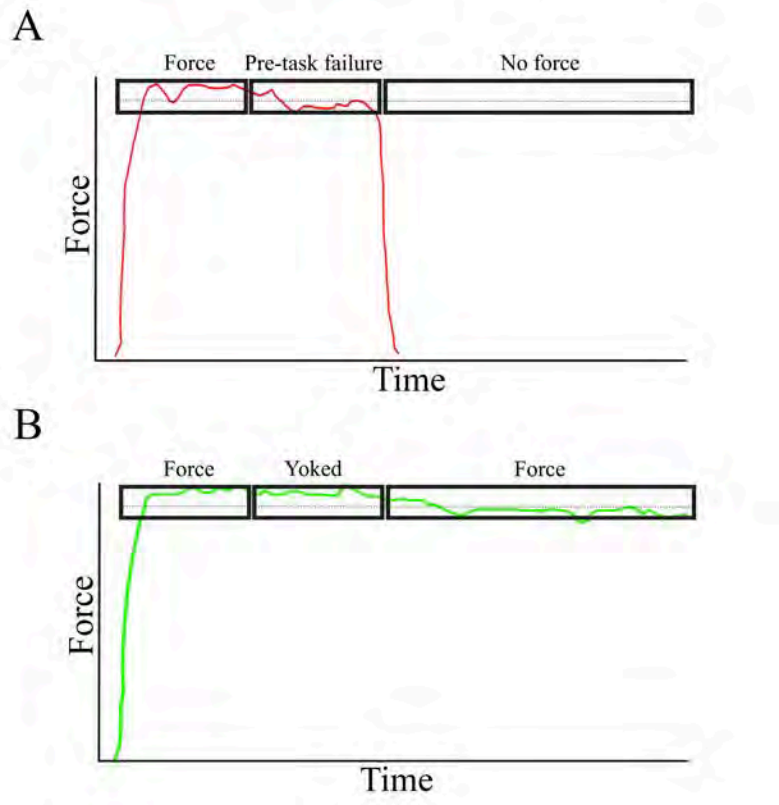

Figure 21. Conceptual diagram illustrating trial characterization of failed (A) and successful (B) trials. Contrasting force windows with no force windows of activity generated grip contrasts (see section 3.3.6.1). Contrasting pre-task failure windows with yoked windows of activity generated pre-task failure contrasts (see section 3.3.6.2).

3.3.6.2 Pre-task failure contrast

In a second design matrix, we modeled all windows in Figure 21 at the first level, except rest. Figure 21A illustrates that failed trials were divided into three sections: 1) force 2) pre-task failure window and 3) no force. Figure 21 B illustrates that successful trials were divided into three sections: 1) force 2) yoked window and 3) second force. Pre-task failure windows were defined individually according to the minimal interval between reaching the target force and releasing the grip dynamometer, regarded over all failed trials. Yoked windows were defined with identical timing as pre-task failure trials and assigned to a randomly selected successful trial. The length of these windows slightly differed between participants (3.11±1.5 s (SD)) given that some failed earlier in a trial than others and thus providing a slightly longer window from which to sample. But for a single participant at the first level analyses, the pre-task failure and yoked windows were the same length. To obtain the neurophysiological event related to task failure we contrasted pre-task failure windows in failed trials with randomly yoked equivalent windows in successful trials. The contrast was pre-task failure windows > yoked windows (Figure 21 A and B).

Despite our instructions to participants - to always to reach the target force - one of the participants uniquely circumvented the paradigm by resting during entire grip trials. There were 13 and 18 instances that the participant did this during placebo and MPH conditions, respectively. Given that this participant did not perform as intended we therefore excluded the participant from our task failure data. Thus, the pre-task failure contrast included data from 14 participants.

3.3.6.3 Psychophysiological interaction and functional connectivity analyses

In order to investigate potential changes in effective connectivity in placebo and MPH conditions we performed PPI analysis using Conn 15.a[316] (downloaded here: http://www.nitrc.org/projects/conn/). We examined PPI in three separate analyses (see below). The first two analyses address the effect of MPH on the interactions between the

IC and motor cortex (M1, SMA) and the third analyses addresses the potential facilitatory mechanisms of MPH during muscle fatigue. Selecting ROIs established from other studies was done in order to circumvent circularity errors described by Vul *et al.* (2009) [217] and others[218] (see section 3.3.7 for ROI definitions).

Both M1 and SMA have extensive corticospinal projections to segments of the spinal cord containing motor neurons controlling the hand[29]. Other motor cortex regions, such as dorsal premotor cortices were not selected since they primarily innervate proximal muscles of the arm (Chapter 38, Kandel *et al*. (2000) [21]). Further, the SMA may be important for M1 influences via mechanisms of motor preparation, or readiness potential[317,318]. Thus, we chose these regions for investigating suboptimal descending drive to the hand in this study. The IC may inhibit the motor cortex during muscle fatigue[116] and was selected from Hilty *et al*. (2010)[2], where it was shown to be involved in the decision to terminate grip force in the identical fatiguing task we have used here. Consequently, we sought to elucidate a potential mechanism of central fatigue by showing IC and motor cortex psychophysiological interactions.

The regions within the facilitation network proposed by Tanaka and Watanabe[174] are thought to perform a facilitating role to compensate for reduced motor drive during fatigue. Increased dopaminergic drive is thought[175] to overcome fatigue and deficits in motor performance[174] by acting on this network. MPH increases motivation and willingness to exert more effort[18,187], which is potentially achieved by increasing synaptic DA and norepinephrine transmission[183,184] in the mesocorticolimbic pathway. Given that the regions of the facilitation network are part of the mesocorticolimbic pathway we sought to assess the potential influence of MPH on PPI within this network in all pairwise relationships. Our PPI analyses were as follows:

1) In order to investigate the potential influence of MPH on IC to M1 PPI connectivity, we examined signals from two empirically derived ROI masks. Our M1 hand motor area was derived from the power grip-related cluster in our ALE analysis in Chapter two[314] and the IC region obtained from a previous study[2] implementing the identical paradigm

used in this study. 2) In order to investigate the potential influence of MPH on IC to SMA PPI connectivity, we examined signals from two empirically derived ROI masks. Our SMA region was derived from the power grip-related cluster in our ALE analysis in Chapter two[314] and the IC region[2] used was identical to the ROI used in hand motor area to IC PPI connectivity analyses. 3) In order to investigate the involvement of the facilitation network, we implemented repeated measures FDR corrected *t* tests for all possible pairwise differences in a connectivity matrix of regions of this network. Without a strong *a priori* hypotheses to investigate two specific ROIs in a single pairwise test we employed FDR corrected testing which is a appropriate statistical correction for exploratory analysis, as discussed in Chapter one (see section 1.10.3). Since PPI well illustrates relative connectivity changes between ROIs but not the absolute connectivity measures (see section 1.10.4) we performed follow-up functional connectivity analysis for any significant PPI interactions.

Both PPI and FC analyses are susceptible to spurious correlations[214,316] caused by temporal confounds such as head motion and physiological signals. Consequently, we used several denoising methods implemented within Conn to address this. Using a principle component analysis based strategy (aCompCor) [316], Conn reduces physiological noise and other temporal confounds. Time series from cerebrospinofluid, motion parameters and their first order derivatives were regressed from the signal time series. Conn employs ArtRepair[319] software before smoothing (downloaded here: http://cibsr.stanford.edu/tools/human-brain-project/artrepair-software.html) that identifies outlier images according to a volume-to-volume motion threshold and a volume-to-volume global signal z-value threshold. Time points that exceed these thresholds are encoded within a first level covariate of no interest that isolates images without deleting or interpolating data time points to ensure continuity. High motion volumes were identified in the regressor as those exceeding a global signal threshold z-value of 3 and motion threshold of 2mm. In order to remove frequencies not associated with the signal of interest (e.g. potential signal noise) we employed a band pass filter (0.008 to 0.09 Hz) and the subsequent despiking before PPI analysis. A more detailed description of Conn's denoising methods can be found in Whitfield-Gabrieli, S. & Nieto-Castanon (2012)[316].

3.3.7 ROI definitions

In order to best define the M1 and SMA areas involved in the power grip we used MRIcron (http://www.mccauslandcenter.sc.edu/mricro/mricron/) to manually identify overlapping voxels between area 4ap and 6 provided by the SPM Anatomy Toolbox[259] with the respective ALE meta-analytic clusters[314] found in Chapter two (Figure 8, clusters 1 and 3, respectively). Thus, the resulting hand motor area and SMA ROIs were composed of only those regions involved in power grip. SPM anatomy toolbox regions are defined in Geyer et al. (1996)[259]. The IC region was selected from IC activations in Hilty et al. (2010)[2] . See Figure 22 for an illustration of these ROIs.

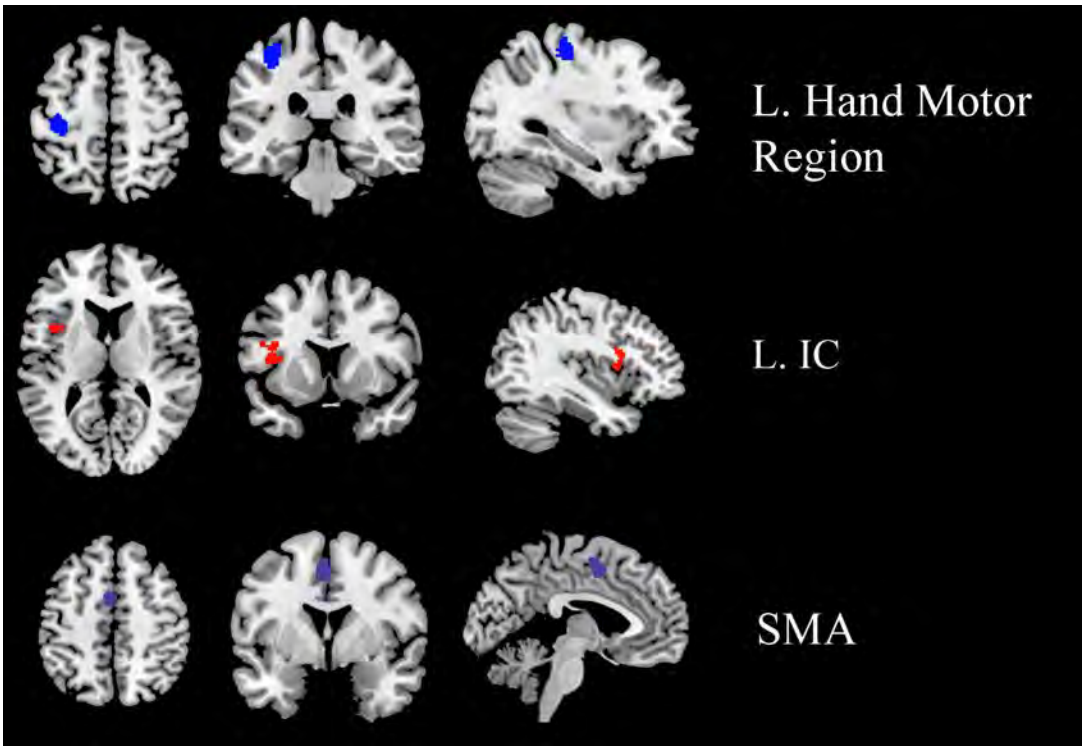

Figure 22. Illustration of ROI used in PPI analyses. The hand motor area ROI is illustrated in blue, insula ROI indicated in red and SMA in purple. The hand motor region and SMA were obtained from overlapping regions of area 4ap and area 6 with respective meta-analytic clusters of handgrip in the power grip position in Chapter two [314] (see section 3.3.7 for details). The IC region was an ROI defined from IC activations in a previous study[2], which implemented the identical paradigm used in this thesis. Displayed MNI coordinate slices of the hand motor area, insula, and SMA were: x = -33, y = -29, z = 56 and x = -39, y = 11, z = 11, x =-4, y = 1 , z = 50, respectively. Abbreviations: ROI – region of interest, PPI - psychophysiological interaction analyses, SMA - supplementary motor area, IC – insula cortex.

To investigate regions of the facilitation network we examined the ACC, right and left OFC, left and right regions of the basal ganglia regions such as the caudate, palladium and putamen, left and right SMA and hand motor area. Except for the hand motor area and SMA which were defined above, these regions were obtained from the Harvard-Oxford brain atlas (http://www.cma.mgh.harvard.edu/fsl_atlas.html), and are defined in Caviness *et al*. (1996)[320]. We implemented the Harvard toolbox since these regions are not yet available by the SPM anatomy toolbox.

3.3.8 Statistical analysis

To answer hypothesis one, we performed a repeated measures *t* test (GraphPad Prism 5.0 software, La Jolla, CA, USA) between mean trial force values in placebo and MPH conditions.

To answer hypothesis two, BOLD images of the grip (force vs. no force) and pre-task failure (pre-task failure vs. yoked) contrasts were compared between placebo and MPH conditions using a repeated measures *t* test using SPM12 within Matlab. We also performed one-sample *t* tests of grip and pre-task failure contrasts in placebo and MPH conditions using SPM12. Images were thresholded at family wise error corrected (FWE) cluster level significance of $p<0.05$. PPI correlation coefficients between the IC and both the hand motor area and SMA during grip and in pre-task failure windows were compared between placebo and MPH using repeated measures *t* test implemented in SPM12 using Conn15a with a significance level of $p<0.05$. In order to test for any differences in PPI correlation values within the facilitation network we created a matrix of PPI correlation values and performed repeated measures *t* tests implemented in SPM12 using Conn15a corrected for multiple comparisons using a FDR corrected significance level of 0.05. Age and sex were used as covariates of no interest for these analyses.

3.3.8.1 Other statistical analysis

We also performed several analyses that did not directly examine our hypotheses. The factors involved and reasoning for performing each are described below. We performed 2 x 2 repeated measure ANOVAs in order to examine the potential effects of MPH on: 1) The forces during pre-task failure and yoked windows. This was done to exclude that any difference in fMRI activity during these windows were related to force coding. The levels of the drug factor were placebo and MPH and the levels of the window type factor were pre-task failure and yoked. 2) The occurrence of pre-failure and yoked successful windows. This was done to ensure that the robustness of data collected from the two time windows was sufficient to allow valid comparisons between each other as well as between drug conditions. We did not expect the number of pre-failure and success windows to be different between placebo and MPH conditions given that the target force is dynamically changed. The levels of the drug factor were placebo and MPH and the levels of the window type factor were pre-failure and yoked successful 3) The proportion of failed to successful trials throughout the experiment. This was done to exclude any temporal effect on the sampled windows that could ocur over the duration of the task. The levels of the drug factor were placebo and MPH and the levels of trial stage factor were the 1st and 2nd half of the experiment.

To illustrate the occurrence of fatigue we calculated the maximum trial forces for each participant per trial and then calculated the slope of these forces over the 40 trials using a linear regression model. We then performed a one-tailed one-sample *t* test on the slope coefficient. In order to compare slopes between placebo and MPH conditions, we compared the respective coefficients by means of a two-tailed repeated measures *t* test. Our reason for using slope-calculated fatigue instead of post-task mean MVCs was that, as part of the study in Chapter four, we sought to determine the effect of the fatiguing task on six minutes of resting state brain activity. Consequently, we wanted to resume scanning as soon as the task was completed, which presumably was best performed immediately after the last trial. We interpret that negative slopes indicate fatigue given

that our instructions were always to reach the target force and that failed trials continued to occur in the second half of the handgrip sessions (see section 3.4.3).

3.3.9 Atlas used and nomenclature

We interpreted our results using the SPM Anatomy Toolbox 1.7, which is a probabilistic atlas used to locate brain regions for neuroimaging research as defined by cytoarchitectural structure[253]. Previous work[256] has recommended that a probabilistic template be used when interpreting the location of activation and consequently we have used it here. The advantage of a probabilistic approach is that it accounts for the inherent variation that exists in human neuroanatomy and provides a probability of a co-ordinate being located in a particular area. In Table 2 and 3, we indicate the probability of significantly activated voxels belonging to an area ascribed by the Anatomy toolbox. However, the disadvantage of the SPM Anatomy toolbox is mixed nomenclature. A complete probabilistic atlas for the whole brain is not yet available and consequently the toolbox assigns an equivalent macroanatomical label using the automated anatomical labeling (aal) atlas (e.g. anterior cingulate) [321] when coordinates fall outside probabilistic maps. As such, we have provided these labels in the results for clarification.

3.4 Results

3.4.1 Force results – hypothesis one

We hypothesized that MPH would improve force output during the task. To examine this we performed a one-tailed paired *t* test of mean trial forces between placebo and MPH conditions. Participants produced significantly greater force in the MPH than placebo condition (Figure 23, $t(14)=2.38$, $p=0.016$, Cohen's $d=0.162$, 120.8±38.17 vs. 127.3±41.93 Newtons (N)).

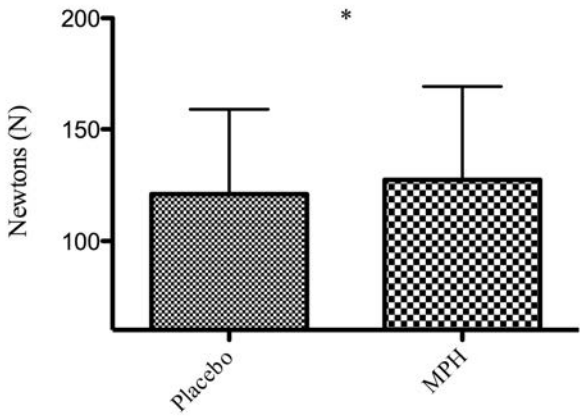

Figure 23. Mean trial grip force is greater in MPH conditions. One tailed paired *t* test demonstrates that participants produced significantly greater force in the MPH than placebo condition. MPH – methylphenidate. T(14)=2.38, p=0.016, Cohen's *d*=0.162, 120.8±38.17 vs. 127.3±41.93 (SD) N. *p<0.05. Abbreviations: MPH – methylphenidate, N - Newtons

3.4.2 Imaging results - hypothesis two

We hypothesized that MPH would alter the BOLD response and effective connectivity during grip force and in the moments prior to task failure. In order to investigate this we performed both whole brain BOLD and ROI-to-ROI PPI analyses. The results of these analyses are described below.

3.4.2.1 Grip contrast

A group level one sample t test of the grip contrast under placebo condition revealed peak activation in R. lobule VI (Vermis), L. supplementary motor area (SMA), and L. BA 6 (Figure 24, Table 10) while a one sample t test of the same contrast during the MPH condition revealed activation in L. BA 6 and 4a (Figure 25, Table 10). A repeated measures t test between placebo and MPH conditions did not reveal statistically significant differences.

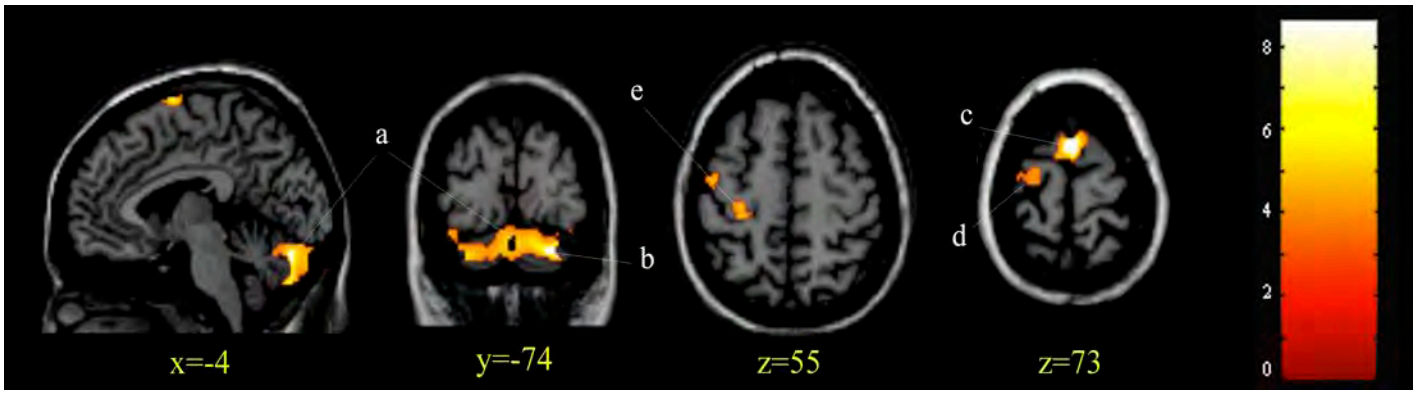

Figure 24. Grip contrast activations in placebo conditions. One sample *t* test reveals activation in the R. lobule (hem) (a), L. lobule (verm) (b), L. SMA (c), L. BA 6 (d) and L. BA 4p (e). Images were thresholded at FWE cluster level significance of $p<0.05$ (see Table 10). MNI coordinates displayed. Abbreviations: BA – Brodmann Area, FWE – Family wise error, SMA – Supplementary motor area.

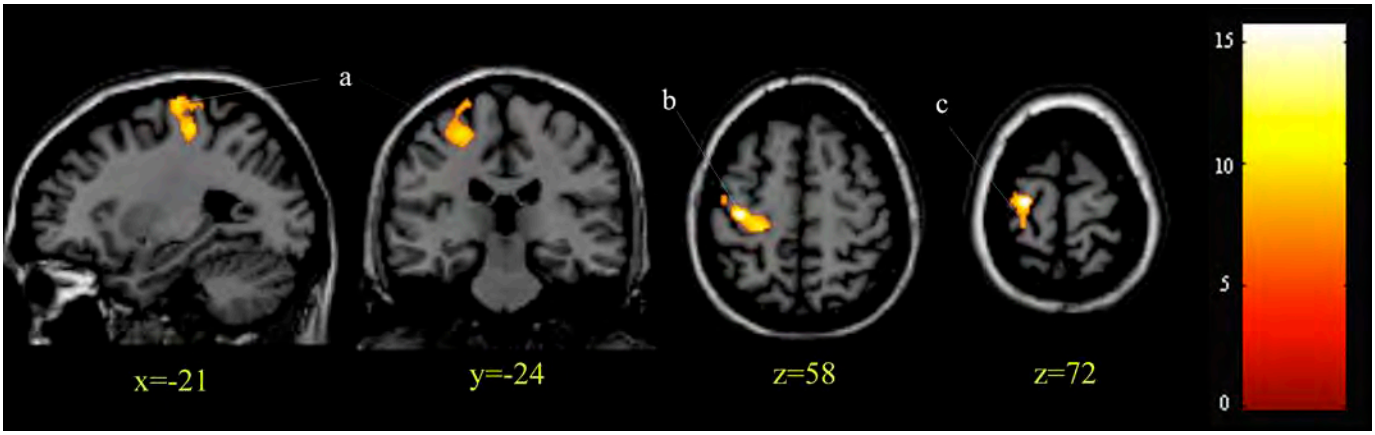

Figure 25. Grip contrast activations in MPH conditions. One sample t test reveals activation in the L. BA 6 (a), L. BA 4a (b) and L. BA 4p (c). Images were thresholded at FWE cluster level significance of $p<0.05$ (see Table 10). MNI coordinates displayed. Abbreviations: BA – Brodmann Area, FWE – Family wise error, MPH – methylphenidate, SMA – Supplementary motor area.

Table 10. Activations for placebo and MPH conditions during grip contrast. Only clusters with FWE cluster level significance of p<0.05 are listed. Coordinates were assigned an area using the SPM Anatomy Toolbox 1.7 and probability indicated in brackets (column 5). When a probability was not provided by the toolbox the coordinate was assigned to macroanatomical label (e.g. L. SMA) [321]. Abbreviations: Hem – hemisphere. FWE – Family wise error, MPH – methylphenidate, SMA – Supplementary motor area.

Condition and Contrast	Cluster Significance	Cluster Size(s) (mm^3)	Z Value	Cytoarchitectonic Area and Probability	Location (x,y,z)	Figure and Label
Placebo Grip	<0.001	2126	4.79	L. lobule VI (Vermis, 47%)	0, -78, -28	Figure 24a
			4.60	R. lobule VIIa (Hem, 95%)	26, -88, -30	Figure 24b
			4.59	R. lobule VIIa (Hem, 83%)	18, -90, -28	Figure 24b
	0.001	566	4.64	L. SMA	0, 4, 74	Figure 24c
			4.50	L. BA 6 (80%)	-18, -12, 78	Figure 24d
			3.81	L. BA 4p (50%)	-28, -30, 58	Figure 24e
MPH Grip	<0.001	663	4.41	L. BA 6 (80%)	-22, -20, 74	Figure 25a
			4.22	L. BA 4a (50%)	-34, -22, 60	Figure 25b
			3.87	L. BA 4p (30%)	-24, -28, 58	Figure 25c

3.4.2.2 Pre-task failure contrast

A group level t test of the pre-task failure contrast in placebo conditions revealed activation in the right (R.) anterior IC and inferior frontal gyrus (IFG, , Table 11) but in MPH conditions the same contrast revealed peak activation in L. posterior IC, BA 3a, R. ACC, R. BA 18, R. BA 6, and R. BA 3b (Figure 27, Table 11). A two-tailed repeated measures t test between placebo and MPH conditions did not reveal statistically significant differences.

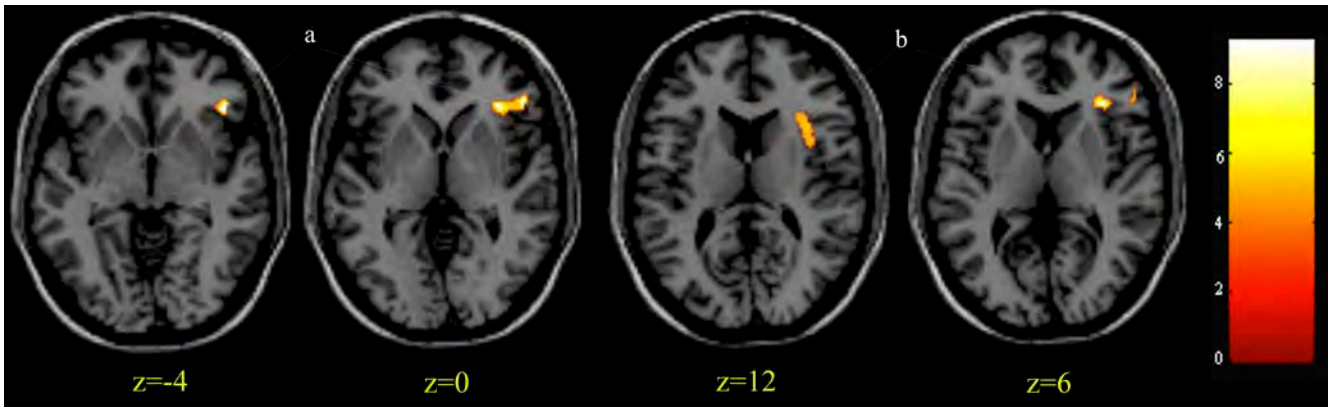

Figure 26. Pre-task failure contrast activations in placebo conditions. One sample *t* test reveals activation in the R. IFG (a) and R. IC (b). Images were thresholded at FWE cluster level significance of p<0.05 (see Table 11). MNI coordinates displayed. Abbreviations: FWE – Family wise error, IC – Insula cortex, IFG – inferior frontal gyrus

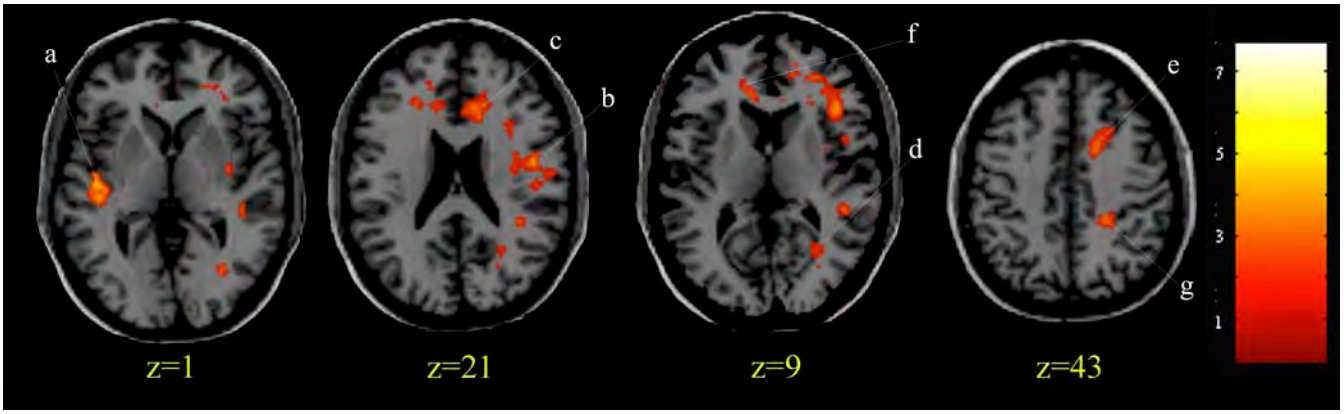

Figure 27. Pre-task failure contrast activations in MPH conditions. One sample *t* test reveals activation in the L. insula (a), R. BA 3a (b), R. ACC and R. IFG (c), R. BA 18, and R. hOC (d), L. BA 9 and L. ACC (f), R. BA 3b (g) and R. BA 6 (e). Images were thresholded at FWE cluster level significance of p<0.05 (see Table 11). Displayed MNI coordinates. Abbreviations: BA – Brodmann Area FWE – Family wise error, MPH – methylphenidate, ACC – anterior cingulate cortex, IFG – inferior frontal gyrus, hOC – human occipital.

Table 11. Activations for placebo and MPH conditions during pre-task failure contrast. Only clusters with FWE cluster level significance of $p<0.05$ are listed. Coordinates were assigned an area using the SPM Anatomy Toolbox 1.7 and probability indicated in brackets (column 5). When a probability was not provided by the toolbox the coordinate was assigned to macroanatomical label (e.g. R. ACC)[321].We reported multiple areas when the assigned probability was equal for two or more areas except for areas that were not assigned a probability. Abbreviations: MPH – methylphenidate, FWE – Family wise error , ACC – anterior cingulate cortex, IC – insula cortex, IFG – Inferior frontal gyrus, SPL – Superior parietal lobule, hOC – human occipital cortex.

Condition and Contrast	**Cluster Significance**	**Cluster Size(s) (mm^3)**	**Z Value**	**Cytoarchitectonic Area and Probability**	**Location (x,y,z)**	**Figure and Label**
Placebo Pre-task failure window	0.007	313	4.51 4.15 3.46	R. IFG (21%) R. IC R. IC	48, 32 -2 36, 18, 12 34, 30, 4	Figure 26a Figure 26b Figure 26b
MPH Pre-task failure window	<0.001	528	5.58 4.40 4.17	L. IC (30%) L. IC (30%) L. IC	-44, -14, 0 -44, -24, 2 -38, 6, -10	Figure 27a Figure 27a Figure 27a
	<0.001	841	4.54 4.16	R. BA 3a (30%) R. rolandic operculum	48, -8, 24 44, 2, 16	Figure 27b Figure 27b
	<0.001	801	4.74 4.50	R. ACC R. IFG (10%)	14, 22, 26 42, 26, 12	Figure 27c Figure 27c
	0.001	372	4.34 4.09 3.98	R. BA 18 (10%) R. SPL (7A, 10%) R. hOC5 (V5, 10%)	26, -58, 16 22, -60, 32 40, -68, -6	Figure 27d Figure 27d Figure 27d
	0.036	180	3.69	R. BA 6 (10%)	20, 14, 46	Figure 27e
	0.007	263	3.88 3.81 3.74	L. BA 9 (30%) L. ACC L. ACC	-24, 32, 22 -16, 40, 14 -10, 34, 10	Figure 27f Figure 27f Figure 27f
	0.050	165	4.16	R. BA 3b (40%)	22, -38, 50	Figure 27g

3.4.2.3 Connectivity results

To determine the effect of MPH on PPI between the left hand motor area and IC we performed a two-tailed repeated measures *t* tests between PPI coefficients in placebo and MPH conditions during grip and pre-task failure windows. A two-tailed repeated measures *t* test demonstrated that MPH resulted in significantly different correlation coefficients (Figure 28, T(14)=2.26, p=0.040, Cohen's *d*=1.01) during grip but not during pre-task failure windows (T(13)=0.95, p=0.358).

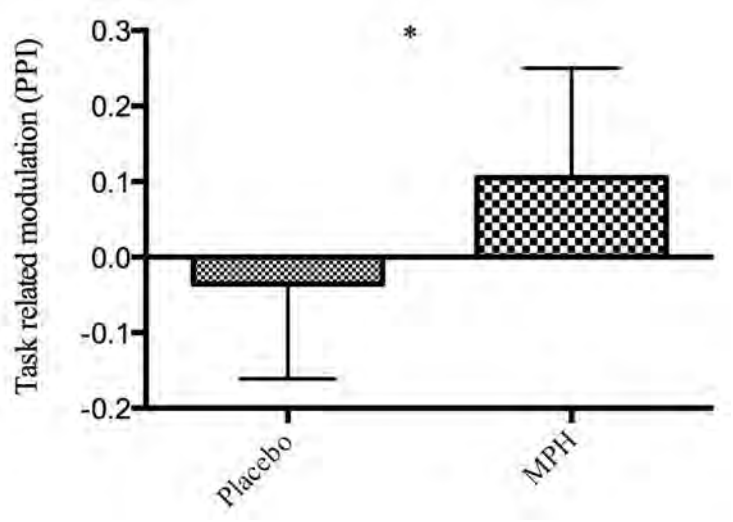

Figure 28. MPH alters psychophysiological connectivity between L. hand motor area and L. insula[2]. A two-tailed repeated measures *t* test revealed that MPH altered effective connectivity during grip (T(14)=2.26, *p=0.040). Abbreviations: MPH – methylphenidate

To determine the effect of MPH on PPI between the SMA and IC we performed a two-tailed repeated measures *t* test which demonstrated that MPH resulted in significantly different correlation coefficients (Figure 29, T(14)=2.15, p=0.049, Cohen's *d*=0.813) during grip but not during pre-task failure windows (T(13)=1.71, p=0.111).

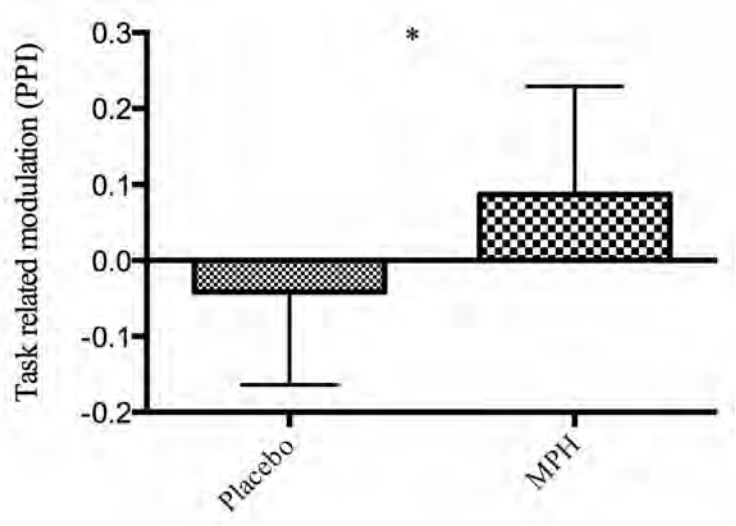

Figure 29. MPH alters psychophysiological connectivity between SMA and L. insula cortex (IC)[2] during grip. A two-tailed repeated measures *t* test revealed that MPH altered effective connectivity during grip (T(14)=2.15, *p=0.0494). Abbreviations: MPH – methylphenidate.

To determine the effect of MPH on PPI within the facilitation network we implemented repeated measures *t* tests for all possible differences in a connectivity matrix of regions of this network with multiple comparisons accounted for using the False Discovery Rate (FDR) correction[212]. In no case did we observe an effect of the pairwise PPI connectivity coefficient values during pre-task failure or grip reach FDR-corrected significance set at 0.05.

To determine the effect of MPH on functional connectivity coefficients between the left hand motor area and IC we performed a two-tailed repeated measures *t* tests between correlation coefficients in placebo and MPH conditions during grip. A two-tailed repeated measures *t* test demonstrated that MPH resulted in significantly increased correlation coefficients (Figure 30, T(14)=2.55, *p=0.023, Cohen's *d*=0.964).

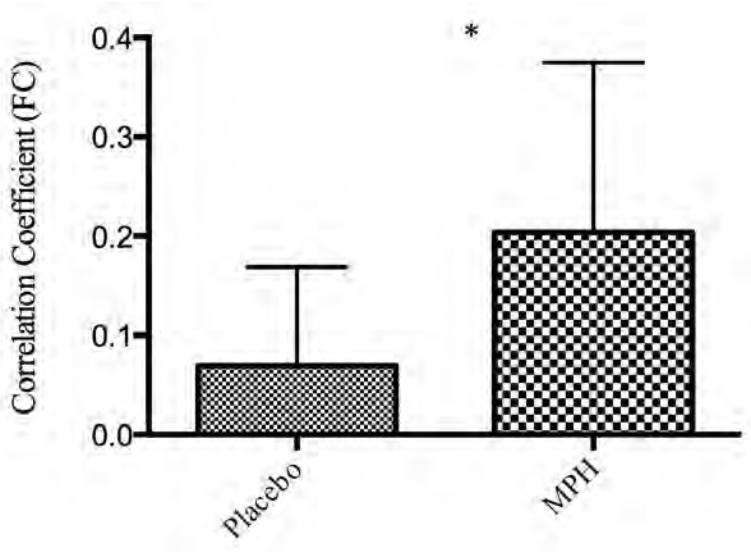

Figure 30. MPH increases functional connectivity coefficients between L. hand motor area and L. insula[2]. A two-tailed repeated measures *t* test revealed that MPH increased functional connectivity during grip (T(14)=2.55, *p=0.023). Abbreviations: MPH – methylphenidate

To determine the effect of MPH on functional connectivity coefficients between the SMA and IC we performed a two-tailed repeated measures *t* tests between correlation coefficients in placebo and MPH conditions during grip. A two-tailed repeated measures *t* test demonstrated that MPH resulted in significantly increased correlation coefficients (Figure 31, T(14)=2.64, *p=0.019, Cohen's *d*=0.998).

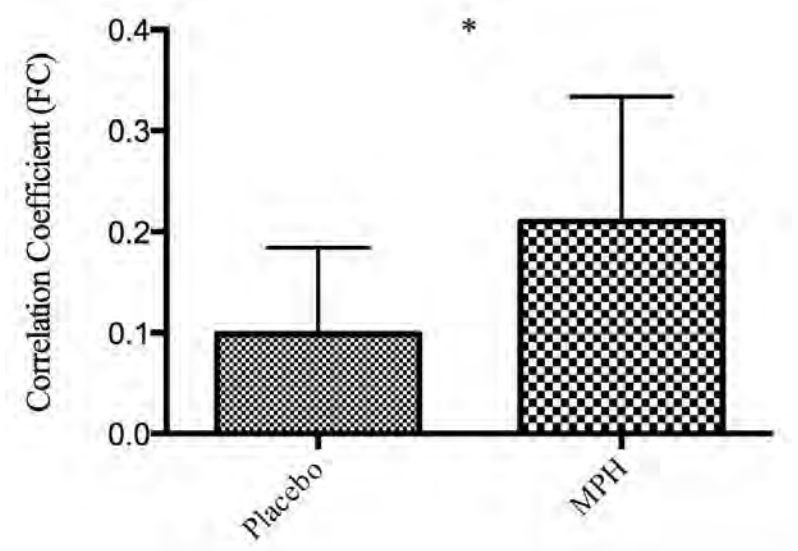

Figure 31. MPH increases functional connectivity coefficients between SMA and L. insula cortex (IC)[2] during grip. A two-tailed repeated measures *t* test revealed that MPH increased functional connectivity during grip (T(14)=2.64, *p=0.019). Abbreviations: MPH – methylphenidate.

3.4.3 Other results

The forces generated in windows from the pre-task failure contrast were not affected by drug (main effect of drug, (Placebo, MPH), F(1,26)=0.813, p=0.376) or window type (main effect of window type (pre-task failure, yoked), F(1,26)=0.584, p=0.452). There was no significant interaction between these factors either (F(1,26)=0.550, p=0.465). Thus, forces in pre-task failure windows were not significantly different from forces in yoked windows in either condition (Figure 32).

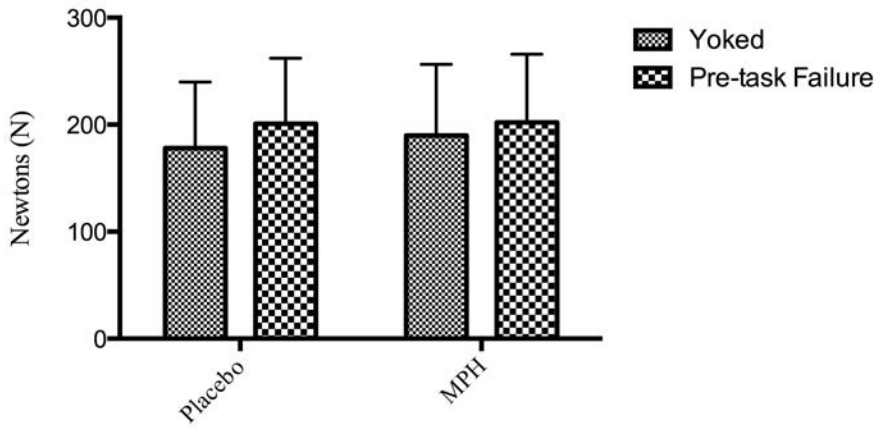

Figure 32. Forces in pre-task failure windows. Forces in pre-task failure windows were not significantly different between conditions. A repeated measures ANOVA demonstrated was no significant interaction (F(1,26)=0.550, p=0.465), main effect of drug (F(1,26)=0.813, p=0.376) or main effect of window type (F(1,26)=0.584, p=0.452). Abbreviations: MPH – methylphenidate

The number of sample windows used in the pre-task failure contrast was not affected by drug (main effect of drug (MPH, Placebo), F(1,26)=0.009., p=0.923) but was affected by window type (main effect of window type, (pre-failure, yoked), (F(1,26)=12.69., p=0.001). Participants produced significantly more yoked than pre-task failure windows, which we previously observed using this task design[2]. Participants produced 21.1±7.49 and 20.1±6.59 (SD) successful windows in the placebo and MPH condition, respectively. Participants produced 11.5± 6.32 and 12.3±6.67 (SD) pre-task failure windows in the placebo and MPH condition, respectively. Pre-task failure and yoked windows were

3.11±1.5 s (SD). There was no interaction between drug and trial type factors ($F(1,26)=1.25.$, $p=0.275$).

The ratio of failed vs. successful trials was not influenced by the drug (main effect of drug (MPH, Placebo), $F(1,26)=1.81$, $p=0.190$), neither by the position within the session (main effect trial stage (1^{st} or 2^{nd} half): $F(1,26)=0.282$, $p=0.600$). There was no significant interaction ($F(1,26)=0.680$, $p=0.417$), between these factors, either.

To demonstrate that participants fatigued during the experiment we calculated the maximum trial force per trial and then the slope of these values over the experiment using linear regression. A one-tailed one-sample *t* test revealed a significantly negative (declining) slope for both placebo ($t(14)=7.26$, $p<0.0001$) and MPH ($t(14)=8.17$, $p<0.0001$) conditions. A two-tailed repeated measures *t* test between slope values revealed no differences in slope between conditions ($t(14)=0.266$, $p=0.397$). Thus, the rate of force decline significantly differed from the start of the handgrip sessions but the rate of force decline did not differ between placebo and MPH conditions.

3.5 Discussion

This chapter reports several interesting findings: 1) MPH improves force output (hypothesis one). 2) MPH caused an increase in connectivity with both the hand motor area and SMA, during grip but not during pre-task failure (hypotheses two). 3) MPH does not appear to modify brain connectivity within the facilitation network during grip or pre-task failure windows (hypotheses two), 4) The IFG may be involved in mediating the decision to terminate exercise, and 5) we confirm that the IC is critical for exercise termination[2]. Thereby, we provide additional support that the IC is a region important for processing a muscle fatiguing task and potentially interoception of fatigue-related disturbed homeostasis[220] . We will next discuss these findings and study limitations.

3.5.1 Increased force output and effective connectivity

The neural correlates of stimulant use during fatiguing exercise are unknown. This chapter sought to explain how MPH, a readily available stimulant, could alter brain activity during a muscle-fatiguing handgrip task. We observed that a 20 mg ingestion of MPH resulted in a 5.1% stronger mean grip force throughout the task (Figure 23, Cohen's $d = 0.162$) than ingestion of a placebo. This increase is in line with previous studies examining the effect of CNS stimulants on muscle contraction[17,193]. Although the observed increase is traditionally viewed as a clinically irrelevant effect, it is known that relatively small increases represent significant improvements when a task is performed at near peak ability or during athletic competition. Thus, this change represents a relevant force effect. Although there were improvements in mean force over the course of the experiment, we observe no differences in the rate of force decay between conditions. Note that this does not indicate a lack of difference in force output. The paradigm was designed to raise or lower the target with 80% probability and thus the rate of decay between conditions should be equal despite higher or lower forces produced.

Previous work [1,14] demonstrated an ergogenic effect of MPH but did not examine brain activity. We investigated brain connectivity during grip and pre-task failure between the motor cortices and IC, which are areas important for performing power grip (Chapter two)[314] and interoception during disturbed homeostasis[79], respectively. Our results indicate that during grip, but not specifically in the moments prior to task failure, there is a MPH-induced increase in connectivity (Figure 28, Figure 30). Although it is not possible to validly assess the direction of influence with the methods employed in this study, PPI and functional connectivity measures suggest that the IC may be providing an excitatory influence on M1. We propose that this excitatory influence may represent an upstream influence on M1, which then leads to increased drive from corticospinal neurons to the hand to increase force. Swart *et al*. (2009)[1] proposed that, "amphetamines may selectively influence the central interpretation of afferent sensory feedback" from exercising muscles, or in other words interoception. Although it may be preemptive to draw strong inferences from our analyses, an alternative interpretation is that MPH could

also influence force output by altering (i.e. perhaps increasing) communication[215] between the motor cortices and IC, even if we refrain from interpreting the direction of influence. Limitations of these interpretations are discussed in section 3.5.4.

Our second set of connectivity analyses show that the IC has the same relationship with the SMA and M1, and although speculative, we suggest that the IC may be affecting descending drive via the SMA as well. The SMA has dense projections to the spinal cord levels (C7-T1) rich in motor neurons controlling the hand[29,30]. Further, SMA micro-stimulation evokes distal limb and digit movement. On the other hand, the SMA is thought to initiate motor drive in a process known as motor readiness or Bereitschaftspotential[317]. Thus, it is possible that the IC provides an excitatory relationship under MPH conditions. Recent research examined the effect of caffeine on RPE and motor-related cortical potential (MRCP)[17]. Authors investigated MRCPs in the SMA, premotor, and M1 cortices before (-1.5-0), during (0-1s, 1-2s) and immediately after contraction (3-4s) and demonstrated a ~5% increase in post-task MVC and reduction in task-related RPE. They proposed that the caffeine-induced reduction in MRCP in these regions during the task was indicative of reduced corollary discharge associated with the concomitant decrease in RPE. Our study also implicates the SMA but we found a potential excitatory influence throughout the task between the IC and SMA in MPH conditions. It is difficult to compare our results given their study implicate the motor cortices in a larger spatial but finer time resolution. It should be noted however that in the moments just prior to grip release (i.e. pre task failure) we observed a near significant increase in PPI ($p=0.11$, see section 3.4.2.3) between the IC and SMA in placebo and MPH conditions. Thus, our results and those of de Morree *et al*. (2014)[17] suggests that stimulants may influence the SMA but how this could lead to altered force output is unclear. These results encourage further research into the effect of MPH on SMA during muscle fatiguing exercise. Alternatively, it is also possible that the IC may be acting on M1 by indirect influence via SMA ending in increased drive. Given the structural[106,108] and functional[107] connections between the IC and SMA and that SMA has been shown to drive M1 activity during motor execution[264,322], it is possible that increased SMA leads to increased force output via indirect actions on M1.

Fatigue is regulated throughout exercise[301 323] and specific neural processes have been isolated just prior to task failure[2]. We show here that MPH has an effect over the course of the task rather than during pre-task failure. Thus, our interpretation is that MPH doesn't influence the neural response to quit the task but has its ergogenic effect throughout. Indeed, this may be reflected by forces in the pre-task failure window were not significantly different between placebo and MPH (Figure 32) but is significantly different over the course of the task (Figure 23). However, the point at which this occurs in this study is unknown, since we did not examine connectivity at specific points throughout the task. Previous work by Deshpande *et al*. (2009)[68] examined fatigue over three time periods, which enabled authors to comment on how fatigue changed over the duration of a fatiguing task. We examined neural activity on a fine (pre-task failure) and coarse (during grip) time resolution. Consequently, we are unable to comment on how activity or connectivity changed as fatigue developed.

The connectivity analyses we performed can be challenging to conclusively interpret since we performed analyses between pairs of ROIs. PPI is unable to rule out the involvement of a third or fourth ROI etc., or whether one ROI influences the relationship between the task and the second ROI (for more details see Figure 5, in Friston *et al*. (1997)[324]). Thus, we may conclude altered connectivity but we cannot exclude the participation of other networks or areas, such as the cerebellum[68] (see section 3.5.4 for further discussion of limitations).

MPH's ergogenic effects may be explained by other factors such as the increase in DA transmission associated with MPH[145], which could increase motivation and willingness to exert more effort[18,187]. MPH binds [188] and acts on the basal ganglia and influences decision making [325] via projections to the frontal cortex during stress or arousal[326]. Indeed, agents that reduce DA transmission cause an increase in fatigue and decrease in motivation[141]. Thus, an increase in the availability of DA and norepinephrine may have resulted in participants being more willing to exert a force near to their maximum than placebo conditions. Although we did not measure motivation levels or subjective fatigue

during the task (see section 3.5.4.2) we investigated changes in PPI connectivity between regions of the proposed facilitation network, which focuses on the importance of motivational input into the basal ganglia and prefrontal cortex[174]. We did not observe any effect of MPH on PPI connectivity within the facilitation system. Areas such as the ventral tegmental area, caudal substantial nigra, and subthalamic nucleus are potential regions for dopaminergic influence. However, these areas are particularly difficult to image given the volume of brain matter[180] approximates to one voxel in the current experiment. Thus, we did not attempt to investigate these regions.

Previous work by Roelands *et al*. (2008) [14] attribute MPH's ergogenic effect to a disruption of thermoregulatory mechanisms leading to increased heat-tolerance during exercise. We cannot conclude a similar temperature-based interpretation given that the body temperature increase during handgrip exercise do not approach intolerable limits (i.e. 41°C) as those that can be achieved during whole body exercise[77]. Instead, we interpret that MPH alters brain connectivity between the IC and motor cortices and increases force output.

3.5.2 Pre-task failure activation

3.5.2.1 Placebo activations

By contrasting task failure with yoked equivalent windows we reveal increased activation in the right inferior frontal gyrus (IFG, Figure 26, label a) and IC (Figure 26, label b) immediately before task failure. Interestingly, the IFG is heavily implicated in response inhibition[327-331]. Further, it is thought to be a critical structure for decision making[332] and allocation of attention[333] during somatosensory tasks[334]. The IFG and IC are thought to interact with feed forward and feedback processing streams in order to make decisions about threats and/or opportunities in the environment based on viscerosensory integration[334]. Consequently, we speculate that IFG activation may represent an inhibitory release response decision subservient to homeostatic signals thought to be integrated in the IC[220] as interoception.

As previously discussed[2], we are not able to differentiate if IC activation is subservient to a cardiovascular response, pain processing, or to the associated emotional response. The IC has been shown to integrate afferent feedback from the periphery[102,303] and is thought to be the site of viscerosensory integration [220] of alarming stimuli[98]. Lesions of the IC result in asymbolia, a peculiar condition where patients can perceive noxious stimuli but do not display an appropriate emotional response[335]. Although we did not measure subjective pain and emotional response during the task, pain and emotion are more likely catalysts of task failure given that the cardiovascular increases during handgrip are relatively insignificant[238] compared to those experienced in whole body exercise. Further, others have associated increases in medial IC activation with pain and exhaustion[120]. Indeed, stimulation of afferent Aδ (group III) and unmyelinated C (group IV) fibers increases activation in the IC and IFG[109]. It is difficult to separate the affective and sensory response to nociceptive stimulation because they are highly correlated. Differentiating between these responses is outside the scope of this investigation. There is a large amount of activation overlap in the IC in response to different homeostatic responses[336] (e.g. air-hunger vs. pain) warranting investigation into other neural mechanisms such as brain connectivity. We further the notion that the IC is a critical site for terminating exercise in the interest of disturbed body physiology[337]. In addition, and in line with others[334], we suggest that the IFG is a cognitive control node that, according to our data, is potentially involved in the decision to terminate exercise.

3.5.2.2 MPH activations

Our study is the first to examine the cortical response associated with the ergogenic effects of MPH. MPH enhances interest[305] and attention [306] and has been shown to increase activation in areas associated with attention control[338], error monitoring[325] and visual processing[339]. The ACC (Figure 27, c) is known to play a role in attention, motor control and processing of pain[340]. Similarly, the left posterior IC (Figure 27, a) is associated with the processing of noxious stimuli[341]. BA 9 (Figure 27, f) of the dorsolateral prefrontal cortex is important for goal directed intentional behaviors[342,343]

(i.e. executive function) and the IFG is important for task inhibition[327-331]. The dorsolateral prefrontal cortex, ACC, and IC are thought to participate in an executive control network important for the top down control of salient stimuli and error processing during motor control[334]. These areas have also been implicated in cognitive restraint of hunger[344], a interoceptive signal to prevent disturbed homeostasis. It is possible the activations we observe here represent enhanced interest and altering of task failure in a failed attempt of cognitive control to prevent grip release. Alternatively, activations in the ACC, IFG and IC together are indicative of cost-benefit decisions that are based on current state and risk assessment[345,346]. However, comparing pre-task failure activations between conditions must be interpreted with caution given that a direct comparison between conditions did not yield significant differences.

3.5.3 Grip activations

To investigate the effect of MPH on brain activation during grip we performed whole brain analysis during grip. In both conditions, grip activation in BA 4p and 6 (Figure 25 and , Table 10) are typical of power grip[314]. In the placebo condition, we observe bilateral cerebellar activation (Figure 25, a and b) in the inferior posterior lobe but not in the MPH condition. A repeated measures comparison between placebo and MPH activations however, did not yield statistically significant results. Thus, we cannot conclusively explain increased force from these activations.

3.5.4 Limitations

3.5.4.1 Analysis limitations

First, we observe increased connectivity between the motor cortices and IC in the MPH condition. To interpret this result it is useful to review the difference between functional and effective connectivity. Functional connectivity is the correlative relationship between two time dependent signals in the brain that may or may not reflect meaningful interactions[324]. However, effective connectivity attempts to determine if regions are

interacting during a task. PPI partially achieves this by inferring that correlations change only in the presence of a particular condition[214]. A limitation of using PPI in a regression analysis is the correlation between the PPI regressor and the task[203], which is inevitable given that the PPI regressor is the product of the task time series and a seed region. Consequently, we include the task time course in the regression model as a covariate of no interest so that the correlation between target and seed represents only those unique to the PPI regressor. Another limitation of PPI is the possibility of different hemodynamic response functions between regions[347]. This may result in different temporal delays that render interactions between regions not indicative of directional influences. Therefore, we do not interpret the direction of influence between ROIs. For a more detailed description of PPI see Friston (1997) [324] and Friston (2011) [214] or O'Rielly *et al*. (2012)[215]. Other effective connectivity methods, such as DCM, are used to measure effective connectivity with directional links between multiple regions in the brain. However, we did not implement DCM. DCM requires task activation in the investigated areas as a prerequisite [214]. Our second level results did not meet this requirement. Further, and of more practical and dissemination reasons, PPI is well translatable [214] to those who do not have a background in mathematics required to fully understand DCM.

Second, we investigated PPI between regions thought to be important for regulating muscle fatigue and force output during a fatiguing handgrip task. Previous work has identified the premotor cortex[24], and parietal[26] cortices as regions that are important for feed forward efference copy. Further, the prefrontal cortex has been implicated in decision to quit maximal exercise[200,348]. We attempted to investigate the role of these regions in our second PPI analysis for all pairwise connections within the facilitation network. However, our analyses did not reveal any significant relationships. Although, analyses including all possible ROI-to-ROI pairwise connections may not be sufficiently sensitive to reveal a significant relationship and we are not aware of any research that would support an *a priori* hypothesis regarding pairwise PPI interactions within this network. Consequently, we do not exclude that connectivity changes between these regions and other aforementioned cognitive control regions may be affected by MPH

during our fatiguing task but recognize that further experiments will need to be conducted in order examine them, or perhaps by using DCM or Granger Causality.

3.5.4.2 Experimental limitations

First, MPH mildly elevates heart rate and blood pressure[349] and one might attribute our findings to this effect. However, previous research[349] indicates that, as expected, the BOLD signal in M1 increases with tapping frequency regardless of the presence or absence of physiological changes induced by MPH. Thus, if the BOLD responses in MPH conditions was simply representing an elevated autonomic response then we anticipate that we would have seen a similar, but increased, activation[103] in placebo conditions, but this was not the case. Further, our PPI analyses implemented an validated principle component based strategy (aCompCor) [316] to remove effects physiological in nature. In a similar light, it might be interpreted that MPH's increase on handgrip force output is peripherally mediated through an increased oxygen delivery to the muscle mediated by an increase in heart rate. This explanation rests on the false assumption that fatigue is primarily a peripheral phenomenon and that the presence of lactate hinders muscle performance. To elaborate, an exclusive peripheral interpretation would erroneously assert that MPH increases oxygen delivery to the muscle and subsequent reduction in anaerobiosis (i.e. reduction in lactate production), which leads to improved force output. However, this interpretation has been discredited by Swart *et al*. (2009)[1] who also demonstrated that participants had higher, not lower, lactate concentrations during MPH-induced performance improvements. Further, lactate is no longer viewed as an anaerobic product causing exercise failure[44]. Thus, we interpret that MPH's peripheral effects are not the source of the observed effects here.

Second, our study is restricted to the brain and does not examine other parts of the CNS. Afferent signals travel through small diameter fibers to the spinal cord where they synapse and ascend to higher cortical areas such as the IC, ACC and sensory cortex (Figure 1 in Craig (2003)[79]) and OFC[104]. Areas such as the periaqueductal grey[86], parabrachial nucleus[220] in the brainstem, and lamina cells in the spinal cord are

components of the afferent signal pathway[79] and are important for homeostatic regulation. Indeed, MPH binds in the medulla, hypothalamus, and spinal cord of the rabbit[350] suggesting that MPH could potentially exert an effect via these areas. Studies implementing the use of transcranial magnetic stimulation are warranted in order to determine if the descending motor command is modulated by MPH in the brainstem or spinal cord.

Thirdly, a key feature of central fatigue theory is that the brain manages exercise of known duration in advance of catastrophic tissue failure[132,351]. While the length of the handgrip experiment remained constant, the target forces were dynamically adjusted throughout the experiment according to trial success or failure (see section 3.3.3.3) and thus we are not able to validly enter a debate of any potential modifications of teleoanticipatory strategies that participants may have performed throughout the experiment. In a similar light, Swart *et al.* (2009)[1] explained that MPH did not alter feed forward mechanisms by showing that initial force output did not differ in a self-paced fixed RPE trial. However, we were not able to perform the same analyses given that this was not a self-selected fixed RPE trial.

Fourthly, the fMRI environment imposed three experimental limitations for our study. 1) Handgrip does not well match the complexity of whole-body exercise involved in most sporting activities. The data collection of fMRI necessitates that the head is in a fixed position and thus exercise involving in large body movement is susceptible to image artifacts. Unfortunately, this is an unavoidable limitation in all fMRI research. 2) We were not able to fully assess fatigue at the end of the experiment via evoked contractions, which would elaborate on the presence of central fatigue[299]. Thus, our measure of fatigue (i.e. calculating the slope of average maximum force) does not differentiate between central and peripheral fatigue[298]. 3) Collecting of RPE is easily achieved during a cycling task. However, verbal collection of RPE during fMRI scanning is difficult to collect over the noise of the scanner. RPE reporting via a MRI compatible keypad or visual scale controlled by handgrip force should be an aim for future studies.

3.5.5 Conclusions

This is the first study to provide neural correlates of fatigue while using the ergogenic stimulant MPH. MPH improves force production throughout the fatiguing handgrip task (Figure 24) and alters brain connectivity (Figure 29) between regions of the motor cortex and IC during a fatiguing handgrip task. This MPH-related change in brain connectivity may represent an upstream influence on the motor cortices during muscle fatigue. This is particularly interesting since the IC has previously been assigned an inhibitory role[2,116,174]. MPH appears to exert its ergogenic effect over the course of the task rather than at a specific point during the task (Figure 33), which supports the notion that exercise is regulated outside the decision to quit[132,301].

In the MPH condition, we see pre-task failure window activations not previously observed (Figure 28)[2] and thus it remains possible that MPH influences neural processes just prior to task failure but these differences are not statistically stable in a direct comparison to placebo. Further research is required to confirm. It is shown here that brain connectivity can be influenced by the use of stimulants during fatiguing exercise. More broadly, this study provides additional support to the line of research suggesting that the CNS acts to regulate motor drive subservient to homeostatic balance.

In the next chapter, I go on to examine the brain connectivity in the six-minute rest period immediately following the fatiguing task in order to determine how brain connectivity is influenced. More specifically, we examine whether the observed connectivity in the current chapter continues into the recovery period after the task has been completed. On the other hand, we also investigate whether the fatiguing task leads to interhemispheric functional connectivity disruption of primary motor cortices, a previous supraspinal symptom during recovery from handgrip muscle fatigue[352].

Chapter Four

Supraspinal mechanisms of muscle fatigue after a fatiguing handgrip task

4.1 Abstract

Muscles do not recover immediately after exercise has ceased and exercise has been shown to have dramatic effects on the CNS in the recovery period. Muscle fatigue and other tasks have been shown to alter functional connectivity (FC) in subsequent resting state scans. In the previous chapter we demonstrated that MPH increases force output during exercise and increases brain connectivity during a fatiguing handgrip task. However, it is not known how MPH alters brain FC in the recovery period after exercise has ceased. In a double blind, crossover design participants ingested MPH or a placebo before performing a fatiguing handgrip task during fMRI. We investigated force output and functional connectivity before and after the task. We found that 1) interhemispheric M1 FC was reduced in the recovery period 2) MPH resulted in a trend toward a more pronounced M1 FC reduction 3) we observe that FC between the IC and hand motor area, but not IC and SMA, changed from negative to positive in the recovery period and 4) FC was reduced between the right OFC and right IC, and ACC. This study demonstrates that 1) performing a fatiguing handgrip task in MPH conditions is associated with a trend towards greater FC disruptions in the recovery period after exercise which are presumably due to the greater forces generated during the task. 2) Task-related brain connectivity continues into the recovery period after exercise is ceased, which could be at least in part due to lasting group III/IV signaling and/or encoding rehearsal of task-related states. 3) Fatigue induced FC disruptions center in the right OFC and may indicate altered processing of interoceptive awareness. To our knowledge, this study is the first to identify the FC changes in the recovery period after exercise following a fatiguing handgrip task performed with an ergogenic stimulant.

4.2 Introduction

Muscle fatigue is a lasting disturbed homeostatic state characterized by a temporary inability to produce or maintain force output[10]. Muscle fatigue has effects on the CNS during and in the recovery period after exercise[123,124,353-355]. For example, muscle fatigue depresses motor evoked potentials[61,354,356,357], increases the cortical silent period[358], increases alpha (7.0 - 12.5 Hz) frequency activity[122-124], and induces asymmetrical functional connectivity (FC) in both frontal[124,125] and primary motor cortices (M1)[126].

Tasks occurring before resting state scanning have been show to dramatically affect subsequent resting state fMRI (RSfMRI) connectivity whereby task-related networks persist into the resting state period (the so called task-related bleeding effect) [222,359] and/or cause network disruption[126]. In Chapter three, we saw that MPH altered effective connectivity between the IC and hand motor area as well as between the IC and SMA. Given the known task related FC effects on subsequent RSfMRI we sought to examine whether these neural relationships continued in the recovery period after exercise has been completed. Further, given the M1 interhemispheric disruptions observed by Peltier *et al.* (2005)[352] we investigated whether increased force production could lead to greater interhemispheric disruption.

Seed based functional connectivity analysis of RSfMRI data examines task-free temporal correlations[214,215] and provides a method of analyses to examine muscle fatigue in the recovery period after exercise. In this study, participants ingested placebo or MPH prior to performing a muscle fatiguing handgrip task in the scanner and then performed a resting state scan during a six-minute recovery period. We firstly examined whether the brain connectivity that we observed between the IC and both the hand motor area and SMA during the task continued into the recovery period. Second, given that MPH[1], and other CNS stimulants[12,13], increase motor drive and allow for exercise closer to maximal ability[1,16], we tested whether MPH would induce greater fatigue-induced interhemispheric M1 disruptions[126] in the recovery period. Finally, we sought to determine other potential FC disturbances associated with fatigue outside the motor

cortices. Given the role of the right OFC[91] (Figure 3 in Craig (2002)[91]), ACC, and IC[79] in the interoception of disturbed homeostasis and their potential role in fatigue[93,131], we also investigated the effect of fatigue and MPH on FC between right OFC and these regions. To our knowledge, this is the first study to examine the effect of MPH administration on FC during the recovery period after exercise.

4.3 Methods

4.3.1 Ethical approval

Participants provided written informed consent before participation. This study was approved by the human research ethics committee of the University of Cape Town, South Africa (REF:214/2003) and was carried out in accordance with the Declaration of Helsinki on the use of human participants in experiments.

4.3.2 Participants

Sixteen right-handed participants (8 male, 8 female) without a history of neuropsychological disease, drug use (e.g. stimulants, amphetamines, tranquilizers), or recent use (1 month) of prescription medication participated in the study. Participants were assessed for handedness using the Edinburgh handedness inventory[307] and completed a neuropsychological evaluation performed by a trained psychologist using the Mini International Neuropsychiatric Interview [308]. Participant data such as age, height, and weight was collected and is displayed in Table 12. This study was partly conducted in parallel with the study described in Chapter three but resting state data collection was not performed for the first two participants. Thus, we recruited three additional participants, whom were not participants in the previous chapter. Consequently, the demographic and force-related data are presented in this chapter to reflect these additional participants.

Table 12 . Subject data illustrating mean and standard deviations of age, height, weight, BMI, and levels of physical activity in METs/week measured by the Generalized Physical Activity Questionnaire. Abbreviations: METs – Metabolic equivalent of task.

Sex	Age	Height (m)	Weight (Kg)	BMI	Physical Activity (METs/week)
8 Male 8 Female	30.08±6.28	12.88±44.66	71.76±11.06	22.91±7.87	588.4±783.2

4.3.3 Experimental design and resting state instructions

In a double blind counter balanced design participants ingested placebo or MPH and subsequently performed three scans 1) pre-task resting state scan 2) task scan during a fatiguing handgrip exercise and 3) post-task resting state scan. Immediately following the completion of the handgrip task participants were instructed that they would now begin resting state acquisition and to keep their eyes closed. Our exact verbal instructions were then "to hang out in the scanner" and was identical between participants. Following the resting state scan we acquired a structural scan. In this study we examined resting data from the 1st and 3rd scan. Participants performed the study in three separate sessions that occurred over 3-4 weeks. The procedures describing the fatiguing handgrip task were reported section 3.3.3.1 and 3.3.3.2 and were identical to those performed in Chapter three. Prior to the start of the task scan participants were asked to verbally rate how they felt on a scale from 1-10, where 1 represented completely calm and 10 represented very nervous[312]. Participants did not differ between placebo and MPH conditions (Figure 33).

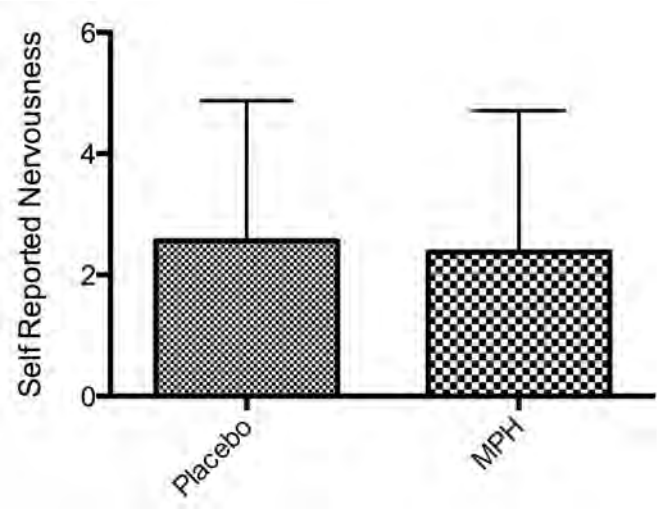

Figure 33. Self reported level of scanner related nervousness. Prior to the start of the scan participants were asked to verbally rate how they felt on a scale from 1-10, where 1 represented completely calm and 10 represented very nervous[312]. Participants did not differ between placebo (PLA) and MPH conditions. Abbreviations: MPH – methylphenidate

4.3.4 Hypotheses

As outlined in Chapter three, MPH alters IC-motor interactions during muscle fatiguing exercise. Brain networks activated during a task have been shown to persist into resting state periods[222,359]. Consequently, we predict that 1) the brain connectivity patterns we observed in Chapter three (Figure 30, Figure 31) will persist during the recovery period. MPH induces exercise performances closer to maximal ability[1] and muscle fatigue has been shown to disrupt interhemispheric M1 FC[126]. Thus, we predict that 2) MPH conditions will result in greater M1 FC disruptions in the recovery period. Further, given the known role of the ACC, IC, and OFC in processing interoception of disturbed homeostasis[79] and their proposed role in fatigue[93] we predicted that (3) a fatiguing handgrip task will alter FC between these regions. Whole brain disruptions of interhemispheric connectivity occur after muscle fatigue and it was interpreted that interhemispheric changes in connectivity were potentially caused by intense processing of sensory information[126]. Given the relationship between muscle fatigue and signals of disturbed homeostasis we chose regions related to interpreting homeostasis described by Craig (2002)[91]– the ACC, IC, and OFC. Indeed, these regions have been proposed as

potential regions for the awareness of muscle fatigue[93]. In addition, Crabbe *et al.* (2004) [124] suggested investigating regions outside the prefrontal cortex (e.g. IC in the temporal cortex) during the recovery from exercise.

4.3.5 Force analysis

As previously found in Chapter three, we anticipated that MPH would improve force output[1]. Consequently, we re-examined our force output hypothesis with a repeated measures *t* test (GraphPad Prism 5.0 software, La Jolla, CA, USA) between mean trial force values in placebo and MPH conditions. To illustrate the occurrence of fatigue we calculated the maximum trial forces for each participant per trial and then calculated the slope of these forces over the 40 trials using a linear regression model. To indicate a significant difference within each condition we performed a one-tailed one-sample *t* test on the slope coefficient. In order to compare slopes between placebo and MPH conditions, we compared the respective coefficients by means of a two-tailed repeated measures *t* test. As previously discussed, our reason for using slope-calculated fatigue instead of post-task MVCs was that we sought to determine the effect of the fatiguing task on resting state brain activity. Consequently, we wanted to start RSfMRI scanning as soon as the task was completed, which presumably would be best conducted immediately after the last trial. We interpret that participants were fatigued given that 1) our instructions were always to reach the target force, yet average maximum trial force continued to decline over the experiment (i.e. significantly declining slope) and 2) that participants continued to fail to reach the target force.

4.3.6 Functional connectivity analysis

RSfMRI FC analysis examines the relationship between fluctuations in BOLD signal between brain regions (e.g. ROIs) and is quantified by Pearson correlation coefficients. We addressed our hypotheses in a 2 x 2 repeated measures design with fatigue and drug as within-participant factors. The levels of the fatigue factor were no fatigue (pre-task)

and recovery (post-task) and the levels of the drug factor were placebo and MPH. At the individual level, we used the Conn toolbox to create a ROI matrix of person correlation coefficients between ROIs (see section 4.3.7) for each participant per condition (i.e. pre-task placebo, post-task placebo, pre-task MPH, post-task MPH). At the group level we then addressed our hypotheses with the following analyses:

1) To address our first hypothesis we implemented an ANCOVA with age and sex as covariates of no interest. We tested for the interaction and main effects of the drug (MPH, placebo) and fatigue (pre- and post-task) on connectivity between the IC and hand motor area as well as between the IC and SMA (see section 4.3.7 for detailed ROI definitions).

2) To address our second hypothesis we implemented an ANCOVA with age and sex as covariates of no interest (MPH, placebo). We tested for the interaction and main effects of the drug and fatigue on connectivity between the left and right M1.

3) To address our third hypothesis we tested for effects of drug, fatigue, and interaction on connectivity between the right OFC and both the right IC, and ACC. First, we examined whether there were any condition effects on connectivity between the right OFC and other ROIs using a repeated measures multivariate ANCOVA with age and sex as covariates of no interest and multiple comparisons accounted for using the False Discovery Rate (FDR) [211,212]. Then, we examined pairwise condition effects for the right OFC-right IC and right OFC-ACC corrected for multiple comparisons using FDR.

4.3.7 *ROI selection and definition*

In order to determine whether a similar pattern of connectivity within the IC and hand motor area was maintained during the recovery period we examined FC changes in the recovery period after exercise between the IC and the hand motor area. We also sought to determine whether there would be a continued pattern of connectivity between this IC region and the SMA. For this analyses we used three ROI masks, derived empirically from other data series in order to circumvent circularity errors described by Vul et al.

(2009)[217] and others[218] 1) a meta-analytically derived hand motor area mask associated with handgrip in the power grip position (Chapter two)[314], which we also used for PPI connectivity analyses in Chapter three, 2) a meta-analytically derived SMA mask associated with handgrip in the power grip (Chapter two) [314] and 3) an IC mask region obtained from task activations in Chapter three (Cluster b, Figure 27).

As in Chapter three, in order to obtain the motor cortex and SMA areas involved in the power grip we used MRIcron (http://www.mccauslandcenter.sc.edu/mricro/mricron/) to manually identify overlapping voxels between the area 4 ap and area 6 ROIs provided by the SPM Anatomy Toolbox[259] with the respective neuroimaging meta-analytic[314] clusters (Chapter two, Figure 8, clusters 1 and 3, respectively). Thus, the resulting hand motor area ROI and SMA were composed of only the regions involved in power grip (Figure 23). However, in the current chapter, the IC ROI was selected from task-failure activations generated in Chapter three (Cluster b, Figure 27). We preferentially chose this region over the task failure region from Hilty et al. (2010)[2] since this region was derived from participants in this study.

In order to test for disruptions of motor cortex connectivity, we used M1 cortices generated by the SPM Anatomy toolbox 1.7 (http://www.fz-juelich.de/inm/inm-1/ DE/Forschung/_docs/SPMAnatomyToolbox/SPMAnatomyToolbox_ node.html), which were defined according area 4 and 6 as in Geyer *et al.* (1996)[259].

To test for effects of drug and fatigue on connectivity between right OFC, right IC, and ACC, we used the right OFC and bilateral ACC of the Harvard-Oxford atlas (http://www.cma.mgh.harvard.edu/fsl_atlas.html), which are defined in Caviness *et al.* (1996)[320]. The right IC was the same ROI used for in first hypotheses of this chapter. An additional reasoning for selecting these three regions instead of a whole brain parcellation of ROIs was that FDR corrected measures are more effective with a fewer statistical tests[360]. Thus, although this test examines for any significant pairwise relationship, it was performed between three interoceptive regions we hypothesized to be influenced by muscle fatigue[91].

4.3.8 Resting state data acquisition

We used a Siemens 3T Magnetom Allegra Syngo MR 2004A cerebral scanner to acquire six minutes of eyes-closed resting state data. There were 180 T2-weighted images per resting scan with a repetition time of 2 s and echo time (TE) of 30 ms. We selected six minutes knowing that the central[124,354]and peripheral[361] effects of the fatiguing handgrip task would be greatest during this interval, without compromising on the recommended time to collect stable resting state data[362]. The field of view was 220 x 220 mm, 33 slices were taken per image and voxel size was 3.4 × 3.4 × 4.0 mm. At the end of each experimental session we collected whole-brain T1-weighted multi-echo fast spoiled gradient (FSPGR) anatomical images (TR=2 s, TE=1.53, 3.21, 4.89, 6.57 ms, voxel = 1×1×1.5 mm, field of view: 256x256 mm, 128 slices), for the purpose of anatomical localization of the FC data. Participant's head were padded with foam to minimize head movement while maintaining comfort.

4.3.9 Image preprocessing and denoising

We performed preprocessing of the resting-state fMRI data using Conn 15.a connectivity toolbox in Matlab 2014b (The MathWorks Inc. Natick, MA, USA). Image data was processed using Conn's default preprocessing pipeline, which implements preprocessing procedures from SPM12 (http://www.fil.ion.ucl.ac.uk/spm/). Two dummy images were collected ahead of the scan to allow the MRI signal to calibrate and were subsequently discarded from the time series before preprocessing. Images were normalized to the ICBM152 MNI template and realigned. Structural images were skull stripped, segmented, and normalized to the brain. Next, functional images were aligned to structural images using movement parameters. Subsequent images were spatially smoothed using a 8mm full-width-at-half-maximum Gaussian filter. ROI mean time series were extracted from unsmoothed images, denoised and averaged (described below).

The results of connectivity RSfMRI are susceptible to spurious correlations[214,316] caused by unwanted temporal confounds, such as head motion and physiological signals. Consequently, we used several denoising methods following preprocessing implemented within Conn to address this. Using a principle component analysis regression-based strategy (aCompCor) [316] Conn mitigates temporal confounds and other physiological noise, such as those originating from the cerebrospinal fluid. Further, Conn employs ArtRepair[319] software that identifies outlier images according to a volume-to-volume motion threshold and a volume-to-volume global signal z-value threshold. Time points that exceed these thresholds are encoded within a first level covariate of no interest that isolates images without deleting or interpolating data time points to ensure continuity. High motion volumes were identified in the regressor as those exceeding a global signal threshold z-value of 3 and motion threshold of 2mm. To ensure that there was no difference between conditions in the number of images that were removed from the analysis we calculated a 2x2 repeated measures ANOVA. In order to remove frequencies not associated with the signal of interest (e.g. potential signal noise) we employed a band pass filter (0.008 to 0.09 Hz) and the subsequent data was despiked before FC analysis. A more detailed description of Conn's denoising methods can be found in Whitfield-Gabrieli and Nieto-Castanon (2012)[316]. It has been suggested that areas of the prefrontal cortex, such as the OFC, are susceptible to signal dropout due to nearby brain tissue/air interfaces. In order to confirm that this did not affect the OFC region from which we extracted our signal, we visually inspected this region in MRIcron on a participant-by-participant basis using unsmoothed images.

4.4 Results

4.4.1 Force results

As found in Chapter three, participants produced significantly greater force in the MPH than placebo condition (Figure 34, T(15)=2.38, p=0.015, Cohen's *d*=0.147, 113.1±37.8 vs. 118.7±39.4 (±SD) Newtons (N)). As previously mentioned in section 4.3.2 we recruited three additional participants, whom were not participants in the previous chapter. Results continue to reflect those observed in Chapter three.

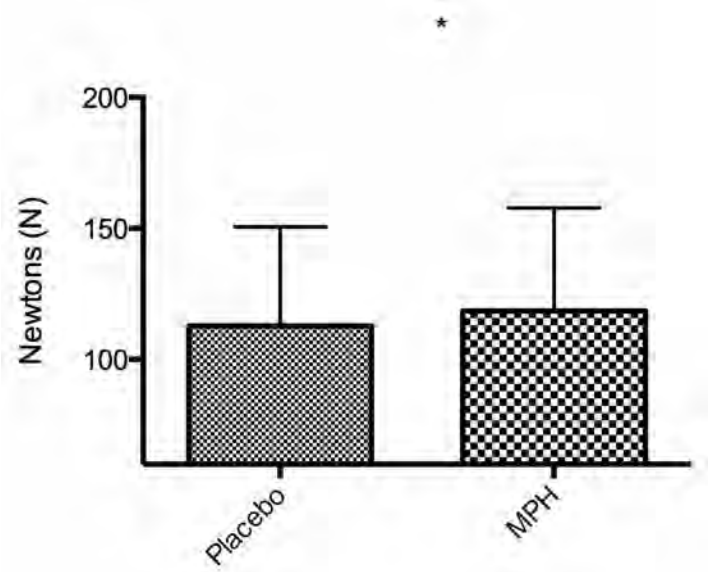

Figure 34. Mean trial grip force is greater in MPH conditions. One tailed paired *t* test demonstrates that participants produced significantly greater force in the MPH than placebo condition. T(15)=2.385, p=0.015, Cohen's *d*=0.147, 113.1±37.8 vs. 118.7±39.4 (±SD) Newtons (N). *p<0.05. Abbreviations: MPH – methylphenidate

To demonstrate that participants fatigued during the experiment we calculated the maximum trial force per trial and the slope of these values over the experiment. A one-tailed one-sample *t* test revealed a significantly negative (declining) slope for placebo (T(15)=12.9, p<0.0001) and MPH (*t*(15)=7.75, p<0.0001) conditions and a two-tailed repeated measures *t* test revealed no difference in slope between placebo and MPH conditions (T(15)=0.1131, p=0.456).

4.4.2 Functional connectivity results

4.4.2.1 Hand motor area to insula cortex (IC)

We observed an effect of drug (F(15)=6.38, p=0.017), interaction between drug and fatigue (F(15)=4.59, p=0.040), but no effect of fatigue (F(15)= 0.086, p=0.771) on functional connectivity (Figure 35). Given the centrality to our hypotheses of potential moderating effects of MPH on changes in FC, we conducted a series of post-hoc tests decomposing the interaction with two *t* tests. The FC in post task placebo conditions was significantly lower (and negative) than the corresponding connectivity estimates in post-task MPH conditions (-0.086.1±0.207 vs. 0.107±0.159 (±SD), T(15)=2.71, *p<0.016), with no differences in connectivity observed between placebo and MPH conditions in the pre-task conditions (-0.015±0.133 vs. 0.013±0.154 (±SD), T(15)=0.63, p=0.541).

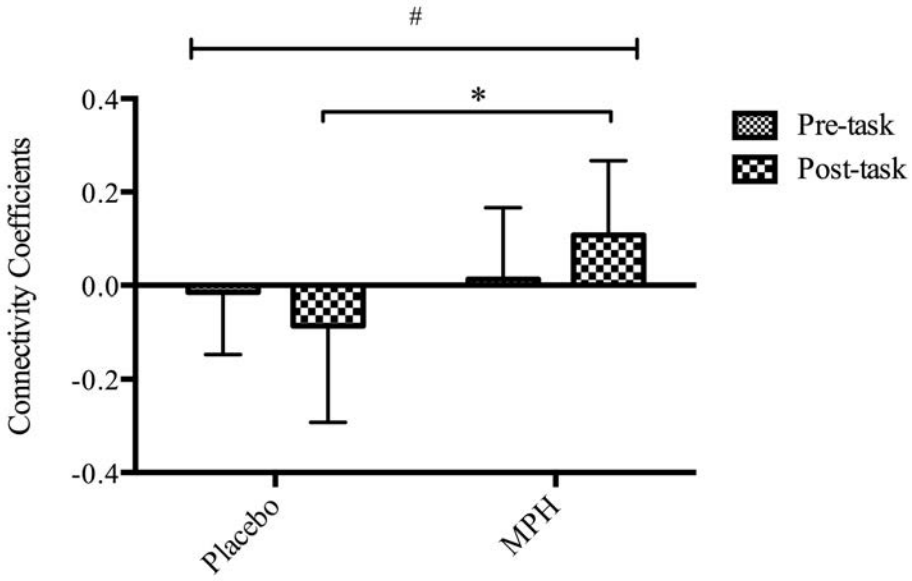

Figure 35. Functional connectivity between IC and hand motor region is altered with MPH. We observed an interaction between fatigue and drug (F(15)=2.370, #p=0.016) and effect of drug (F(15)=3.05, p=0.008) but no effect of fatigue (F(15)= 0.086, p=0.771). T tests show no difference between drug pre-task (T(15) = 0.63, p=0.541) but are significantly different post-task (T(15) = 2.71, p=0.016). *p<0.05. Abbreviations: IC – insula cortex, MPH – methylphenidate

4.4.2.2 Supplementary motor area to insula cortex (IC)

We observed no effect of drug (F(15)=0.58, p=0.716), fatigue (F(15)=0.380, p=0.710) or interaction (F(15)=0.02, p=0.985) between the SMA and IC (Figure 36).

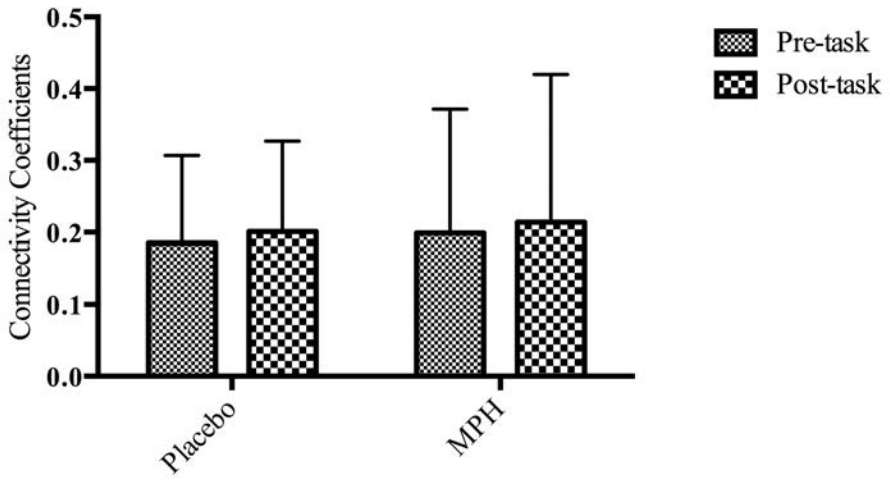

Figure 36. Functional connectivity in the recovery period between SMA and IC is not altered with administration of MPH. There was no effect of drug (F(15)=0.58, p=0.716), fatigue (F(15)=0.380, p=0.710) or interaction (F(15)=0.02, p=0.985). Abbreviations: SMA - supplementary motor area, IC – insula cortex, MPH - methylphenidate

4.4.2.3 Interhemispheric primary motor cortex (M1)

We observed both a main effect of fatigue (F(15)=2.17, p=0.046) and main effect of drug (F(15)=2.89, p=0.01) where both factors reduced connectivity. Although we did not observe an interaction effect, a trend was present (F(15)=1.92, p=0.074, Figure 37). To explore this trend, we performed a post hoc *t* test between post-task in placebo and post-task in MPH conditions revealed a highly significant difference between conditions (T(15)=4.73, p=0.0003).

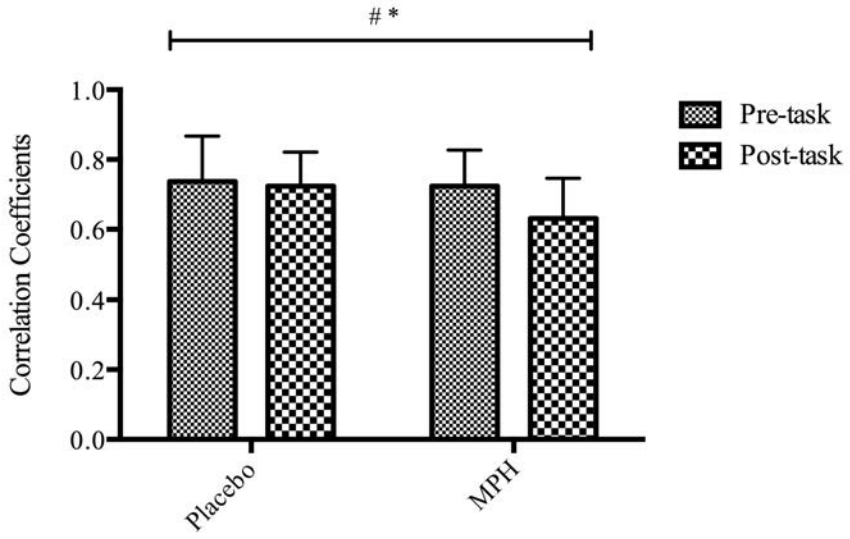

Figure 37. MPH and a fatiguing handgrip task reduced interhemispheric primary motor cortex (M1) activity functional connectivity. We observed both a main effect of fatigue, F(15)=2.17, $^{\#}$p=0.046) and main effect of drug,(F(15)=2.89, *p=0.01) where both factors reduced connectivity. Although we did not observe an interaction effect, a trend was present (F(15)=1.92, p=0.074). MPH - methylphenidate

4.4.2.4 Right orbital frontal, anterior cingulate and insula cortex

In the multivariate test to examine any effect for connectivity with the right OFC, we observed a main effect of fatigue F(13)=19.76, p=0.0002) but no main effect of drug (F(13)=0.08, p=0.971) or interaction (F(13)=0.85, p=0.65). Post-tests to address specific relationships between the right OFC and both the ACC and IC indicate significant decreases in FC for main effect of fatigue between right OFC and ACC F(15)=5.75, p<0.0001 (Figure 38) and IC F(15)=3.17, p<0.0096 (Figure 39).

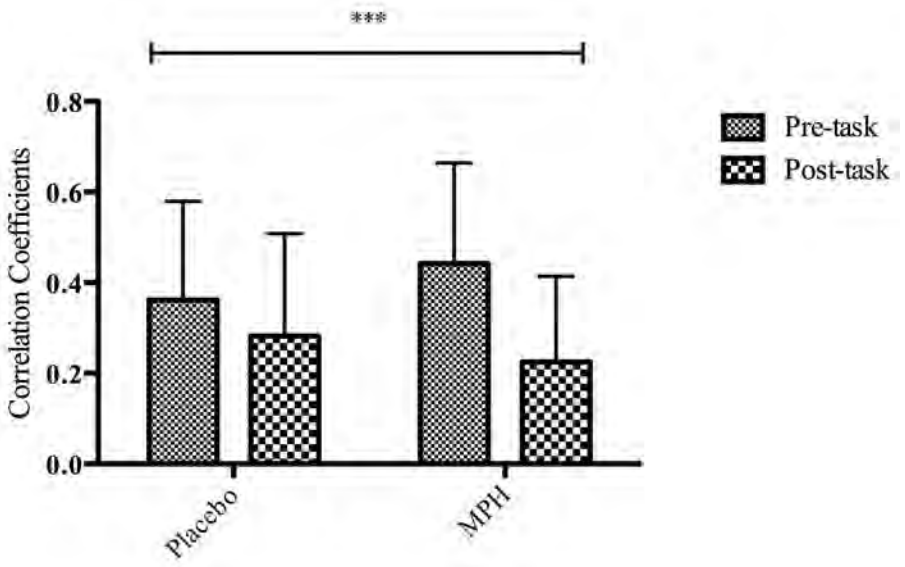

Figure 38. Functional connectivity between the right OFC and ACC is significantly decreased with fatigue. F(15)=5.75, ***p<0.0001. Abbreviations: OFC: Orbital frontal cortex, ACC – anterior cingulate cortex, MPH – methylphenidate.

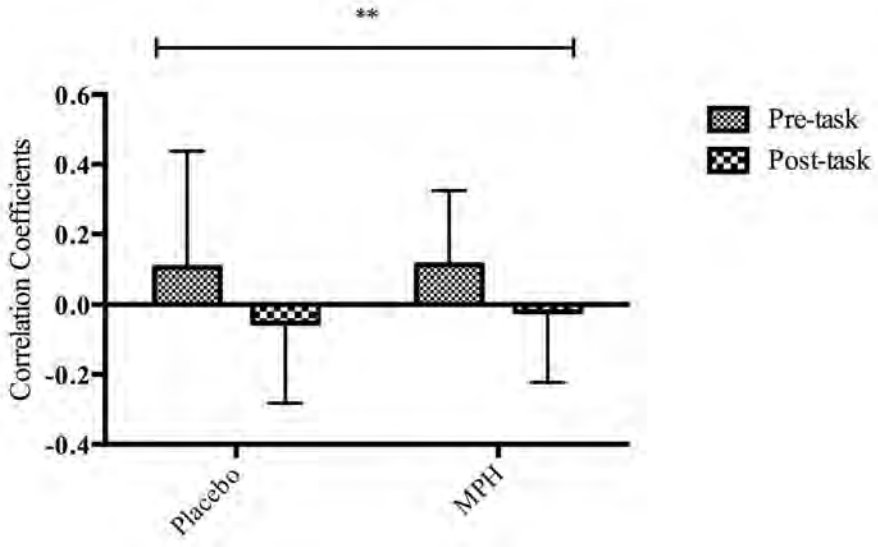

Figure 39. Functional connectivity between the right OFC and IC is significantly decreased with fatigue. F(15)=3.17, **p<0.0064. Abbreviations: OFC: Orbital frontal cortex, IC – Insula cortex, MPH – methylphenidate.

4.4.3 Denoising results

During denoising Conn isolated outlier images that were used as first level covariates from participants. There was no effect of drug ($F(30)=0.610$, $p=0.649$) or fatigue ($F(30)=0.520$, $p=0.381$) or interaction ($F(30)<0.00$, $p=1.00$) on the number of volumes that exceeded the motion or global signal threshold. The mean number of images isolated were 7.13±4.53, 8.0±6.06, 7.94±6.20, and 8.81±6.88 for placebo pre-fatigue, placebo post-fatigue, MPH pre-fatigue, and MPH post-fatigue, respectively.

4.5 Discussion

4.5.1 Main findings

This study examined the effect of MPH on handgrip force and changes in RSfMRI FC in the recovery period after exercise. We demonstrated several interesting findings: 1) The ingestion of 20 mg of MPH and performing a fatiguing handgrip task resulted in a change from negative to positive FC between the IC and hand motor area (Figure 35) 2) An MPH-related improved force output (Figure 34) during the task led to a trend of greater interhemispheric M1 FC reduction (Figure 37). 3) FC was reduced in the recovery period after a fatiguing handgrip task between the right OFC and both right IC cortex, and ACC.

4.5.2 Insula and hand motor area connectivity

The IC is thought to integrate interoceptive homeostatic information[91,363] from the periphery[102,303] and to be important for the termination of exercise[2]. The IC is heavily integrated with the motor cortices[111] and as seen in Chapter three the IC may provide an excitatory influence on the motor cortices under MPH conditions during muscle fatiguing exercise[2,116]. Interestingly, we observed that MPH shifted FC from a negative to positive between the IC and hand motor area in the recovery period after exercise. It is possible that the observed FC changes are 1) lasting afferent signaling or 2) a bleeding

effect[222]/cognitive inertia, whereby similar network activity is maintained after a task is complete [359].

The FC we observed in a six minute recovery period may reflect an inhibitory effect in placebo conditions and excitatory effect in MPH conditions independent of executing handgrip task. In non-exercising muscles, a pain-inducing injection of hypertonic saline leads to lasting decreased cortical excitability[364]. Afferent signals are generated in response to painful mechanical and chemical stimuli[80] (e.g. phosphate[82]) associated with fatiguing muscle contraction and have been shown to inhibit motor neuron firing rates[88]. Further, these fibers continue to fire after muscle contraction has stopped[82]. The connectivity changes we observe are independent of force generation since participants were at rest. Thus, the FC we observe in a six minute recovery period may reflect an inhibitory effect in placebo conditions and excitatory effect in MPH conditions independent of executing handgrip task. This observation is inline with the finding that connectivity during a task maintains similar activity in the rest period after the task [222]. The so-called bleeding effect, or cognitive inertia, may reflect active task disengagement, rehearsal, and/or encoding of previous states, which continue post-task[356]. Although we cannot confirm the persistent activation of afferent fibers, we suggest that the connectivity pattern observed in placebo conditions could be at least in part due to lasting group III/IV signaling or task disengagement, while the connectivity pattern observed in MPH conditions could represent encoding rehearsal or task-related encoding of previous states. It should be noted that the current chapter utilized a different IC ROI than what has been used for connectivity during the task in Chapter three (right and left IC, respectively, see ROI selection and definition) suggesting that this relationship (Figure 35) is not simply inertia of activation in the same regions but perhaps a meaningful effect between the motor cortices and IC extending into the recovery period, which is influenced by MPH.

Additionally, the observed change in connectivity between placebo and MPH may represent secondary widespread MPH–induced alterations of network activity. MPH has previously been shown to alter RSfMRI[365]. For instance, there is evidence that MPH

affects connectivity of striatal networks, although the exact nature of these changes and MPH's role in the motor network is not clear. MPH-induced decreased connectivity was reported for the cortico-striatal-thalamic network at rest, with increases in connectivity concomitantly observed in the sensory motor network[366]. Conflicting with this, evidence shows that MPH increases striatal connectivity, while sulpiride, a DA antagonist, has the opposite effect[367]. The ROI pairwise analysis we have performed excludes the examination of the potential involvement of striatal regions, and as such our data interpretations cannot enter into the debate on striatal involvement. Instead, we suggest that MPH may have induced the motor cortex or IC[368] to become involved in competing networks[369], although, we do not have the data to support this interpretation. Nonetheless, the FC between these regions did not differ before the fatiguing task. Thus, in line with the data shown here, we interpret that MPH and fatigue interact to alter FC changes in the brain but whether this occurs through an IC-motor cortex relationship or network switching cannot be conclusively confirmed.

In Chapter three, we saw MPH increased effective connectivity during fatigue between the IC and SMA. However, we did not observe the same bleeding effect of brain connectivity between these regions (Figure 36) as was observed between IC and the hand motor area (Figure 35). The study of task influence on resting state periods is a relatively new field of research[221] and ROI-specific relationships have not been well investigated. Conflicting evidence by Tailby *et al.* (2015)[222] demonstrates pervasive task-related increases in connectivity after a non-fatiguing motor task regardless of ROI. In agreement with the current findings Roth *et al.* (2014) found SMA connectivity to vary between task and rest, where some connections remained stable, and others not.

Our RSfMRI data support the notion that task related changes between the IC and motor cortex, but not IC and SMA, continue to be present after muscle-fatiguing exercise has ceased but certain analysis limitations of FC should be considered. Similar to PPI, FC cannot validly assess direction of influence and thus we cannot confirm directional influences but only an interaction among brain regions during the task and a residual relationship after the task. In addition, analysis methods commonly used in functional

connectivity, such as global signal regression, have raised issues with interpreting negative connectivity[370]. However, The aCompCor method[316] used in our analyses does not employ global signal regression and thus improves inference regarding anti-correlations. Although speculative, we propose here that MPH could be altering communication between the hand motor cortex and IC in the recovery period after a fatiguing exercise task.

4.5.3 Interhemispheric motor cortex connectivity

We show that participants increased force output during MPH conditions (Figure 2, Cohen's $d = 0.147$) and that this led to a disrupted neuronal state in the brain as measured by interhemispheric M1 FC [126]. Although, the observed increase in force was small, it is in line with previous effects of simulants on force output[17,182,193]. In line with our hypothesis, MPH-induced force increase coincided with a more pronounced reduction in interhemispheric connectivity, albeit at a trend ($p=0.074$) level.

The effect of fatigue on interhemispheric M1 FC could be caused by a number of processes. For example, the volume of activation in the sensorimotor cortex[371] is more affected on the contralateral side of the task after a fatiguing handgrip task and motor evoked potentials induced by TMS have been shown to be reduced on the contralateral side after handgrip[361] as well as in other fatiguing exercise[356,357]. Further, the cortical silent period, which reduces the probability of neuronal firing[372] and partly arises from intracortical inhibition, is lengthened following fatiguing exercise[358]. Cortical silent periods, or refractory period, which have been shown to be dependent on group III/IV afferent fibers[75], could be acting as a central mechanism to reduce neuronal firing. Indeed, type III/IV afferent fibers respond to metabolites generated during exercise and continue to fire after muscle contraction has stopped[82], suggesting a potential lasting inhibitory effect. On the other hand, prolonged motor cortex activation during grip may lead to post synaptic receptor activation via indirect gating of metabotropic receptors, which modulate neuronal state (e.g. excitability and activation) lasting for minutes in duration, which would disproportionately affect discharge rate on the contralateral side

(Figure 10-8 in Kandel et al. (2000)[21]). Together, reduced motor evoked potentials, lengthened cortical silent periods, and prolonged activation may modify M1 excitability and consequently neural activity that would affect FC between the contralateral and ipsilateral M1, which has not been activated to the same extent[63] (Chapter two, Figure 8). Indeed, reduced excitability of the motor cortex is thought to be a core aspect of central fatigue[54,55].

We observed a trend towards a significant interaction between drug and fatigue. Although not statistically significant, a Cohen's *d* of 0.85 was obtained for post-hoc repeated measures *t* test between placebo and MPH in the recovery period, suggesting a strong effect difference between conditions. A potential reason for why interhemispheric connectivity may not have been significantly more pronounced in MPH conditions was that more intense contractions may have led to greater recruitment from ipisilateral M1 neurons[177] in an attempt to overcome fatigue[63,65,174], which if utilized would reduce M1 asymmetry during the task. We interpret that MPH allows participants to reach stronger grip forces that were not previously possible in placebo conditions[1], which in turn resulted in larger interhemispheric M1 disruptions. Swart *et al.* (2009)[1] demonstrated that in MPH conditions participants had higher peripheral indicators of exertion such as lactate, oxygen consumption, heart rate and breathing rate, which indicates participants were able to withstand higher work rates in MPH conditions. MPH's ergogenic effects may be explained by the increase in DA transmission associated with MPH[145], which could increase willingness to exert more effort[18,187]. Since the goal of the task was to always reach a force level, which was dynamically changed in the current experiment (see section 3.3.3.3) to encourage fatigue regardless of stronger forces applied, we interpret that MPH in our study did not prevent the occurrence of fatigue via a restoring effect (indeed both conditions displayed a negative slope of force) but raised the force output that participants performed in order to complete the task, perhaps via IC-motor cortices excitatory mechanisms proposed in Chapter three.

4.5.4 OFC, ACC and IC network connectivity

We observed FC changes in response to muscle fatiguing task centralized in the right OFC. EEG studies [124,125,355,373] have well-established that exercise disrupts frontal alpha interhemispheric symmetry and whole brain disruptions of interhemispheric connectivity. Peltier *et al. (*2011)[221] interpreted that the fatigue-induced changes in wide spread interhemispheric connectivity (i.e. between hemispheres) were potentially caused by intense recruitment or processing of information associated with a muscle fatiguing task[126]. While on the other hand Tailby *et al.* (2015) demonstrated increases in connectivity regardless of ROI after a motor task. Thus, it was not clear whether to expect task-related increase or decreases in connectivity within these regions in our study. Post-task decreased FC was observed between the OFC and both the ACC, and right IC.

Muscle fatigue can be viewed as a state of disturbed homeostasis[374] and disturbed homeostasis is associated with increased activation in the ACC [375] and insular cortex[79], perhaps reflecting processing of interoception[91]. In humans, the IC projects to the OFC[104,108] and ACC[111]. Muscle fatigue activates the IC[2] as well as the OFC after fatigue[127], which are both activated in response to sympathetic arousal[103,376]. Indeed, a viscerosensory network that includes the IC and OFC, has independently proposed by multiple research groups [91,104,105] (see Figure 3 in Craig *et al*. (2002)[91]). Pain, which is an inseparable part of muscle fatiguing exercise, generates both a sensory and emotional response[91], which is partly processed by the OFC[91]. The IC and ACC have both been associated with the response to pain[109,375]. The pain response is thought to be formed when sensory information from the IC is relayed to the OFC, which is thought to be important for interoception of homeostatic signals[377]. Indeed, afferent fibers continue to fire after muscle contraction has stopped[82]. Interestingly, acupuncture, a pain reduction treatment, increases ACC connectivity in the default mode and sensorimotor network network[378].

Although we cannot confirm, it is possible that the fatigued state alters resting processing between the OFC and these regions in response to interoception of pain related to performing the handgrip task. Future studies should address differential effects of these various aspects of fatigue on OFC intrinsic connectivity, and the implications of reduced connectivity between this structure and other task-relevant brain regions for physical fatigue. On the other hand, connectivity disruption in the OFC is interesting given the proposed role of mental fatigue in exercise[27]. Mental fatigue, which is an inseparable component of physically demanding exercise[130], is associated with activation the OFC[128] and functional connectivity in the medial frontal gyrus[379]. Given that the OFC has been implicated in processes of sensory integration, muscle fatigue, pain, and mental fatigue, it is possible that connectivity within these regions suffers a post-task depression similar to the effect we observed between interhemispheric motor cortices.

4.5.5 Limitations

There are a number of limitations to this study that should be borne in mind when interpreting our results. Firstly, RSfMRI connectivity is based on correlational findings, and with the possible exception of task related methods like Dynamic Causal Modeling and Granger Causality Analysis any connectivity-based conclusion provides limited support for arguments of causality. Since RSfMRI is a task-free analysis we are unable to interpret FC to be associated with a specific task or event. Secondly, there are different hemodynamic response functions between individuals and cortical regions that may result in different temporal delays [347], which make it difficult to interpret temporal correlations of neuronal activity (a criticism also applied to Granger Causality). Thirdly, connectivity fMRI is particularly susceptible to spurious correlations[214,316] caused by unwanted temporal confounds such as head motion and physiological signals. While Conn's aCompCor method[316] has been shown to be effective in removing unwanted confounds[380] without the use of global signal regression, it is not possible to guarantee the removal of all physiological noise. For example, there are HR increases associated with handgrip and MPH. The potential influence of HR noise originating from MPH can be excluded since we did not observe any pre-task differences in placebo and MPH conditions. Further, it

has been shown that heart rate returns to baseline within less than a minute of ending a repetitive 16 s 80% MVCs[381]. Thus, it is unlikely that the FC changes we observe are a consequence of the physiological noise. Indeed, we applied a motion and global signal threshold and illustrated that there were no differences between the numbers of outlier images identified between conditions. Fourthly, despite showing a significantly declining slope of force we were not able to fully assess fatigue at the end of the experiment via evoked contractions, which would allowed us to elaborate on the presence of central fatigue[299]. Thus, our measure of fatigue (i.e. calculating the slope of average trial force) does not differentiate between central and peripheral fatigue[298]. Fifthly, while we demonstrate a potential post-exercise relationship between the IC and the hand motor area, we cannot determine other motor pathway components that may be involved. For instance, stimulants such as caffeine have been shown to increase submaximal muscle force[195]. However, evidence suggests that the effect of stimulants can be attributed to supraspinal effects rather than on the muscle itself[193]. Finally, due to pre-post study design constraints we were not able to address the possible effect of time-in-the-scanner as a potential confounding variable in influencing our FC results.

4.5.6 Conclusions

Firstly, administration of 20 mg of MPH causes a positive shift in connectivity between the IC and hand motor area in the recovery period after exercise has ceased (Figure 35). Further, the observed increase in MPH connectivity during recovery supports the so-called bleeding effect. Secondly, increased force production during a fatiguing handgrip task (Figure 34) is potentially associated with a more pronounced functional connectivity disruption (Figure 37) in interhemispheric M1. Lastly, this study demonstrates novel disruptions of FC with the right OFC and key interoceptive regions, such as the IC and ACC, supporting the possibility that participants have altered interoception following a fatiguing task, which are perhaps due to the symptoms of muscle fatigue (e.g. pain, discomfort). The results of this study support that central fatigue processes are ongoing after exercise has ceased[80,352].

In confirming the observation that preceding tasks can influence subsequent resting state connectivity, a broader conclusion of this study is that caution should be taken when performing resting state connectivity experiments. This is particularly applicable to projects that pool the acquisition of functional and resting state data into a single data collection session, or the pooling of larger multi center projects that may not have controlled for previous tasks prior to resting state scanning.

Chapter Five

Synthesis of research

5.1 Review

The earliest hominids gained an evolutionary advantage over their counterparts by its ability to grip and manipulate objects into tools for hunting, eating, and aggressive behavior. In the present day, this ubiquitous action remains equally important for how we interact with our environment. However, like all muscular contractions, handgrip is regulated partly by a multitude of peripheral and central mechanisms that lead to muscle fatigue. Peripheral fatigue theory attempts to explain the mechanisms that occur downstream of the neuromuscular junction, where as central fatigue theory addresses mechanisms from the neuromuscular junction to the brain. Central fatigue theory proposes fatigue is perceived and interpreted by similar neural structures that regulate homeostasis. A sub-component of central fatigue specifically examines the reduced descending drive from the motor cortex, which is known as supraspinal fatigue. However, the supraspinal mechanisms that influence the motor cortices to reduce force output have remained elusive to central fatigue theory. In order to investigate this we used a muscle fatiguing handgrip task completed within a MRI scanner. We first investigated the brain regions responsible for the performance of handgrip in its most fundamental type and pattern and generated ROIs characterizing the areas important for handgrip. Then, using these regions we examined the central mechanisms of handgrip fatigue, with a particular focus on the IC, in three separate time resolutions: 1) throughout the task (during grip), in the moments just prior to task failure (pre-task failure), and during the recovery period after the task (post-fatigue).

5.1.1 Main findings

Our main findings were:

Chapter two:

i. Grip type and pattern generate both unique and shared brain activation.
ii. Precision and dynamic grip generate stronger activation than power and static, respectively.

iii. Despite these differences there is a striking regional similarity between the areas involved in different grip type and pattern.

Collectively, chapter two demonstrates that different forms of handgrip are not only characterized by location and strength of activation but possibly by other mechanisms such as brain connectivity, neural coding, or oscillations in electrophysiological activity.

Chapter three:

i. The IC and inferior frontal gyrus are important structures for task failure.
ii. MPH improves force output throughout a fatiguing handgrip task but not in the moments prior to task failure. This supports the notion that the ergogenic effect of MPH is evident throughout exercise rather than in the moments just before quitting exercise.
iii. MPH alters brain connectivity between the IC and each of the hand motor cortex hand area and SMA This suggests an excitatory relationship and/or increased communication in MPH conditions.
iv. Despite the potential influences that MPH may have on motivational input into the facilitator network, we did not observe any evidence to suggest that MPH influences effective connectivity between regions during grip or task failure.

Our findings from Chapter three suggest that MPH alters effective brain connectivity between the motor cortices and the IC throughout a muscle-fatiguing task rather than in the moments prior to task failure. This change in effective connectivity may represent an upstream supraspinal mechanism acting to increase force output under the influence of ergogenic stimulants. The results of chapter three are consistent with the CGM and neurotransmitter model of fatigue. Unfortunately, since we did not directly control for feedback or feed forward mechanisms, we are unable to enter into debate of how our results apply to the psychobiological model.

Chapter four:

i. MPH-induced increased in task-related force output may induce a trend towards greater interhemispheric M1 FC disruption.
ii. Task-related EC between the IC and hand motor area appears to persist into the recovery period as indicated by a similar FC relationship. However, this is not true for IC and SMA connectivity.
iii. A fatiguing handgrip task reduces FC in regions known to be important for the interoception of disturbed homeostasis.

Chapter four demonstrates that a fatiguing handgrip task leads to both a persistence and disruption of FC in the recovery period in regions related to the task and interoception of homeostasis, respectively. More broadly, this chapter shows that caution should be taken when fMRI research initiatives contain a series of resting state or task scans.

> ***Thesis contribution****:* Handgrip is a complex task partly orchestrated by network brain regions including the motor cortices (e.g. M1, SMA) (Chapter two), which interact with homeostatic brain regions (e.g. the IC) under fatiguing conditions (Chapter three). Ingestion of MPH leads to increase in force output and alters task-related brain connectivity (Chapter three), which continues to be influenced after the handgrip task ceases (Chapter four).

5.2 Relevance of findings, limitations and future directions

This thesis makes a novel contribution to the understanding of the supraspinal processes of handgrip, handgrip muscle fatigue, and increases our understanding of how CNS stimulants lead to changes in force output during exercise.

We began our analyses in Chapter two with an ALE of the brain regions involved in handgrip. An intriguing finding of this chapter was that dynamic and static handgrip shared activation in area 2. This region has been implicated in the evolution of hand and tool use[268]. The old world monkeys and the cebus monkey are the only primates besides humans that have a well-developed area 2 and an opposable thumb[423]. It would be interesting to perform similar ALE analysis in primates, particularly with the old world monkeys[268], in order to investigate potential differences between species, which may shed light on this important trait. Although, this line of research poses challenges due to a lack of studies and species related brain structural differences.

In Chapter three we investigated the neural correlates of the ergogenic effect of MPH. The ergogenic effect of CNS stimulants have been long known[12,13]. It is for this reason

that MPH and other readily available stimulants, such as Adderall[382], are illicitly used in competitive sports. For example, 33% of the resolved cases in 2013 by the US anti-doping agency were for stimulant use and 31% of 234 NCAA athletes reported using performance-enhancing drugs, which included stimulant use, despite that these athletes were all subject to random drug testing throughout the academic year[383]. The 2015 world leader in the 100m sprint, Justin Gatlin, tested positive for amphetamines in 2001. Gatlin defended these allegations by claiming therapeutic use for attention deficit hyperactivity disorder (ADHD). The incidence of ADHD-related therapeutic use exemption in major league baseball has reached nearly 8%, which has nearly quadrupled since the organization banned amphetamine use [384]. This is highly suggestive that athletes are attempting to exploit MPH for its performance benefits. MPH, which is commonly used to treat ADHD, is a world anti-doping agency band substance, yet how it acts to improve performance is unknown. The results of Chapter three suggests that MPH alters IC-motor cortex connectivity during a fatiguing handgrip task leading to increased force output but further research is warranted to investigate its causal relationship to improved performance. These results have implications for the question of whether those with ADHD should be allowed to use MPH during competition in sport. The rationale for therapeutic use is that those with ADHD are at a cognitive disadvantage and should be allowed therapeutic use exception[385]. However, in a double blind MPH baseball trial, boys with ADHD increased their game-related attention but this did not improve their skill performance[386]. Further, the proposed ergogenic mechanism of MPH in this thesis acts on interoception-related brain structures, which we assume function no differently during muscle fatigue between those with or without ADHD. Thus, regardless of diagnosis, we propose that MPH should not be permitted because it may lead to an unfair advantage (i.e. increased force output). Mild stimulants such as caffeine are permitted and frequently used in competitive sport. However, unlike caffeine, MPH and bupropion may disrupt normal heat regulatory mechanisms[14] that are important for preventing exercise-induced hyperthermia. As such, MPH and other drugs alike should not be allowed in sports associated with intense cardiovascular exercise based on safety measures alone, notwithstanding the unfair advantage they may provide.

Discussion of population-specific responses to DA stimulants warrants highlighting the question of whether DA tone is an important factor for the efficacy of ergogenic stimulants. Rat populations that are bred for increased voluntary wheel running have higher DA tone than controls[191] and do not ergogenically respond to MPH[192], while the opposite is true for control rats. Similarly, rats genetically predisposed to obesity also display higher levels of DA tone in comparison to controls[182]. Investigating the relationship between DA tone and ergogenic response to stimulants would be relevant given the recent proposal of stimulant use to increase physical activity in low activity/overweight populations[182]. Indeed, all participants received a 20 mg dose of MPH regardless of body weight. Unfortunately, we were unable to collect blood plasma samples and thus have no measure of individual drug bioavailability for our participants. Future experiments could employ PET to quantify the relationship between the ergogenic response (e.g. percent mean force improvement) with the binding potential of MPH to DA[387] transporters as well as a measurement of DA receptor availability [388], which together would reflect DA tone and the efficacy of the drug, respectively.

In a similar light, the hemodynamic response is not well understood and may be driven by neurotransmitters such as dopamine[207]. For example, dopaminergic modulation has been associated with both increases[207] and decreases[208] in cerebral blood flow. Dilation or constriction of microvessels is thought to be mediated by dopaminergic post-synaptic action of astrocytes and/or dopaminergic receptors on microvessels. Since the BOLD signal is partly a measure of cerebral blood flow this confound should be kept in mind. However, given that the study of neurotransmitter-mediated microvascular modulation is an inchoate line of research, and thus not well understood, it is unclear how the interpretations of this thesis should be modified.

Handgrip induces intense sensations of muscle fatigue but it does not generate all the sensations associated with whole body exercise (e.g. increase in temperature[137] and air hunger[100]). Excessive body heat, for example, is an important factor regulating exercise performance[136]. Temperature is assumed not to be a relevant experimental factor related to performance in the context of handgrip exercise. As mentioned, ergogenic drugs

similar to MPH, such as bupropion, are thought to prolong exercise through a disruption of heat regulatory mechanisms[148,300]. Given the constraints of the fMRI environment, we were unable to investigate the involvement of stimulant-related temperature effects during whole body exercise. Future studies should be conducted in order to examine the impact of MPH on brain activity during fatiguing cycling, perhaps using an EEG design as implemented in Hilty *et al*. (2011)[116]. Some have successfully investigated low exertion cycling in the fMRI[389]. However, any exercise that generates high physiological responses (i.e. perspiration, increase in heart rate, respiration) is highly susceptible to false activations. Further, the supine and upright cycling do not generate the same metabolic response[390,391] or RPE and thus a cycling design does not perfectly model exercise either. We are aware of previous work[392] that has attempted this but decided that it would not be an appropriate line of research to pursue for these reasons.

Other fMRI methodological constraints include reduced communication with the research participant. The voice of a participant is inaudible over the noise of the scanner, which makes verbal collection of RPE difficult. At the time of data collection we were not able to implement a solution for collecting RPE such as an MRI compatible keypad or visual scale controlled by handgrip force. Thus, collection of RPE during and after the task should be an aim for future studies in order to determine subjective sensations of fatigue. Given the ergogenic effect of MPH and the importance of interoception of disturbed homeostatic signals during exercise fatigue[93] it may be useful to assess how consciously aware the participant is of the effort he/she is making during the task effort awareness scale[393]. Task effort awareness is an RPE scale designed to measure the psychological effort associated with the performance of a physical task and was developed by Swart *et al*. (2012)[393] at Exercise Science and Sports Medicine, University of Cape Town.

Recent research[17] demonstrated a caffeine induced 5% increase in post-task MVC and reduction in task-related RPE and motor related cortical potential (MRCP) in the motor cortices. Authors proposed that the reduction in MRCP was indicative of reduced corollary discharge associated with the concomitant decrease in perception of effort. Chapter three also implicates the SMA but we found a potential excitatory influence

between the IC and SMA in MPH conditions. It is difficult to compare our results given that they examined the combined EEG activity of the premotor, SMA, and M1 on fine time resolutions (1.5s before, 0-1s and 1-2 during and 3-4s during recovery). Nonetheless, this encourages further research using EEG to examine the effect of MPH on other potential electrophysiological mechanisms', such as changes in the bereitschaftspotential associated with motor initiation or state changes (e.g. arousal, see section 2.5.5.). Alternatively, we could investigate caffeine's potential ergogenic effect within the context of the current handgrip/fMRI design. This would be particularly relevant to sport competition given that caffeine is currently permitted by the world anti-doping agency.

In Chapter four we observed task-related FC changes during six minutes of resting state. This duration was selected knowing that the central[124,354]and peripheral[361] effects of the fatiguing handgrip task would be greatest during this interval. However, we did not address the temporal profile of these FC changes. As a future direction of research, it would be interesting to investigate when FC changes return to baseline and whether this differs between ROIs. In order to examine the FC temporal profile, we would implement a longer resting state period (e.g. twelve minutes) or perhaps two segmented resting scans separated by a brief inter-scan period. The latter approach was recommended by Dijk *et al*. (2010)[362], who demonstrated identical resting state results between a twelve-minute continuous scan and two closely timed sequential six minute scans. The advantage to a segmented scan is that it may allow improved data collection from potentially difficult participant populations (e.g. children, older adults) and more practically, it prevents having to split resting sessions during data pre-processing.

5.3 Conclusions

This thesis demonstrates that the regulation and interoception of a muscle fatiguing handgrip task involves multiple brain areas. In order to properly understand muscle fatigue, further investigations should examine brain connectivity between multiple ROIs given that muscle fatiguing exercise engenders disturbed signals of homeostasis,

interoception of those signals, and ensuing modifications of motor drive by the motor network involved in the task.

References

1. Swart, J. *et al.* Exercising with reserve: evidence that the central nervous system regulates prolonged exercise performance. *Br. J. Sports Med.* **43,** 782–788 (2009).
2. Hilty, L., Jäncke, L., Luechinger, R., Boutellier, U. & Lutz, K. Limitation of physical performance in a muscle fatiguing handgrip exercise is mediated by thalamo-insular activity. *Hum. Brain Mapp.* **32,** 2151–2160 (2010).
3. Leakey, L. S., Tobias, P. V. & R, N. J. A New Species Of The Genus Homo From Olduvai Gorge. *Nature* **202,** 7–9 (1964).
4. Napier, R. J. The prehensile movements of the human hand. *J Bone Joint Surg Br* **38-B,** 902–913 (1956).
5. Young, R. W. Evolution of the human hand: the role of throwing and clubbing. *J. Anat.* **202,** 165–174 (2003).
6. Marzke, M. W. & Marzke, R. F. Evolution of the human hand: approaches to acquiring, analysing and interpreting the anatomical evidence. *J. Anat.* **197 (Pt 1),** 121–140 (2000).
7. Landsmeer, J. M. Power grip and precision handling. *Ann. Rheum. Dis.* **21,** 164–170 (1962).
8. Sasaki, H., Kasagi, F., Yamada, M. & Fujita, S. Grip Strength Predicts Cause-Specific Mortality in Middle-Aged and Elderly Persons. *Am. J. Med.* **120,** 337–342 (2007).
9. Armstrong, T. *et al.* Muscle responses to simulated torque reactions of hand-held power tools. *Ergonomics* (2010). doi:10.1080/001401399185856
10. Enoka, R. M. & Stuart, D. G. Neurobiology of muscle fatigue. *J Appl Physiol* **72,** 1631–1648 (1992).
11. Noakes, T. D. From catastrophe to complexity: a novel model of integrative central neural regulation of effort and fatigue during exercise in humans: summary and conclusions. *Br. J. Sports Med.* **39,** 120–124 (2005).
12. Cuthberson, D. P. & Knox, J. A. C. The Effects Of Analeptics On The Fatigued Subject. *J. Physiol* **106,** 42–58 (1947).
13. Smith, G. M. & Beecher, H. K. Amphetamine sulfate and athletic performance. I. Objective effects. *J Am Med Assoc* **170,** 542–557 (1959).
14. Roelands, B. *et al.* The effects of acute dopamine reuptake inhibition on performance. *Medicine & Science in Sports & Exercise* **40,** 879–885 (2008).
15. Borg, G., Edström, C. G., Linderholm, H. & Marklund, G. Changes in physical performance induced by amphetamine and amobarbital. *Psychopharmacologia* **26,** 10–18 (1972).
16. Roelands, B. *et al.* A dopamine/noradrenaline reuptake inhibitor improves performance in the heat, but only at the maximum therapeutic dose. *Scand J Med Sci Spor* **22,** e93–e98 (2012).
17. de Morree, H. M., Klein, C. & Marcora, S. M. Cortical substrates of the effects of caffeine and time-on-task on perception of effort. *J. Appl. Physiol.* **117,** 1514–1523 (2014).
18. Chong, T. T. J. *et al.* Dopamine enhances willingness to exert effort for

reward in Parkinson's disease. *Cortex* **69,** 40–46 (2015).
19. Long, C., Conrad, P. W., Hall, E. A. & Furler, S. L. Intrinsic extrinsic muscle control of the hand in power grip and precision handling. An electromyographic study. *J Bone Joint Surg Am* **52,** 853–867 (1970).
20. Hunt, C. C. The reflex activity of mammalian small-nerve fibres. *J. Physiol* **115,** 456–469 (1951).
21. Kandel, E., Schwartz, J. H. & Jessell, T. M. *Principles of Neural Science*. McGraw-Hill Companies, 4th Edition, NY, New York.
22. Flanagan, J. R. & Johansson, R. S. Action plans used in action observation. *Nature* **424,** 769–771 (2003).
23. Sperry, R. W. Neural basis of the spontaneous optokinetic response produced by visual inversion. *J Comp Physiol Psychol* **43,** 482–489 (1950).
24. Ellaway, P. H., Prochazka, A., Chan, M. & Gauthier, M. J. The sense of movement elicited by transcranial magnetic stimulation in humans is due to sensory feedback. *J. Physiol* **556,** 651–660 (2004).
25. Haggard, P. & Whitford, B. Supplementary motor area provides an efferent signal for sensory suppression. *Brain Res Cogn Brain Res* **19,** 52–58 (2004).
26. Christensen, M. S. *et al.* Premotor cortex modulates somatosensory cortex during voluntary movements without proprioceptive feedback. *Nature Neuroscience* **10,** 417–419 (2007).
27. Marcora, S. M. Do we really need a central governor to explain brain regulation of exercise performance? *European J. Appl. Physiol.* **104,** 929–931 (2008).
28. Blakemore, S.-J., Frith, C. D. & Wolpert, D. M. The cerebellum is involved in predicting the sensory consequences of action. *Neuroreport* **12,** 1879 (2001).
29. Dum, R. P. & Strick, P. L. Spinal Cord Terminations of the Medial Wall Motor Areas in Macaque Monkeys. *J. Neurosci* **16,** 6513–6525 (1996).
30. Dum, R. & Strick, P. Motor areas in the frontal lobe of the primate. *Physiology & Behavior* **77,** 677–682 (2002).
31. Kuhtz-Buschbeck, J. P. *et al.* Brain activity is similar during precision and power gripping with light force: An fMRI study. *NeuroImage* **40,** 1469–1481 (2008).
32. Thickbroom, G. W., Phillips, B. A., Morris, I., Byrnes, M. L. & Mastaglia, F. L. Isometric force-related activity in sensorimotor cortex measured with functional MRI. *Exp Brain Res* 1–6 (1998).
33. Cramer, S. C. *et al.* Motor cortex activation is related to force of squeezing. *Hum. Brain Mapp.* **16,** 197–205 (2002).
34. Dettmers, C. *et al.* Relation between cerebral activity and force in the motor areas of the human brain. *J. Neurophysiol* **74,** 802–815 (1995).
35. Takasawa, M. *et al.* Cerebral and cerebellar activation in power and precision grip movements: an H2 15O positron emission tomography study. *J. Cereb. Blood Flow Metab.* **23,** 1378–1382 (2003).
36. Ehrsson, H. H. *et al.* Cortical activity in precision- versus power-grip tasks: an fMRI study. *J. Neurophysiol* **83,** 528–536 (2000).
37. Kuhtz-Buschbeck, J. P., Ehrsson, H. H. & Forssberg, H. Human brain

activity in the control of fine static precision grip forces: an fMRI study. *Eur J Neurosci* **14,** 382–390 (2001).
38. Ehrsson, H. H., Fagergren, E. & Forssberg, H. Differential fronto-parietal activation depending on force used in a precision grip task: an fMRI study. *J. Neurophysiol* **85,** 2613–2623 (2001).
39. Ward, N. S. & Frackowiak, R. S. Age-related changes in the neural correlates of motor performance. *Brain* **126,** 873–888 (2003).
40. Keisker, B., Hepp-Reymond, M.-C., Blickenstorfer, A. & Kollias, S. S. Differential representation of dynamic and static power grip force in the sensorimotor network. *European J. Neurosci* **31,** 1483–1491 (2010).
41. Liu, J. Z., Zhang, L., Yao, B., Sahgal, V. & Yue, G. H. Fatigue induced by intermittent maximal voluntary contractions is associated with significant losses in muscle output but limited reductions in functional MRI-measured brain activation level. *Brain Research* **1040,** 44–54 (2005).
42. Dettmers, C., Lemon, R. N., Stephan, K. M., Fink, G. R. & Frackowiak, R. S. Cerebral activation during the exertion of sustained static force in man. *Neuroreport* **7,** 2103–2110 (1996).
43. Hill, A. V., Long, C. & Lupton, H. Muscular Exercise, Lactic Acid, and the Supply and Utilisation of Oxygen on JSTOR. in (1924). doi:10.2307/81066
44. Brooks, G. A. Lactate: link between glycolytic and oxidative metabolism. *Sports Med* **37,** 341–343 (2007).
45. Bergström, J., Hermansen, L., Hultman, E. & Saltin, B. Diet, muscle glycogen and physical performance. *Acta Physiol. Scand.* **71,** 140–150 (1967).
46. Heald, D. E. Influence of ammonium ions on mechanical and electrophysiological responses of skeletal muscle. *Am. J. Physiol.* **229,** 1174–1179 (1975).
47. Mortimer, J. T., Magnusson, R. & Petersén, I. Conduction velocity in ischemic muscle: effect on EMG frequency spectrum. *Am. J. Physiol.* **219,** 1324–1329 (1970).
48. Taylor, A. D., Bronks, R., Smith, P. & Humphries, B. Myoelectric evidence of peripheral muscle fatigue during exercise in severe hypoxia: some references to m. vastus lateralis myosin heavy chain composition. *Eur J Appl Physiol Occup Physiol* **75,** 151–159 (1997).
49. Swart, J. *et al.* Exercising with reserve: exercise regulation by perceived exertion in relation to duration of exercise and knowledge of endpoint. *Br. J. Sports Med.* **43,** 775–781 (2009).
50. Amann, M. *et al.* Arterial oxygenation influences central motor output and exercise performance via effects on peripheral locomotor muscle fatigue in humans. *J. Physiol* **575,** 937–952 (2006).
51. Taylor, J. L. & Gandevia, S. C. A comparison of central aspects of fatigue in submaximal and maximal voluntary contractions. *J. Appl. Physiol.* **104,** 542–550 (2008).
52. Peters, E. J. & Fuglevand, A. J. Cessation of human motor unit discharge during sustained maximal voluntary contraction. *Neuroscience Letters* **274,** 66–70 (1999).

53. Kernell, D. D. & Monster, A. W. Time course and properties of late adaptation in spinal motoneurones of the cat. *Exp Brain Res* **46,** 191–196 (1982).
54. Butler, J. E., Taylor, J. L. & Gandevia, S. C. Responses of Human Motoneurons to Corticospinal Stimulation during Maximal Voluntary Contractions and Ischemia. *J. Neurosci* **23,** 10224–10230 (2003).
55. Andersen, B., Westlund, B. & Krarup, C. Failure of activation of spinal motoneurones after muscle fatigue in healthy subjects studied by transcranial magnetic stimulation. *J. Physiol* **551,** 345–356 (2003).
56. Johnson, K. V. B., Edwards, S. C., Van Tongeren, C. & Bawa, P. Properties of human motor units after prolonged activity at a constant firing rate. *Exp Brain Res* **154,** 479–487 (2003).
57. Bongiovanni, L. G. & Hagbarth, K. E. Tonic vibration reflexes elicited during fatigue from maximal voluntary contractions in man. *J. Physiol* **423,** 1–14 (1990).
58. Spielmann, J. M. *et al.* Adaptation of cat motoneurons to sustained and intermittent extracellular activation. *J. Physiol* **464,** 75–120 (1993).
59. Sawczuk, A., Powers, R. K. & Binder, M. D. Contribution of outward currents to spike-frequency adaptation in hypoglossal motoneurons of the rat. *J. Neurophysiol* **78,** 2246–2253 (1997).
60. Todd, G., Taylor, J. L. & Gandevia, S. C. Measurement of voluntary activation of fresh and fatigued human muscles using transcranial magnetic stimulation. *J. Physiol* **551,** 661–671 (2003).
61. Gandevia, S. C., Allen, G. M., Butler, J. E. & Taylor, J. L. Supraspinal factors in human muscle fatigue: evidence for suboptimal output from the motor cortex. *J. Physiol* **490,** 529–536 (1996).
62. Dai, T., Liu, J., Sahgal, V., Brown, R. & Yue, G. Relationship between muscle output and functional MRI-measured brain activation. *Experimental Brain Research* **140,** 290–300 (2001).
63. Liu, J. Z. Human Brain Activation During Sustained and Intermittent Submaximal Fatigue Muscle Contractions: An fMRI Study. *J. Neurophysiol* **90,** 300–312 (2003).
64. Noble, J. W., Eng, J. J., Kokotilo, K. J. & Boyd, L. A. Aging effects on the control of grip force magnitude: An fMRI study. *EXG* **46,** 453–461 (2011).
65. Liu, J. Z., Dai, T. H., Sahgal, V., Brown, R. W. & Yue, G. H. Nonlinear cortical modulation of muscle fatigue: a functional MRI study. *Brain Research* (2002).
66. Johnston, J., Rearick, M. & Slobounov, S. Movement-related cortical potentials associated with progressive muscle fatigue in a grasping task. *Clin Neurophysiol* **112,** 68–77 (2001).
67. Jiang, Z., Wang, X.-F., Kisiel-Sajewicz, K., Yan, J. H. & Yue, G. H. Strengthened functional connectivity in the brain during muscle fatigue. *NeuroImage* **60,** 728–737 (2012).
68. Deshpande, G., LaConte, S., James, G. A., Peltier, S. & Hu, X. Multivariate Granger causality analysis of fMRI data. *Human Brain Mapping* **30,** 1361–1373 (2009).

69. Taylor, A. D. & Bronks, R. *Changes in iEMG and metabolite accumulation during submaximal work under various degrees of acute hypoxia*. (Proceedings of the XVth Congress of the International …, 1995).
70. Logothetis, N. K. What we can do and what we cannot do with fMRI. *Nature* **453,** 869–878 (2008).
71. Shibasaki, H. Human brain mapping: hemodynamic response and electrophysiology. *Clin Neurophysiol* **119,** 731–743 (2008).
72. Marcora, S. M. Perception of effort during exercise is independent of afferent feedback from skeletal muscles, heart, and lungs. *J. Appl. Physiol.* **106,** 2060–2062 (2009).
73. Marcora, S. M. Is peripheral locomotor muscle fatigue during endurance exercise a variable carefully regulated by a negative feedback system? *J. Physiol* **586,** 2027–8– author reply 2029–30 (2008).
74. Amann, M., Proctor, L. T., Sebranek, J. J., Pegelow, D. F. & Dempsey, J. A. Opioid-mediated muscle afferents inhibit central motor drive and limit peripheral muscle fatigue development in humans. *J. Physiol* **587,** 271–283 (2009).
75. Hilty, L. *et al.* Spinal opioid receptor-sensitive muscle afferents contribute to the fatigue-induced increase in intracortical inhibition in healthy humans. *Experimental Physiology* **96,** 505–517 (2011).
76. Cooper, S. J. From Claude Bernard to Walter Cannon. Emergence of the concept of homeostasis. *Appetite* **51,** 419–427 (2008).
77. Rae, D. E. *et al.* Heatstroke during endurance exercise: is there evidence for excessive endothermy? *Medicine & Science in Sports & Exercise* **40,** 1193–1204 (2008).
78. Amann, M. Significance of Group III and IV muscle afferents for the endurance exercising human. *Clin Exp Pharmacol Physiol* **39,** 831–835 (2012).
79. Craig, A. D. A new view of pain as a homeostatic emotion. *Trends Neurosci.* **26,** 303–307 (2003).
80. Bigland-Ritchie, B. R., Dawson, N. J., Johansson, R. S. & Lippold, O. C. Reflex origin for the slowing of motoneurone firing rates in fatigue of human voluntary contractions. *J. Physiol* **379,** 451–459 (1986).
81. Hayes, S. G., Kindig, A. E. & Kaufman, M. P. Comparison between the effect of static contraction and tendon stretch on the discharge of group III and IV muscle afferents. *J. Appl. Physiol.* **99,** 1891–1896 (2005).
82. Kniffki, K. D., Mense, S. & Schmidt, R. F. Responses of group IV afferent units from skeletal muscle to stretch, contraction and chemical stimulation. *Exp Brain Res* **31,** 511–522 (1978).
83. Mense, S. Nervous outflow from skeletal muscle following chemical noxious stimulation. *J. Physiol* **267,** 75–88 (1977).
84. Rotto, D. M. & Kaufman, M. P. Effect of metabolic products of muscular contraction on discharge of group III and IV afferents. *J. Appl. Physiol.* **64,** 2306–2313 (1988).
85. Potts, J. T., Spyer, K. M. & Paton, J. F. Somatosympathetic reflex in a working heart-brainstem preparation of the rat. *Brain Research Bulletin* **53,**

59–67 (2000).
86. Bandler, R., Carrive, P. & Zhang, S. P. Integration of somatic and autonomic reactions within the midbrain periaqueductal grey: viscerotopic, somatotopic and functional organization. *Prog. Brain Res.* **87,** 269–305 (1991).
87. Craig, A. D. Significance of the insula for the evolution of human awareness of feelings from the body. *Annals of the New York Academy of Sciences* **1225,** 72–82 (2011).
88. Garland, S. J. & Kaufman, M. P. in *Fatigue* **384,** 271–278 (Springer US, 1995).
89. Martin, P. G., Smith, J. L., Butler, J. E., Gandevia, S. C. & Taylor, J. L. Fatigue-sensitive afferents inhibit extensor but not flexor motoneurons in humans. **26,** 4796–4802 (2006).
90. Kennedy, D. S., McNeil, C. J., Gandevia, S. C. & Taylor, J. L. Fatigue-related firing of distal muscle nociceptors reduces voluntary activation of proximal muscles of the same limb. *J. Appl. Physiol.* **116,** 385–394 (2014).
91. Craig, A. D. How do you feel? Interoception: the sense of the physiological condition of the body. *Nature Publishing Group* **3,** 655–666 (2002).
92. Beckstead, R. M., Morse, J. R. & Norgren, R. The nucleus of the solitary tract in the monkey: projections to the thalamus and brain stem nuclei. *J. Comp. Neurol.* **190,** 259–282 (1980).
93. Gibson, A. S. C. *et al.* The Conscious Perception of the Sensation of Fatigue. *Sports Med* **33,** 167–176 (2003).
94. Noakes, T. D. Fatigue is a Brain-Derived Emotion that Regulates the Exercise Behavior to Ensure the Protection of Whole Body Homeostasis. *Front Physiol* **3,** (2012).
95. Bramble, D. M. & Lieberman, D. E. Endurance running and the evolution of Homo. *Nature* **432,** 345–352 (2004).
96. Noakes, T. & Spedding, M. Olympics: Run for your life. *Nature* **487,** 295–296 (2012).
97. Craig, A. D., Bushnell, M. C., Zhang, E. T. & Blomqvist, A. A thalamic nucleus specific for pain and temperature sensation. *Nature* **372,** 770–773 (1994).
98. Reiman, E. M. The application of positron emission tomography to the study of normal and pathologic emotions. *J Clin Psychiatry* **58 Suppl 16,** 4–12 (1997).
99. Vogt, B. A. Pain and emotion interactions in subregions of the cingulate gyrus. *Nature Publishing Group* **6,** 533–544 (2005).
100. Liotti, M. *et al.* Brain responses associated with consciousness of breathlessness (air hunger). *PNAS* **98,** 2035–2040 (2001).
101. Denton, D. *et al.* Correlation of regional cerebral blood flow and change of plasma sodium concentration during genesis and satiation of thirst. *Proc. Natl. Acad. Sci. U.S.A.* **96,** 2532–2537 (1999).
102. Williamson, J. W. *et al.* Brain activation by central command during actual and imagined handgrip under hypnosis. *J. Appl. Physiol.* **92,** 1317–1324 (2002).
103. Williamson, J. W., McColl, R., Mathews, D., Ginsburg, M. & Mitchell, J. H.

Activation of the insular cortex is affected by the intensity of exercise. *J. Appl. Physiol.* **87,** 1213–1219 (1999).
104. Öngür, D. & Price, J. L. The Organization of Networks within the Orbital and Medial Prefrontal Cortex of Rats, Monkeys and Humans. *Cereb. Cortex* **10,** 206–219 (2000).
105. Floyd, N. S., Price, J. L., Ferry, A. T., Keay, K. A. & Bandler, R. Orbitomedial prefrontal cortical projections to distinct longitudinal columns of the periaqueductal gray in the rat. *J Comp Neurol* **422,** 556–578 (2000).
106. Passingham, R. E. Premotor cortex and preparation for movement. *Exp Brain Res* **70,** 590–596 (1988).
107. Flynn, F. G. Anatomy of the insula functional and clinical correlates. *Aphasiology* (1999). doi:10.1080/026870399402325
108. Mufson, E. J. & Mesulam, M. M. Insula of the old world monkey. II: Afferent cortical input and comments on the claustrum. *J. Comp. Neurol.* **212,** 23–37 (1982).
109. Weiss, T. *et al.* Brain activation upon selective stimulation of cutaneous C- and Aδ-fibers. *NeuroImage* **41,** 1372–1381 (2008).
110. Mazzola, L., Isnard, J., Peyron, R., Guénot, M. & Mauguière, F. Somatotopic organization of pain responses to direct electrical stimulation of the human insular cortex. *Pain* **146,** 99–104 (2009).
111. Mesulam, M. M. & Mufson, E. J. Insula of the old world monkey. III: Efferent cortical output and comments on function. *J. Comp. Neurol.* **212,** 38–52 (1982).
112. Henderson, L. A., Gandevia, S. C. & Macefield, V. G. Somatotopic organization of the processing of muscle and cutaneous pain in the left and right insula cortex: a single-trial fMRI study. *Pain* **128,** 20–30 (2007).
113. Macefield, V. G., Gandevia, S. C. & Henderson, L. A. Discrete changes in cortical activation during experimentally induced referred muscle pain: a single-trial fMRI study. *Cereb. Cortex* **17,** 2050–2059 (2007).
114. Williamson, J. W. New insights into central cardiovascular control during exercise in humans: a central command update. *Experimental Physiology* **91,** 51–58 (2005).
115. Williamson, J. W. & Fadel, P. J. New insights into central cardiovascular control during exercise in humans: a central command update - Williamson - 2005 - Experimental Physiology - Wiley Online Library. *Experimental Physiology* (2006).
116. Hilty, L., Langer, N., Pascual-Marqui, R., Boutellier, U. & Lutz, K. Fatigue-induced increase in intracortical communication between mid/anterior insular and motor cortex during cycling exercise. *European J. Neurosci* **34,** 2035–2042 (2011).
117. Wong, S. W. *et al.* Sex differences in forebrain and cardiovagal responses at the onset of isometric handgrip exercise: a retrospective fMRI study. *J. Appl. Physiol.* **103,** 1402–1411 (2007).
118. Gibson, A. & Noakes, T. D. Evidence for complex system integration and dynamic neural regulation of skeletal muscle recruitment during exercise in humans. *Br. J. Sports Med.* **38,** 797–806 (2004).

119. Gibson, A. S. C., Schabort, E. J. & Noakes, T. D. Reduced neuromuscular activity and force generation during prolonged cycling. *Am. J. Physiol. Regul. Integr. Comp. Physiol.* **281,** R187–R196 (2001).
120. Jouanin, J.-C., Pérès, M., Ducorps, A. & Renault, B. A dynamic network involving M1-S1, SII-insular, medial insular, and cingulate cortices controls muscular activity during an isometric contraction reaction time task. *Human Brain Mapping* **30,** 675–688 (2009).
121. Pitcher, J. B. & Miles, T. S. Alterations in corticospinal excitability with imposed vs. voluntary fatigue in human hand muscles. *J. Appl. Physiol.* **92,** 2131–2138 (2002).
122. Nielsen, B., Hyldig, T., Bidstrup, F., Gonzalez-Alonso, J. & Christoffersen, G. R. J. Brain activity and fatigue during prolonged exercise in the heat. *Pflügers Arch - Eur J Physiol* **442,** 41–48 (2001).
123. Schneider, S., Brümmer, V., Abel, T., Askew, C. D. & Strüder, H. K. Changes in brain cortical activity measured by EEG are related to individual exercise preferences. *Physiology & Behavior* **98,** 447–452 (2009).
124. Crabbe, J. B. & Dishman, R. K. Brain electrocortical activity during and after exercise: a quantitative synthesis. *Psychophysiol* **41,** 563–574 (2004).
125. Hall, E. E., Ekkekakis, P. & Petruzzello, S. J. Regional brain activity and strenuous exercise: predicting affective responses using EEG asymmetry. *Biological Psychology* **75,** 194–200 (2007).
126. Peltier, S. J. *et al.* Reductions in interhemispheric motor cortex functional connectivity after muscle fatigue. *Brain Research* **1057,** 10–16 (2005).
127. van Duinen, H., Renken, R., Maurits, N. & Zijdewind, I. Effects of motor fatigue on human brain activity, an fMRI study. *NeuroImage* **35,** 1438–1449 (2007).
128. Tajima, S. *et al.* Medial Orbitofrontal Cortex Is Associated with Fatigue Sensation. *Neurology Research International* **2010,** 1–5 (2010).
129. Temesi, J., Arnal, P. J. & Davranche, K. Does central fatigue explain reduced cycling after complete sleep deprivation. *Med Sci Sports* (2013).
130. Marcora, S. M., Staiano, W. & Manning, V. Mental fatigue impairs physical performance in humans. *J. Appl. Physiol.* **106,** 857–864 (2009).
131. van Duinen, H., Renken, R., Maurits, N. & Zijdewind, I. Effects of motor fatigue on human brain activity, an fMRI study. *NeuroImage* **35,** 1438–1449 (2007).
132. St Clair Gibson, A. *et al.* The role of information processing between the brain and peripheral physiological systems in pacing and perception of effort. *Sports Med* **36,** 705–722 (2006).
133. Borg, G. A. Psychophysical bases of perceived exertion. *Medicine & Science in Sports & Exercise* (1982).
134. Martin, B. J. Effect of sleep deprivation on tolerance of prolonged exercise. *Eur J Appl Physiol Occup Physiol* **47,** 345–354 (1981).
135. Glass, S. C., Knowlton, R. G. & Becque, M. D. Accuracy of RPE from graded exercise to establish exercise training intensity. *Medicine & Science in Sports & Exercise* **24,** 1303–1307 (1992).
136. Tucker, R. & Noakes, T. D. The physiological regulation of pacing strategy

during exercise: a critical review. *Br. J. Sports Med.* **43,** e1–e1 (2009).
137. Tucker, R., Marle, T., Lambert, E. V. & Noakes, T. D. The rate of heat storage mediates an anticipatory reduction in exercise intensity during cycling at a fixed rating of perceived exertion. *J Physiol* **574,** 905–915 (2006).
138. Heyes, M. P., Garnett, E. S. & Coates, G. Central dopaminergic activity influences rats ability to exercise. *Life Sci.* **36,** 671–677 (1985).
139. Meeusen, R., Watson, P., Hasegawa, H., Roelands, B. & Piacentini, M. F. P. F. Brain neurotransmitters in fatigue and overtraining. *Applied Physiology, Nutrition, and Metabolism* (2007). doi:10.1139/H07-080
140. Jankovic, J. Parkinson's disease: clinical features and diagnosis. *J Neurol, Neurosurgery & Psychiatry* **79,** 368–376 (2008).
141. Capuron, L. *et al.* Dopaminergic Mechanisms of Reduced Basal Ganglia Responses to Hedonic Reward During Interferon Alfa Administration. *Arch Gen Psychiatry* **69,** 1044–1053 (2012).
142. Tobler, P. N., Fiorillo, C. D. & Schultz, W. Adaptive coding of reward value by dopamine neurons. *Science* (2005). doi:10.1126/science.1106267
143. Robbins, T. W. Arousal systems and attentional processes. *Biological Psychology* **45,** 57–71 (1997).
144. Davis, J. M. & Bailey, S. P. Possible mechanisms of central nervous system fatigue during exercise. *Medicine & Science in Sports & Exercise* **29,** 45–57 (1997).
145. Roelands, B. & Meeusen, R. Alterations in central fatigue by pharmacological manipulations of neurotransmitters in normal and high ambient temperature. *Sports Medicine* **40,** 229–246 (2010).
146. Piacentini, M. F. *et al.* No effect of a noradrenergic reuptake inhibitor on performance in trained cyclists. *Medicine & Science in Sports & Exercise* **34,** 1189–1193 (2002).
147. Piacentini, M., Meeusen, R., Buyse, L., Schutter, G., & De Meirleir, K. (2002) No Effect of a Selective Serotonergic/Noradrenergic Reuptake Inhibitor on Endurance Performance, *Eur J Sport Sci*, 2:6, 1-10
148. Roelands, B. *et al.* Acute norepinephrine reuptake inhibition decreases performance in normal and high ambient temperature. *J. Appl. Physiol.* **105,** 206–212 (2008).
149. Bailey, S. P., Davis, J. M. & Ahlborn, E. N. Effect of increased brain serotonergic activity on endurance performance in the rat. *Acta Physiol. Scand.* **145,** 75–76 (1992).
150. Bailey, S. P., Davis, J. M. & Ahlborn, E. N. Serotonergic agonists and antagonists affect endurance performance in the rat. *Int J Sports Med* **14,** 330–333 (1993).
151. Newsholme, E. A. & Blomstrand, E. Branched-chain amino acids and central fatigue. *J. Nutr.* **136,** 274S–6S (2006).
152. Blomstrand, E., Hassmén, P. & Newsholme, E. A. Effect of branched-chain amino acid supplementation on mental performance. *Acta Physiol. Scand.* **143,** 225–226 (1991).
153. Wilson, W. M. & Maughan, R. J. Evidence for a possible role of 5-

hydroxytryptamine in the genesis of fatigue in man: administration of paroxetine, a 5-HT re-uptake inhibitor, reduces the capacity to perform prolonged exercise - Wilson - 1992 - Experimental Physiology - Wiley Online Library. *Experimental Physiology* (1992). doi:10.1113/expphysiol.1992.sp003660/abstract

154. Strüder, H. K. *et al.* Influence of paroxetine, branched-chain amino acids and tyrosine on neuroendocrine system responses and fatigue in humans. *Horm Metab Res* **30,** 188–194 (1998).

155. Sutton, E. E., Coill, M. R. & Deuster, P. A. Ingestion of tyrosine: effects on endurance, muscle strength, and anaerobic performance. *Int J Sport Nutr Exerc Metab* **15,** 173–185 (2005).

156. Parise, G., Bosman, M. J., Boecker, D. R., Barry, M. J. & Tarnopolsky, M. A. Selective serotonin reuptake inhibitors: Their effect on high-intensity exercise performance. *Archives of Physical Medicine and Rehabilitation* **82,** 867–871 (2001).

157. Meeusen, R., Piacentini, M. F., Van Den Eynde, S., Magnus, L. & De Meirleir, K. Exercise performance is not influenced by a 5-HT reuptake inhibitor. *Int J Sports Med* **22,** 329–336 (2001).

158. Knab, A. M. & Lightfoot, J. T. Does the difference between physically active and couch potato lie in the dopamine system? *Int J Biol Sci* **6,** 133–150 (2010).

159. Marshall, J. F. & Berrios, N. Movement disorders of aged rats: reversal by dopamine receptor stimulation. *Science* **206,** 477–479 (1979).

160. Hallman, H., Olson, L. & Jonsson, G. Neurotoxicity of the meperidine analogue N-methyl-4-phenyl-1,2,3,6-tetrahydropyridine on brain catecholamine neurons in the mouse. *Eur. J. Pharmacol* **97,** 133–136 (1984).

161. Burns, R. S., LeWitt, P. A., Ebert, M. H., Pakkenberg, H. & Kopin, I. J. The Clinical Syndrome of Striatal Dopamine Deficiency. *N Engl J Med* **312,** 1418–1421 (1985).

162. Davis, G. C. *et al.* Chronic parkinsonism secondary to intravenous injection of meperidine analogues. *Psychiatry Research* **1,** 249–254 (1979).

163. Fredriksson, A., Plaznik, A. & Sundström, E. MPTP‐Induced Hypoactivity in Mice: Reversal by L‐Dopa. *Pharmacology & …* (1990). doi:10.1111/j.1600-0773.1990.tb00833.x

164. Meeusen, R. & De Meirleir, K. Exercise and brain neurotransmission. *Sports Medicine* (1995). doi:10.2165/00007256-199520030-00004

165. Wang, G. J. *et al.* PET studies of the effects of aerobic exercise on human striatal dopamine release. *J. Nucl. Med.* **41,** 1352–1356 (2000).

166. Sheldon, M. I., Sorscher, S. & Smith, C. B. A comparison of the effects of morphine and forced running upon the incorporation of 14-C-tyrosine into 14-C-catecholamines in mouse brain, heart and spleen. *J. Pharmacol. Exp. Ther.* **193,** 564–575 (1975).

167. Sudo, A. Time course of the changes of catecholamine levels in rat brain during swimming stress. *Brain Research* **276,** 372–374 (1983).

168. Cheramy, A., Leviel, V. & Glowinski, J. Dendritic release of dopamine in the substantia nigra. *Nature* (1981).

169. Chesselet, M. F. & Delfs, J. M. Basal ganglia and movement disorders: an update. *Trends Neurosci.* (1996). doi:10.1016/0166-2236(96)10052-7
170. Wise, R. A. Dopamine, learning and motivation. *Nature Publishing Group* **5,** 483–494 (2004).
171. Bertolucci-D'Angio, M., Serrano, A. & Scatton, B. Mesocorticolimbic dopaminergic systems and emotional states. *J. Neurosci Methods* **34,** 135–142 (1990).
172. Alexander, G. E., Crutcher, M. D. & DeLong, M. R. Basal ganglia-thalamocortical circuits: parallel substrates for motor, oculomotor, "prefrontal" and 'limbic' functions. *Prog. Brain Res.* **85,** 119–146 (1990).
173. Alexander, G. E. & Crutcher, M. D. Functional architecture of basal ganglia circuits: neural substrates of parallel processing. *Trends Neurosci.* **13,** 266–271 (1990).
174. Tanaka, M. & Watanabe, Y. Supraspinal regulation of physical fatigue. *Neuroscience & Biobehavioral Reviews* **36,** 727–734 (2012).
175. Chaudhuri, A. & Behan, P. O. Fatigue and basal ganglia. *J Neurol Sci* **179,** 34–42 (2000).
176. Chaudhuri, A. & Behan, P. O. Fatigue in neurological disorders. *The Lancet* **363,** 978–988 (2004).
177. Liu, J. Z. *et al.* Shifting of activation center in the brain during muscle fatigue: An explanation of minimal central fatigue? *NeuroImage* **35,** 299–307 (2007).
178. Rouiller, E. M., Liang, F., Babalian, A., Moret, V. & Wiesendanger, M. Cerebellothalamocortical and pallidothalamocortical projections to the primary and supplementary motor cortical areas: a multiple tracing study in macaque monkeys. *J. Comp. Neurol.* **345,** 185–213 (1994).
179. Tarsy, D. *Surgical treatment of Parkinson's disease and other movement disorders*. (Humana Press Inc, 2003).
180. Hamani, C., Saint Cyr, J. A., Fraser, J., Kaplitt, M. & Lozano, A. M. The subthalamic nucleus in the context of movement disorders. *Brain* **127,** 4–20 (2004).
181. Noakes, T. D. Time to move beyond a brainless exercise physiology: the evidence for complex regulation of human exercise performance. *Appl. Physiol. Nutr. Metab.* **36,** 23–35 (2011).
182. Marcora, S. M. Can Doping be a Good Thing? Using Psychoactive Drugs to Facilitate Physical Activity Behaviour. *Sports Medicine* 1–5 (2015). doi:10.1007/s40279-015-0412-x
183. Hannestad, J. *et al.* Clinically Relevant Doses of Methylphenidate Significantly Occupy Norepinephrine Transporters in Humans In Vivo. *BPS* **68,** 854–860 (2010).
184. Sasaki, T. *et al.* Quantification of Dopamine Transporter in Human Brain Using PET with 18F-FE-PE2I. *J. Nucl. Med.* **53,** 1065–1073 (2012).
185. Pan, D. *et al.* Binding of bromine-substituted analogs of methylphenidate to monoamine transporters. *Eur. J. Pharmacol* **264,** 177–182 (1994).
186. Scheel-Krüger, J. Comparative studies of various amphetamine analogues demonstrating different interactions with the metabolism of the

catecholamines in the brain. *Eur. J. Pharmacol* **14,** 47–59 (1971).
187. Treadway, M. T. *et al.* Dopaminergic mechanisms of individual differences in human effort-based decision-making. **32,** 6170–6176 (2012).
188. Volkow, N. D., Fowler, J. S., Wang, G., Ding, Y. & Gatley, S. J. Mechanism of action of methylphenidate: insights from PET imaging studies. *J Atten Disord* **6 Suppl 1,** S31–43 (2002).
189. Hasegawa, H. *et al.* Influence of brain catecholamines on the development of fatigue in exercising rats in the heat. *J. Physiol* **586,** 141–149 (2008).
190. Committee for Proprietary Medicinal Products. Bupropion hydrochloride, international non-proprietary name (INN): bupropion. European Agency for the Evaluation of Medicinal Products, 1–25 (2002).
191. Mathes, W. F. *et al.* Dopaminergic dysregulation in mice selectively bred for excessive exercise or obesity. *Behavioural Brain Research* **210,** 155–163 (2010).
192. Rhodes, J. S. & Garland, T., Jr. Differential sensitivity to acute administration of Ritalin, apormorphine, SCH 23390, but not raclopride in mice selectively bred for hyperactive wheel-running behavior - Springer. *Psychopharmacology* (2003).
193. Warren, G. L., Park, N. D., Maresca, R. D., McKibans, K. I. & Millard-Stafford, M. L. Effect of caffeine ingestion on muscular strength and endurance: a meta-analysis. *Medicine & Science in Sports & Exercise* **42,** 1375–1387 (2010).
194. Kalmar, J. M. & Cafarelli, E. Effects of caffeine on neuromuscular function. *J. Appl. Physiol.* **87,** 801–808 (1999).
195. Lopes, J. M., Aubier, M., Jardim, J., Aranda, J. V. & Macklem, P. T. Effect of caffeine on skeletal muscle function before and after fatigue. *J Appl Physiol Respir Environ Exerc Physiol* **54,** 1303–1305 (1983).
196. Davis, D. J. K. & Green, J. M. Caffeine and Anaerobic Performance. *Sports Med* **39,** 813–832 (2009).
197. Garrett, B. E. & Griffiths, R. R. The Role of Dopamine in the Behavioral Effects of Caffeine in Animals and Humans. *Pharmacology Biochemistry and Behavior* **57,** 533–541 (1997).
198. Garrett, B. E. & Holtzman, S. G. D1 and D2 dopamine receptor antagonists block caffeine-induced stimulation of locomotor activity in rats. *Pharmacology Biochemistry and Behavior* **47,** 89–94 (1994).
199. Morree, H. M., Klein, C. & Marcora, S. M. Perception of effort reflects central motor command during movement execution. *Psychophysiol* **49,** 1242–1253 (2012).
200. Subudhi, A. W., Miramon, B. R., Granger, M. E. & Roach, R. C. Frontal and motor cortex oxygenation during maximal exercise in normoxia and hypoxia. *J. Appl. Physiol.* **106,** 1153–1158 (2009).
201. Buxton, R. B. Introduction to Functional Magnetic Resonance Imaging: Principles and Techniques, SECOND EDITION. 1–479 (2009).
202. Savoy, R. L. Functional magnetic resonance imaging (fMRI). *Encyclopedia of Neuroscience* (1999).
203. Poldrack, R. A., Mumford, J. & Nichols, T. E. Handbook of Functional MRI

Data Analysis. (2011). Cambridge University Press, NY, New York
204. Magri, C., Logothetis, N. K. & Panzeri, S. Investigating static nonlinearities in neurovascular coupling. *Magnetic Resonance Imaging* **29,** 1358–1364 (2011).
205. Attwell, D. & Laughlin, S. B. An Energy Budget for Signaling in the Grey Matter of the Brain. *J. Cereb. Blood Flow Metab.* 1133–1145 (2001). doi:10.1097/00004647-200110000-00001
206. Attwell, D. & Iadecola, C. The neural basis of functional brain imaging signals. *Trends Neurosci.* **25,** 621–625 (2002).
207. Choi, J.-K., Chen, Y. I., Hamel, E. & Jenkins, B. G. Brain hemodynamic changes mediated by dopamine receptors: Role of the cerebral microvasculature in dopamine-mediated neurovascular coupling. *NeuroImage* **30,** 700–712 (2006).
208. Nehlig, A., Daval, J. L. & Debry, G. Caffeine and the central nervous system: mechanisms of action, biochemical, metabolic and psychostimulant effects. *Brain Res. Brain Res. Rev.* **17,** 139–170 (1992).
209. Eickhoff, S. B., Bzdok, D., Laird, A. R., Kurth, F. & Fox, P. T. Activation likelihood estimation meta-analysis revisited. *NeuroImage* **59,** 2349–2361 (2012).
210. Friston, K. J., Holmes, A., Poline, J. B., Price, C. J. & Frith, C. D. Detecting activations in PET and fMRI: levels of inference and power. *NeuroImage* **4,** 223–235 (1996).
211. Benjamini, Y. & Hochberg, Y. Controlling the False Discovery Rate: A Practical and Powerful Approach to Multiple Testing. *Journal of the Royal Statistical Society Series B* (1995). doi:10.2307/2346101
212. Genovese, C. R., Lazar, N. A. & Nichols, T. Thresholding of statistical maps in functional neuroimaging using the false discovery rate. *NeuroImage* **15,** 870–878 (2002).
213. Storey, J. D. The positive false discovery rate: a Bayesian interpretation and the q-value. *Annals of statistics* (2003).
214. Friston, K. J. Functional and Effective Connectivity: A Review. *Brain Connectivity* **1,** 13–36 (2011).
215. O'Reilly, J. X., Woolrich, M. W., Behrens, T. E. J., Smith, S. M. & Johansen-Berg, H. Tools of the trade: psychophysiological interactions and functional connectivity. *Social Cognitive and Affective Neuroscience* **7,** 604–609 (2012).
216. Liu, J. Z., Huang, H. B., Sahgal, V. & Hu, X. P. Deterioration of cortical functional connectivity due to muscle fatigue. *Proc Intl Soc Mag …* (2005).
217. Vul, E., Harris, C., Winkielman, P. & Pashler, H. Puzzlingly High Correlations in fMRI Studies of Emotion, Personality, and Social Cognition. *Perspectives on Psychological Science* **4,** 274–290 (2009).
218. Poldrack, R. A. & Mumford, J. A. Independence in ROI analysis: where is the voodoo? *Social Cognitive and Affective Neuroscience* **4,** 208–213 (2009).
219. Caulo, M. *et al.* New Morphologic Variants of the Hand Motor Cortex as Seen with MR Imaging in a Large Study Population. *AJNR Am J Neuroradiol* **28,** 1480–1485 (2007).

220. Craig, A. D. Interoception: the sense of the physiological condition of the body. *Current Opinion in Neurobiology* **13,** 500–505 (2003).
221. Peltier, S. J. & Shah, Y. Biophysical Modulations of Functional Connectivity. *Brain Connectivity* **1,** 267–277 (2011).
222. Tailby, C., Masterton, R. A. J., Huang, J. Y., Jackson, G. D. & Abbott, D. F. Resting state functional connectivity changes induced by prior brain state are not network specific. *NeuroImage* **106,** 428–440 (2015).
223. Schmidt, L. *et al.* Get Aroused and Be Stronger: Emotional Facilitation of Physical Effort in the Human Brain. **29,** 9450–9457 (2009).
224. Sclocco, R. *et al.* EEG-informed fMRI analysis during a hand grip task - Sclocco. *Conf Proc IEEE Eng Med Biol Soc* 1–4 (2012).
225. Ward, N. S., Swayne, O. B. C. & Newton, J. M. Age-dependent changes in the neural correlates of force modulation: An fMRI study. *Neurobiology of Aging* **29,** 1434–1446 (2008).
226. Goswami, R., Frances, M. F. & Shoemaker, J. K. Representation of somatosensory inputs within the cortical autonomic network. *NeuroImage* **54,** 1211–1220 (2011).
227. Sulzer, J. S., Chib, V. S., Hepp-Reymond, M.-C., Kollias, S. & Gassert, R. BOLD correlations to force in precision grip: an event-related study. *Conf Proc IEEE Eng Med Biol Soc* **2011,** 2342–2346 (2011).
228. Neely, K. A., Coombes, S. A., Planetta, P. J. & Vaillancourt, D. E. Segregated and overlapping neural circuits exist for the production of static and dynamic precision grip force. *Hum. Brain Mapp.* **34,** 698–712 (2013).
229. Prodoehl, J., Corcos, D. M. & Vaillancourt, D. E. Basal ganglia mechanisms underlying precision grip force control. *Neuroscience & Biobehavioral Reviews* **33,** 900–908 (2009).
230. Hardwick, R. M., Rottschy, C., Miall, R. C. & Eickhoff, S. B. A quantitative meta-analysis and review of motor learning in the human brain. *NeuroImage* **67,** 283–297 (2013).
231. Leslie, R. A. & James, M. F. Pharmacological magnetic resonance imaging: a new application for functional MRI. *Trends Pharmacol. Sci.* **21,** 314–318 (2000).
232. Thickbroom, G. W. *et al.* Differences in functional magnetic resonance imaging of sensorimotor cortex during static and dynamic finger flexion. *Exp Brain Res* **126,** 431–438 (1999).
233. Radua, J. & Mataix-Cols, D. Meta-analytic methods for neuroimaging data explained. *Biology of Mood & Anxiety Disorders* **2,** 6 (2012).
234. Moher, D., Liberati, A., Tetzlaff, J. & Altman, D. G. Reprint—preferred reporting items for systematic reviews and meta-analyses: the PRISMA statement. *Phys Ther* **89,** 873–880 (2009).
235. Poldrack, R. A. *et al.* Guidelines for reporting an fMRI study. *NeuroImage* **40,** 409–414 (2008).
236. Mosier, K., Lau, C., Wang, Y., Venkadesan, M. & Valero-Cuevas, F. J. Controlling instabilities in manipulation requires specific cortical-striatal-cerebellar networks. *J. Neurophysiol* **105,** 1295–1305 (2011).
237. van Nuenen, B. F. L., Kuhtz-Buschbeck, J., Schulz, C., Bloem, B. R. &

Siebner, H. R. Weight-Specific Anticipatory Coding of Grip Force in Human Dorsal Premotor Cortex. **32,** 5272–5283 (2012).
238. Wong, S. W., Massé, N., Kimmerly, D. S., Menon, R. S. & Shoemaker, J. K. Ventral medial prefrontal cortex and cardiovagal control in conscious humans. *NeuroImage* **35,** 698–708 (2007).
239. Spraker, M. B., Prodoehl, J., Corcos, D. M., Comella, C. L. & Vaillancourt, D. E. Basal ganglia hypoactivity during grip force in drug naïve Parkinson's disease. *Hum. Brain Mapp.* **31,** 1928–1941 (2010).
240. Cosottini, M. *et al.* Structural and functional evaluation of cortical motor areas in Amyotrophic Lateral Sclerosis. *Experimental Neurology* **234,** 169–180 (2012).
241. Kurniawan, I. T. *et al.* Choosing to Make an Effort: The Role of Striatum in Signaling Physical Effort of a Chosen Action. *J. Neurophysiol* **104,** 313–321 (2010).
242. Vaillancourt, D. E., Thulborn, K. R. & Corcos, D. M. Neural basis for the processes that underlie visually guided and internally guided force control in humans. *J. Neurophysiol* **90,** 3330–3340 (2003).
243. Galléa, C., de Graaf, J. B., Bonnard, M. & Pailhous, J. High level of dexterity: differential contributions of frontal and parietal areas. *Neuroreport* **16,** 1271–1274 (2005).
244. Ehrsson, H. H., Fagergren, A., Ehrsson, G. O. & Forssberg, H. Holding an object: neural activity associated with fingertip force adjustments to external perturbations. *J. Neurophysiol* **97,** 1342–1352 (2007).
245. Spraker, M. B., Corcos, D. M. & Vaillancourt, D. E. Cortical and subcortical mechanisms for precisely controlled force generation and force relaxation. *Cerebral Cortex* **19,** 2640–2650 (2009).
246. Holmström, L. *et al.* Dissociation of brain areas associated with force production and stabilization during manipulation of unstable objects. *Exp Brain Res* **215,** 359–367 (2011).
247. Wasson, P., Prodoehl, J., Coombes, S. A., Corcos, D. M. & Vaillancourt, D. E. Predicting grip force amplitude involves circuits in the anterior basal ganglia. *NeuroImage* **49,** 3230–3238 (2010).
248. Galléa, C., Graaf, J. B. de, Pailhous, J. & Bonnard, M. Error processing during online motor control depends on the response accuracy. *Behavioural Brain Research* **193,** 117–125 (2008).
249. McCrea, D. A. & Rybak, I. A. Organization of mammalian locomotor rhythm and pattern generation. *Brain Research Reviews* **57,** 134–146 (2008).
250. Whelan, P. Control of Locomotion in the Decerebrate Cat. *Progress in Neurobiology* **49,** 481–515 (1996).
251. Jordan, L. M., Liu, J., Hedlund, P. B., Akay, T. & Pearson, K. G. Descending command systems for the initiation of locomotion in mammals. *Brain Research Reviews* **57,** 183–191 (2008).
252. Brown, G. The intrinsic factors in the act of progression in the mammal. *Proceedings of the Royal Society B Biological Sciences* **84,** 308–319 (1911).
253. Eickhoff, S. B. *et al.* A new SPM toolbox for combining probabilistic cytoarchitectonic maps and functional imaging data. *NeuroImage* **25,** 1325–

1335 (2005).
254. Amunts, K. & Zilles, K. Advances in cytoarchitectonic mapping of the human cerebral cortex. *Neuroimaging Clinics of North America* **11,** 151–69–vii (2001).
255. Fox, P. T., Parsons, L. M. & Lancaster, J. L. Beyond the single study: function/location metanalysis in cognitive neuroimaging. *Current Opinion in Neurobiology* **8,** 178–187 (1998).
256. Amunts, K., Malikovic, A., Mohlberg, H., Schormann, T. & Zilles, K. Brodmann's areas 17 and 18 brought into stereotaxic space-where and how variable? *NeuroImage* **11,** 66–84 (2000).
257. Geyer, S., Schormann, T., Mohlberg, H. & Zilles, K. Areas 3a, 3b, and 1 of Human Primary Somatosensory Cortex. *NeuroImage* **11,** 684–696 (2000).
258. Grefkes, C., Geyer, S., Schormann, T., Roland, P. & Zilles, K. Human Somatosensory Area 2: Observer-Independent Cytoarchitectonic Mapping, Interindividual Variability, and Population Map. *NeuroImage* **14,** 617–631 (2001).
259. Geyer, S. *et al.* Two different areas within the primary motor cortex of man. *Nature* **382,** 805–807 (1996).
260. Ehrsson, H. H. Imagery of Voluntary Movement of Fingers, Toes, and Tongue Activates Corresponding Body-Part-Specific Motor Representations. *J. Neurophysiol* **90,** 3304–3316 (2003).
261. Engel, A. K. & Fries, P. Beta-band oscillations -signalling the status quo? *Current Opinion in Neurobiology* **20,** 156–165 (2010).
262. Rauch, H. G. L., Schönbächler, G. & Noakes, T. D. Neural correlates of motor vigour and motor urgency during exercise. *Sports Med* **43,** 227–241 (2013).
263. Chen, H., Yang, Q., Liao, W., Gong, Q. & Shen, S. Evaluation of the effective connectivity of supplementary motor areas during motor imagery using Granger causality mapping. *NeuroImage* **47,** 1844–1853 (2009).
264. Kasess, C. H. *et al.* The suppressive influence of SMA on M1 in motor imagery revealed by fMRI and dynamic causal modeling. *NeuroImage* **40,** 828–837 (2008).
265. König, P. & Engel, A. K. Correlated firing in sensory-motor systems. *Current Opinion in Neurobiology* **5,** 511–519 (1995).
266. Evarts, E. V., Fromm, C., Kröller, J. & Jennings, V. A. Motor Cortex control of finely graded forces. *J. Neurophysiol* **49,** 1199–1215 (1983).
267. Foltys, H. *et al.* Power grip disinhibits the ipsilateral sensorimotor cortex: a TMS and fMRI study. *NeuroImage* **19,** 332–340 (2003).
268. Eickhoff, S. B., Grefkes, C., Fink, G. R. & Zilles, K. Functional Lateralization of Face, Hand, and Trunk Representation in Anatomically Defined Human Somatosensory Areas. *Cerebral Cortex* **18,** 2820–2830 (2008).
269. Cadoret, G. & Smith, A. M. Comparison of the neuronal activity in the SMA and the ventral cingulate cortex during prehension in the monkey. *J. Neurophysiol* **77,** 153–166 (1997).
270. Beissner, F., Meissner, K., Bär, K.-J. & Napadow, V. The autonomic brain:

an activation likelihood estimation meta-analysis for central processing of autonomic function. **33,** 10503–10511 (2013).
271. Barnabi, F. & Cechetto, D. F. Neurotransmitters in the thalamus relaying visceral input to the insular cortex in the rat. *Am. J. Physiol. Regul. Integr. Comp. Physiol.* **281,** R1665–74 (2001).
272. Heitger, M. H. *et al.* Motor learning-induced changes in functional brain connectivity as revealed by means of graph-theoretical network analysis. *NeuroImage* **61,** 633–650 (2012).
273. Calautti, C., Serrati, C. & Baron, J. C. Effects of Age on Brain Activation During Auditory-Cued Thumb-to-Index Opposition : A Positron Emission Tomography Study. *Stroke* **32,** 139–146 (2001).
274. Tanné-Gariépy, J., Rouiller, E. M. & Boussaoud, D. Parietal inputs to dorsal versus ventral premotor areas in the macaque monkey: evidence for largely segregated visuomotor pathways. *Exp Brain Res* **145,** 91–103 (2002).
275. Fagg, A. H. & Arbib, M. A. Modeling parietal-premotor interactions in primate control of grasping. *Neural Netw* **11,** 1277–1303 (1998).
276. Jeannerod, M., Arbib, M. A., Rizzolatti, G. & Sakata, H. Grasping objects: the cortical mechanisms of visuomotor transformation. *Trends Neurosci.* **18,** 314–320 (1995).
277. Rizzolatti, G. & Luppino, G. The cortical motor system. *Neuron* **31,** 889–901 (2001).
278. Binkofski, F. *et al.* A fronto-parietal circuit for object manipulation in man: evidence from an fMRI-study. *European J. Neurosci* **11,** 3276–3286 (1999).
279. Decety, J. *et al.* Mapping motor representations with positron emission tomography. *Nature* **371,** 600–602 (1994).
280. Hattori, N. *et al.* Discrete Parieto-Frontal Functional Connectivity Related to Grasping. *J. Neurophysiol* **101,** 1267–1282 (2009).
281. Renzi, C. *et al.* The Effects of Visual Control and Distance in Modulating Peripersonal Spatial Representation. *PLoS ONE* **8,** e59460 (2013).
282. Gao, Q., Duan, X. & Chen, H. Evaluation of effective connectivity of motor areas during motor imagery and execution using conditional Granger causality. *NeuroImage* **54,** 1280–1288 (2011).
283. Solodkin, A. Fine Modulation in Network Activation during Motor Execution and Motor Imagery. *Cerebral Cortex* **14,** 1246–1255 (2004).
284. Haller, S., Chapuis, D., Gassert, R., Burdet, E. & Klarhöfer, M. Supplementary motor area and anterior intraparietal area integrate fine-graded timing and force control during precision grip. *Eur J Neurosci* **30,** 2401–2406 (2009).
285. Vaillancourt, D. E. Intermittent Visuomotor Processing in the Human Cerebellum, Parietal Cortex, and Premotor Cortex. *J. Neurophysiol* **95,** 922–931 (2005).
286. Chao, L. L. & Martin, A. Representation of Manipulable Man-Made Objects in the Dorsal Stream. *NeuroImage* **12,** 478–484 (2000).
287. Binkofski, F. *et al.* Human anterior intraparietal area subserves prehension: a combined lesion and functional MRI activation study. *Neurology* **50,** 1253–1259 (1998).

288. Steriade, M., McCormick, D. A. & Sejnowski, T. J. Thalamocortical Oscillations in the Sleeping and Aroused Brain. 1–8 (1993).
289. Rosanova, M. *et al.* Natural Frequencies of Human Corticothalamic Circuits. **29,** 7679–7685 (2009).
290. Kilner, J. M. *et al.* Task-dependent modulation of 15-30 Hz coherence between rectified EMGs from human hand and forearm muscles. *J. Physiol* **516 (Pt 2),** 559–570 (1999).
291. Friston, K. J. Another neural code? *NeuroImage* **5,** 213–220 (1997).
292. Radua, J. & Mataix-Cols, D. Voxel-wise meta-analysis of grey matter changes in obsessive-compulsive disorder. *Br J Psychiatry* **195,** 393–402 (2009).
293. Harel, N., Lee, S.-P., Nagaoka, T., Kim, D.-S. & Kim, S.-G. Origin of negative blood oxygenation level-dependent fMRI signals. *J. Cereb. Blood Flow Metab.* **22,** 908–917 (2002).
294. Frey, S. H., Vinton, D., Norlund, R. & Grafton, S. T. Cortical topography of human anterior intraparietal cortex active during visually guided grasping. *Cognitive Brain Research* **23,** 397–405 (2005).
295. Ono, M., Kubick, S. & Albernathey, C. D. Atlas of the Cerebral Sulci - Michio Ono, Michio Ono (M.D.), Stefan Kubik, Chad D. Abernathey - Google Books. (1990).
296. Rehme, A. K., Eickhoff, S. B., Rottschy, C., Fink, G. R. & Grefkes, C. Activation likelihood estimation meta-analysis of motor-related neural activity after stroke. *NeuroImage* **59,** 2771–2782 (2012).
297. Herz, D. M., Eickhoff, S. B., Løkkegaard, A. & Siebner, H. R. Functional neuroimaging of motor control in Parkinson's disease: a meta-analysis. *Human Brain Mapping* **35,** 3227–3237 (2014).
298. Amann, M. & Calbet, J. A. L. Convective oxygen transport and fatigue. *J. Appl. Physiol.* **104,** 861–870 (2008).
299. Gandevia, S. C. Spinal and Supraspinal Factors in Human Muscle Fatigue. *Physiological Reviews* **81,** 1725–1789 (2001).
300. Meeusen, R. & Roelands, B. Central fatigue and neurotransmitters, can thermoregulation be manipulated? *Scand J Med Sci Spor* **20,** 19–28 (2010).
301. Billaut, F., Bishop, D. J., Schaerz, S. & Noakes, T. D. Influence of Knowledge of Sprint Number on Pacing during Repeated-Sprint Exercise. *Medicine & Science in Sports & Exercise* **43,** 665–672 (2011).
302. Neyroud, D., Maffiuletti, N. A., Kayser, B. & Place, N. Mechanisms of fatigue and task failure induced by sustained submaximal contractions. *Medicine & Science in Sports & Exercise* **44,** 1243–1251 (2012).
303. King, A. B., Menon, R. S., Hachinski, V. & Cechetto, D. F. Human forebrain activation by visceral stimuli. *J. Comp. Neurol.* **413,** 572–582 (1999).
304. Sinita, E. & Coghill, D. The use of stimulant medications for non-core aspects of ADHD and in other disorders. *Neuropharmacology* **87,** 161–172 (2014).
305. Volkow, N. D. *et al.* Evidence that methylphenidate enhances the saliency of a mathematical task by increasing dopamine in the human brain. *Am J Psychiatry* **161,** 1173–1180 (2004).

306. Vaidya, C. J. *et al.* Selective effects of methylphenidate in attention deficit hyperactivity disorder: a functional magnetic resonance study. *Proc. Natl. Acad. Sci. U.S.A.* **95,** 14494–14499 (1998).
307. Oldfield, R. C. The assessment and analysis of handedness: The Edinburgh inventory. *Neuropsychologia* **9,** 97–113 (1971).
308. Sheehan, D. V. *et al.* The Mini-International Neuropsychiatric Interview (M.I.N.I.): the development and validation of a structured diagnostic psychiatric interview for DSM-IV and ICD-10. *J Clin Psychiatry* **59 Suppl 20,** 22–33–quiz 34–57 (1998).
309. Bull, F. C., Maslin, T. S. & Armstrong, T. Global physical activity questionnaire (GPAQ): nine country reliability and validity study. *J Phys Act Health* **6,** 790–804 (2009).
310. Kimko, H. C., Cross, J. T. & Abernethy, D. R. Pharmacokinetics and clinical effectiveness of methylphenidate. *Clin Pharmacokinet* **37,** 457–470 (1999).
311. Noseworthy, M. D., Alfonsi, J. & Bells, S. Attenuation of brain BOLD response following lipid ingestion. *Hum. Brain Mapp.* **20,** 116–121 (2003).
312. Noonan, V. & Dean, E. Submaximal exercise testing: clinical application and interpretation. *Phys Ther* **80,** 782–807 (2000).
313. Taylor, J. L., Todd, G. & Gandevia, S. C. Evidence for a supraspinal contribution to human muscle fatigue. *Clin Exp Pharmacol Physiol* **33,** 400–405 (2006).
314. King, M., Rauch, H. G., Stein, D. J. & Brooks, S. J. The handyman's brain: a neuroimaging meta-analysis describing the similarities and differences between grip type and pattern in humans. *NeuroImage* **102 Pt 2,** 923–937 (2014).
315. Semmler, J. G., Tucker, K. J., Allen, T. J. & Proske, U. Eccentric exercise increases EMG amplitude and force fluctuations during submaximal contractions of elbow flexor muscles. *J. Appl. Physiol.* **103,** 979–989 (2007).
316. Whitfield-Gabrieli, S. & Nieto-Castanon, A. Conn: A Functional Connectivity Toolbox for Correlated and Anticorrelated Brain Networks. *Brain Connectivity* **2,** 125–141 (2012).
317. Shibasaki, H. & Hallett, M. What is the Bereitschaftspotential? *Clinical Neurophysiology* **117,** 2341–2356 (2006).
318. Deecke, L. Planning, preparation, execution, and imagery of volitional action. *Cognitive Brain Research* **3,** 59–64 (1996).
319. Mazaika, P., Hoeft, F., Glover, G. H. & Reiss, A. L. Methods and Software for fMRI Analysis for Clinical Subjects. in 1–1 (2009).
320. Caviness, V. S., Meyer, J., Makris, N. & Kennedy, D. N. MRI-Based Topographic Parcellation of Human Neocortex: An Anatomically Specified Method with Estimate of Reliability. *J Cogn Neurosci* **8,** 566–587 (1996).
321. Tzourio-Mazoyer, N. *et al.* Automated anatomical labeling of activations in SPM using a macroscopic anatomical parcellation of the MNI MRI single-subject brain. *NeuroImage* **15,** 273–289 (2002).
322. Bönstrup, M., Schulz, R., Feldheim, J., Hummel, F. C. & Gerloff, C. Dynamic causal modelling of EEG and fMRI to characterize network architectures in a simple motor task. *NeuroImage* **124,** 498–508 (2016).

323. St Clair Gibson, A. Evidence for complex system integration and dynamic neural regulation of skeletal muscle recruitment during exercise in humans. *Br. J. Sports Med.* **38,** 797–806 (2004).
324. Friston, K. J. *et al.* Psychophysiological and Modulatory Interactions in Neuroimaging. *NeuroImage* **6,** 218–229 (1997).
325. Pauls, A. M. *et al.* Methylphenidate Effects on Prefrontal Functioning During Attentional-Capture and Response Inhibition. *BPS* **72,** 142–149 (2012).
326. Robbins, T. W. Chemical neuromodulation of frontal-executive functions in humans and other animals. *Exp Brain Res* **133,** 130–138 (2000).
327. Hirose, S. *et al.* Changes in cerebro-cerebellar interaction during response inhibition after performance improvement. *NeuroImage* **99,** 142–148 (2014).
328. Brass, M. & Haggard, P. To do or not to do: the neural signature of self-control. **27,** 9141–9145 (2007).
329. Zhang, S. & Li, C. S. R. Functional networks for cognitive control in a stop signal task: independent component analysis. *Human Brain Mapping* **33,** 89–104 (2012).
330. Garavan, H., Ross, T. J. & Stein, E. A. Right hemispheric dominance of inhibitory control: an event-related functional MRI study. *Proc. Natl. Acad. Sci. U.S.A.* **96,** 8301–8306 (1999).
331. Krämer, U. M. *et al.* The role of the lateral prefrontal cortex in inhibitory motor control. *Cortex* **49,** 837–849 (2013).
332. Auksztulewicz, R., Spitzer, B., Goltz, D. & Blankenburg, F. Impairing somatosensory working memory using rTMS. *Eur J Neurosci* **34,** 839–844 (2011).
333. Preuschhof, C., Heekeren, H. R., Taskin, B., Schubert, T. & Villringer, A. Neural correlates of vibrotactile working memory in the human brain. **26,** 13231–13239 (2006).
334. Tops, M. & Boksem, M. A. S. A potential role of the inferior frontal gyrus and anterior insula in cognitive control, brain rhythms, and event-related potentials. *Front Psychol* **2,** 330 (2011).
335. Berthier, M., Starkstein, S. & Leiguarda, R. Asymbolia for pain: A sensory-limbic disconnection syndrome. *Annals of Neurology* **24,** 41–49 (1988).
336. Kurth, F., Zilles, K., Fox, P. T., Laird, A. R. & Eickhoff, S. B. A link between the systems: functional differentiation and integration within the human insula revealed by meta-analysis. *Brain Struct Funct* **214,** 519–534 (2010).
337. Craig, A. D. Once an island, now the focus of attention. *Brain Struct Funct* **214,** 395–396 (2010).
338. Tomasi, D. *et al.* Methylphenidate enhances brain activation and deactivation responses to visual attention and working memory tasks in healthy controls. *NeuroImage* **54,** 3101–3110 (2011).
339. Hodzhev, Y. *et al.* Methylphenidate (MPH) promotes visual cortical activation in healthy adults in a cued visuomotor task. *J Neural Transm* **119,** 1455–1464 (2012).
340. Koyama, T., McHaffie, J. G., Laurienti, P. J. & Coghill, R. C. The subjective

experience of pain: where expectations become reality. *Proc. Natl. Acad. Sci. U.S.A.* **102,** 12950–12955 (2005).
341. Hofbauer, R. K., Rainville, P., Duncan, G. H. & Bushnell, M. C. Cortical representation of the sensory dimension of pain. *J. Neurophysiol* **86,** 402–411 (2001).
342. Kübler, A., Dixon, V. & Garavan, H. Automaticity and reestablishment of executive control-an fMRI study. *J Cogn Neurosci* **18,** 1331–1342 (2006).
343. Fassbender, C. *et al.* A topography of executive functions and their interactions revealed by functional magnetic resonance imaging. *Brain Res Cogn Brain Res* **20,** 132–143 (2004).
344. Brooks, S. J. *et al.* Thinking about eating food activates visual cortex with reduced bilateral cerebellar activation in females with anorexia nervosa: an fMRI study. *PLoS ONE* **7,** e34000 (2012).
345. Singer, T., Critchley, H. D. & Preuschoff, K. A common role of insula in feelings, empathy and uncertainty. *Trends in Cognitive Sciences* **13,** 334–340 (2009).
346. Rudebeck, P. H., Walton, M. E., Smyth, A. N., Bannerman, D. M. & Rushworth, M. F. S. Separate neural pathways process different decision costs. *Nature Neuroscience* **9,** 1161–1168 (2006).
347. Handwerker, D. A., Ollinger, J. M. & D'Esposito, M. Variation of BOLD hemodynamic responses across subjects and brain regions and their effects on statistical analyses. *NeuroImage* **21,** 1639–1651 (2004).
348. Santos-Concejero, J. *et al.* Maintained cerebral oxygenation during maximal self-paced exercise in elite Kenyan runners. *J. Appl. Physiol.* **118,** 156–162 (2015).
349. Rao, S. M. *et al.* Effects of methylphenidate on functional MRI blood-oxygen-level-dependent contrast. *Am J Psychiatry* **157,** 1697–1699 (2000).
350. Shah, N. S., Powell, D. A. & Shah, A. Regional localization of [14C] methylphenidate in rabbit brain. *Prog Neuro-Psychopharmacol Biol. Psychiat* **7,** 101–106 (1983).
351. Robson-Ansley, P. & Gibson, A. S. C. Anticipatory pacing strategies during supra-maximal exercise lasting more than 30 s. *Medicine & Science …* (2004). doi:10.1249/01.MSS.0000113474.31529.C6
352. Peltier, S. J. *et al.* Functional connectivity changes with concentration of sevoflurane anesthesia. *Neuroreport* **16,** 285–288 (2005).
353. Woo, M., Kim, S., Kim, J., Petruzzello, S. J. & Hatfield, B. D. Examining the exercise-affect dose–response relationship: Does duration influence frontal EEG asymmetry? *Int J of Psychophysiol* **72,** 166–172 (2009).
354. Pitcher, J. B., Robertson, A. L., Clover, E. C. & Jaberzadeh, S. Facilitation of cortically evoked potentials with motor imagery during post-exercise depression of corticospinal excitability. *Exp Brain Res* **160,** 409–417 (2005).
355. Petruzzello, S. J. & Tate, A. K. Brain activation, affect, and aerobic exercise: An examination of both state-independent and state-dependent relationships. *Psychophysiol* **34,** 527–533 (1997).
356. McKay, W. B., Tuel, S. M., Sherwood, A. M., Stokić, D. S. & Dimitrijević, M. R. Focal depression of cortical excitability induced by fatiguing muscle

contraction: a transcranial magnetic stimulation study. *Exp Brain Res* **105,** 276–282 (1995).
357. Brasil Neto, J. P., Cohen, L. G. & Hallett, M. Central fatigue as revealed by postexercise decrement of motor evoked potentials. *Muscle Nerve* **17,** 713–719 (1994).
358. Taylor, J. L., Butler, J. E. & Allen, G. M. Changes in motor cortical excitability during human muscle fatigue. *J Physiol* **490.2**, 519-528 (1996)
359. Hasson, U., Nusbaum, H. C. & Small, S. L. Task-dependent organization of brain regions active during rest. *Proc. Natl. Acad. Sci. U.S.A.* **106,** 10841–10846 (2009).
360. Groppe, D. M., Urbach, T. P. & Kutas, M. Mass univariate analysis of event-related brain potentials/fields I: a critical tutorial review. *Psychophysiol* **48,** 1711–1725 (2011).
361. Coco, M. *et al.* Changes in cortical excitability and blood lactate after a fatiguing hand-grip exercise. *Somatosensory & Motor Research* (2015). doi:10.3109/08990220.2013.834816
362. Van Dijk, K. R. A. *et al.* Intrinsic functional connectivity as a tool for human connectomics: theory, properties, and optimization. *J. Neurophysiol* **103,** 297–321 (2010).
363. Brannan, S. *et al.* Neuroimaging of cerebral activations and deactivations associated with hypercapnia and hunger for air. *Proc. Natl. Acad. Sci. U.S.A.* **98,** 2029–2034 (2001).
364. Le Pera, D. *et al.* Inhibition of motor system excitability at cortical and spinal level by tonic muscle pain. *Clinical Neurophysiology* **112,** 1633–1641 (2001).
365. Konova, A. B., Moeller, S. J., Tomasi, D., Volkow, N. D. & Goldstein, R. Z. Effects of Methylphenidate on Resting-State Functional Connectivity of the Mesocorticolimbic Dopamine Pathways in Cocaine Addiction. *JAMA Psychiatry* **70,** 857–868 (2013).
366. Mueller, S. *et al.* The effects of methylphenidate on whole brain intrinsic functional connectivity. *Human Brain Mapping* **35,** 5379–5388 (2014).
367. Honey, G. D. Dopaminergic drug effects on physiological connectivity in a human cortico-striato-thalamic system. *Brain* **126,** 1767–1781 (2003).
368. Sridharan, D., Levitin, D. J. & Menon, V. A critical role for the right fronto-insular cortex in switching between central-executive and default-mode networks. *PNAS* **105,** 12569–12574 (2008).
369. Fox, M. D. *et al.* The human brain is intrinsically organized into dynamic, anticorrelated functional networks. *Proc. Natl. Acad. Sci. U.S.A.* **102,** 9673–9678 (2005).
370. Fox, M. D., Zhang, D., Snyder, A. Z. & Raichle, M. E. The global signal and observed anticorrelated resting state brain networks. *J. Neurophysiol* **101,** 3270–3283 (2009).
371. Benwell, N. M., Mastaglia, F. L. & Thickbroom, G. W. Reduced functional activation after fatiguing exercise is not confined to primary motor areas. *Exp Brain Res* **175,** 575–583 (2006).
372. Butler, J. E., Larsen, T. S., Gandevia, S. C. & Petersen, N. T. The nature of

corticospinal paths driving human motoneurones during voluntary contractions. *J. Physiol* **584,** 651–659 (2007).
373. Petruzzello, S. J., Hall, E. E. & Ekkekakis, P. Regional brain activation as a biological marker of affective responsivity to acute exercise: Influence of fitness. *Psychophysiol* **38,** 99–106 (2001).
374. Noakes, T. D. From catastrophe to complexity: a novel model of integrative central neural regulation of effort and fatigue during exercise in humans. *Br. J. Sports Med.* **38,** 511–514 (2004).
375. Coghill, R. C., Sang, C. N., Maisog, J. M. & Iadarola, M. J. Pain intensity processing within the human brain: a bilateral, distributed mechanism. *J. Neurophysiol* **82,** 1934–1943 (1999).
376. Critchley, H. D. Human cingulate cortex and autonomic control: converging neuroimaging and clinical evidence. *Brain* **126,** 2139–2152 (2003).
377. Naqvi, N. H. & Bechara, A. The insula and drug addiction: an interoceptive view of pleasure, urges, and decision-making. *Brain Struct Funct* **214,** 435–450 (2010).
378. Dhond, R. P., Yeh, C., Park, K., Kettner, N. & Napadow, V. Acupuncture modulates resting state connectivity in default and sensorimotor brain networks. *Pain* **136,** 407–418 (2008).
379. Esposito, F., Otto, T., Zijlstra, F. R. H. & Goebel, R. Spatially distributed effects of mental exhaustion on resting-state FMRI networks. *PLoS ONE* **9,** e94222 (2014).
380. Chai, X. J., Castañón, A. N., Öngür, D. & Whitfield-Gabrieli, S. Anticorrelations in resting state networks without global signal regression. *NeuroImage* **59,** 1420–1428 (2012).
381. Macey, P. M. *et al.* Differential responses of the insular cortex gyri to autonomic challenges. *Autonomic Neuroscience: Basic and Clinical* **168,** 72–81 (2012).
382. Veliz, P., Boyd, C. & McCabe, S. E. Adolescent athletic participation and nonmedical Adderall use: an exploratory analysis of a performance-enhancing drug. *J Stud Alcohol Drugs* **74,** 714–719 (2013).
383. Buckman, J. F., Yusko, D. A., White, H. R. & Pandina, R. J. Risk profile of male college athletes who use performance-enhancing substances. *J Stud Alcohol Drugs* **70,** 919–923 (2009).
384. Eichner, E. R. Stimulants in Sports. *Current Sports Medicine Reports* **7,** 244–245 (2008).
385. Hickey, G. & Fricker, P. Attention Deficit Hyperactivity Disorder, CNS Stimulants and Sport. *Sports Med* **27,** 11–21 (1999).
386. Pelham, W. E. *et al.* Methylphenidate and baseball playing in ADHD children: Who's on first? *J Consult Clin Psych* **58,** 130–133 (1990).
387. Bonab, A. A., Dougherty, D. D. & Martin, J. A PET study examining pharmacokinetics and dopamine transporter occupancy of two long-acting formulations of methylphenidate in adults. *International …* (2010). doi:10.3892/ijmm_00000339
388. Slifstein, M. *et al.* COMT genotype predicts cortical-limbic D1 receptor availability measured with [11C]NNC112 and PET. *Mol. Psychiatry* **13,**

821–827 (2008).
389. Christensen, L. O. D. *et al.* Cerebral activation during bicycle movements in man. *Exp Brain Res* **135,** 66–72 (2000).
390. Egaña, M., O'Riordan, D. & Warmington, S. A. Exercise performance and VO2 kinetics during upright and recumbent high-intensity cycling exercise. *Eur J Appl Physiol* **110,** 39–47 (2010).
391. Koga, S. *et al.* Kinetics of oxygen uptake during supine and upright heavy exercise. *J. Appl. Physiol.* **87,** 253–260 (1999).
392. Fontes, E. B. *et al.* Brain activity and perceived exertion during cycling exercise: an fMRI study. *Br. J. Sports Med.* (2013). doi:10.1136/bjsports-2012-091924
393. Swart, J., Lindsay, T. R., Lambert, M. I., Brown, J. C. & Noakes, T. D. Perceptual cues in the regulation of exercise performance – physical sensations of exercise and awareness of effort interact as separate cues. *Br. J. Sports Med.* **46,** 42–48 (2012).